UPPSALA
UNIVERSITET

Digital Comprehensive Summaries of Uppsala Dissertations from the Faculty of Science and Technology 1809

Photoinduced Electron Transfer in Luminescent Lanthanide Complexes

DANIEL KOVACS

ACTA
UNIVERSITATIS
UPSALIENSIS
UPPSALA
2019

ISSN 1651-6214
ISBN 978-91-513-0657-5
urn:nbn:se:uu:diva-381905

Dissertation presented at Uppsala University to be publicly examined in Häggsalen, 10132, Ångstömlaboratoriet, Lägerhyddsvägen 1, Uppsala, Monday, 10 June 2019 at 09:15 for the degree of Doctor of Philosophy. The examination will be conducted in English. Faculty examiner: Professor Stephen Faulkner (University of Oxford, Department of Chemistry).

Abstract

Kovacs, D. 2019. Photoinduced Electron Transfer in Luminescent Lanthanide Complexes. *Digital Comprehensive Summaries of Uppsala Dissertations from the Faculty of Science and Technology* 1809. 99 pp. Uppsala: Acta Universitatis Upsaliensis. ISBN 978-91-513-0657-5.

Luminescence from the trivalent lanthanides is used for detection in biological systems. Lanthanide luminescence is usually sensitized by a light-harvesting organic chromophore (’antenna’). An ideal emitter has an antenna that efficiently transfers energy to the lanthanide, and a ligand that shields the metal from quenching solvent molecules.

Additional photophysical processes can impact the luminescence quantum yield. One such process is electron transfer from the excited state antenna to the lanthanide, yielding a lanthanide(II) and an antenna radical cation. Back electron transfer returns the antenna and a lanthanide(III), which, may or may not emit a photon.

This thesis summarizes my work on the investigation of the photoinduced electron transfer in lanthanide complexes. Chapter 1 is a brief introduction. Chapter 2 describes a structure-activity relationship in a focused library of lanthanide complexes. PeT was observed with most antennae and in a larger of lanthanides than previously assumed.

In Chapter 3, the role of the linker connecting the antenna and the metal binding site is investigated. Replacement of the secondary amide linker with a tertiary amide yielded unexpectedly high luminescence quantum yields. This was attributed to an improved sensitization efficiency due to a combination of factors (structural as well as electronic) in the Eu complexes, and a reduced back energy transfer in the Tb complexes.

In Chapter 4, the role of the ligand in PeT was investigated. Stabilization of the lanthanide(III) state by encapsulation of the ion in a highly negatively charged ligand resulted in a recovery of some of the excitation energy lost to PeT. The addition of external a strongly coordinating anionic ligand, fluoride, which could replace the charge-neutral water ligand, had a similar effect. The changes in the lanthanide redox potential was confirmed by cyclic voltammetry.

Finally, complexes equipped with azide and alkyne reactive handles are described. The introduction of bioconjugatable groups had only a small effect on the luminescent properties of the compounds. We attempted to improve the luminescence quantum yields by excluding the lanthanide-bound water molecule that has been occupying the ninth coordination. However, the nonadentate ligands did not yield appreciably better emitters due to a carbostyril-to-pyridine PeT.

Keywords: Lanthanide, Luminescence, Photoinduced electron transfer

Daniel Kovacs, Department of Chemistry - Ångström, Box 523, Uppsala University, SE-75120 Uppsala, Sweden.

ISSN 1651-6214
ISBN 978-91-513-0657-5
urn:nbn:se:uu:diva-381905 (http://urn.kb.se/resolve?urn=urn:nbn:se:uu:diva-381905)

To my beloved family

List of Papers

This thesis is based on the following papers, which are referred to in the text by their Roman numerals.

I Kovacs D., Lu X., Mészáros S. L., Ott M., Andres J., Borbas K. E. (2017) Photophysics of coumarin and carbostyril-sensitized luminescent lanthanide complexes: Implications for complex design in multiplex detection. *J. Am. Chem. Soc.*, 139, 5756-5767.

II Kovacs D., Phipps D., Orthaber A., Borbas K. E. (2018) Highly luminescent lanthanide complexes sensitised by tertiary amide-linked carbostyril antennae. *Dalton Trans.*, 47, 10702-10714.

III Kovacs D., Mathieu E., Kiraev S., Demeyere E., Sipos A., Andres J., Borbas K.E. (2019) Photoinduced electron transfer in europium complexes. In manuscript.

IV Kovacs D., Mathieu E., Kiraev S., Borbas K. E. (2019) Controlling the Yb sensitization pathway in luminescent complexes through the modulation of the Yb(II)/Yb(III) redox potential. In manuscript.

V Kovacs D., Kiraev S., Orthaber A., Borbas K. E. (2019) Highly emissive Eu- and Tb-emitting bioconjugatable complexes of octa- and nonadentate macrocyclic ligands. In manuscript.

Contribution Report

Paper I	Contributed to the synthetic work and characterization. Performed all the photophysical measurements. Contributed to the writing of the manuscript.
Paper II	Performed all the synthetic work and characterization as well as the photophysical measurements, except X-ray. Contributed to the writing of the manuscript.
Paper III	Performed all the synthetic work and characterization and photophysical measurements. Electrochemical characterization was performed by Dr. Emilie Mathieu. X-ray crystallography was done by Dr. Andreas Orthaber. Wrote the first draft of the manuscript and supporting information.
Paper IV	Performed the major part of the synthetic work and executed characterization and photophysical measurements. Electrochemical characterization was performed by Dr. Emilie Mathieu. X-ray crystallography was done by Dr. Andreas Orthaber. Wrote the first draft of the manuscript and supporting information.
Paper V	Performed all the synthetic work and compound characterization. Contributed to the writing of the manuscript.

Papers not included in this thesis:

VI Xiong R., Arkhypchuk A. I., Kovacs D., Orthaber A., Borbas K. E. (2016) Directly linked hydroporphyrin dimers. *Chem. Commun.*, 52, 9056-9058.

VII Vithanarachchi S. M., Kovacs D., Borbas K. E. (2017) Synthesis and photophysical characterization of luminescent lanthanide complexes of nucleotide-functionalized cyclen- and dipicolinate-based ligands. *Inorg. Chim. Acta.*, 460, 148-158.

VIII Kovacs D., Borbas K. E. (2018) The role of photoinduced electron transfer in the quenching of sensitized Europium emission. *Coord. Chem. Rev.*, 364, 1-9.

IX Arkhypchuk A. I., Orthaber A., Kovacs D., Borbas K. E. (2018) Isolation and characterization of a monoprotonated hydroporphyrin. *Eur. J. Org. Chem.*, 7051-7056.

X Arnold L. P., Purkis M. J., Rutkauskaite R., Kovacs D., Love B. J., Austin J. (2019) Controlled photocatalytic hydrocarbon oxidation by uranyl complexes. *ChemCatChem,* DOI: 10.1002/cctc.201900037.

Contents

Abbreviations

)))	Sonication
AIBN	Azobisisobutyronitrile
BET	Back energy transfer
$Bim(Py)_2$	*N*-((1*H*-benzo[d]imidazole-2-yl)methyl)-1-(pyridine-2-yl)-*N*-(piridin-2-ylmethyl)methanamine
Boc	*Tert*-buthyloxycarbonyl
BODIPY	4,4-difluoro-4-bora-3a,4a-diaza-s-indacene
Boc-OSu	*N*-(*tert*-Butyloxycarbonyloxy)succinimide
CBZ-Cl	Benzyloxycarbonyl chloride
cs124	7-amino-4-methyl-2-(1*H*)-quinolinone
CV	Cyclic voltammetry
DAPI	4',6-Diamidino-2-phenylindole
DCC	*N*,*N*'-Dicyclohexylcarbodiimide
DIPEA	*N*,*N*-Diisopropylethylamine
DNA	Deoxyribonucleic acid
DO3A	1,4,7,10-tetraazacyclododecane-1,4,7-triacetic acid
DOTA	1,4,7,10-Tetraazacyclododecane-1,4,7,10-tetraacetic acid
DTPA	Diethylenetriaminepentaacetic acid
dppf	1,1'-Bis(diphenylphosphino)ferrocene
$E_{1/2}$	Half-wave potential
EDANS	5-((2-Aminoethyl)amino)naphthalene-1-sulfonic acid
EDCI	1-Ethyl-3-(3-dimethylaminopropyl)carbodiimide
ET	Electron transfer
EnT	Energy transfer
ESI-MS	Electrospray ionization mass spectrometry
EWG	Electron withdrawing group
FRET	Förster resonance energy transfer
GM	Goeppert-Mayer
ICP-MS	Inductively coupled plasma mass spectrometry
ILCT	Intraligand charge-transfer
ISC	Intersystem crossing
HPLC-MS	High performance liquid chromatography - mass spectrometry
LC-MS	Liquid chromatography - mass spectrometry
LRET	Luminescence resonance energy transfer
LMCT	Ligand-to-metal charge-transfer
HATU	1-[Bis(dimethylamino)methylene]-1*H*-1,2,3-triazolo[4,5-b]pyridinium 3-oxide hexafluorophosphate

HEPES	4-(2-hydroxyethyl)-1-piperazineethanesulfonic acid
IPA	Isopropyl alcohol
LB	Lysogeny broth
Ln	Lanthanide
MOM	Methoxymethyl ether
MRI	Magnetic Resonance Imaging
NADH	Nicotinamide adenine dinucleotide, reduced form
n.d.	Not determined
NBS	*N*-bromosuccinamide
NHE	Normal hydrogen electrode
NIR	Near-infrared
NMR	Nuclear Magnetic Resonance
OD_{600}	Optical density at 600 nm
ovnt.	Overnight
PeT	Photoinduced electron transfer
PIPES	Piperazine-*N*,*N*′-bis(2-ethanesulfonic acid)
q	Hydration state
r.t.	Room temperature
RNA	Ribonucleic acid
S/N	Signal-to-noise ratio
TACN	1,4,7-Triazacyclononane
TRIS	Tris(hydroxymethyl)aminomethane
TTHA	Triethylenetetramine-*N*,*N*,*N*′,*N*″,*N*‴,*N*⁗-hexaacetic acid
UV	Ultraviolet
UV-Vis	Ultraviolet - Visible
η_{sens}	Sensitization efficiency
τ	Luminescence lifetime
Φ	Quantum yield of luminescence

1. Introduction

Lanthanides are comprised of the elements La-Lu (Z = 57–71), and together with Sc and Y, they are also called the "rare earths". They are the quintessential Scandinavian elements.[1] Many of them were first isolated in Sweden, which is reflected in their names. Holmium and Thulium are derived from the Latin names of Stockholm and Sweden, respectively. Gadolinium is named after the Finnish-Swedish scientist Johan Gadolin. Ytterbium, Erbium and Terbium (along with the honorary lanthanide Yttrium) got their names after Ytterby, a village just north of Stockholm that is home to the now closed mine that yielded lanthanide-rich ores. Today, most lanthanides are mined in China, with considerable deposits in the United States, Russia and Australia.[2] Recently, even the bottom of the Pacific Ocean was found to contain several lanthanides in amounts that are worth mining despite challenging conditions.[3] This reflects both an increasing demand for lanthanides, as well as an almost complete lack of their recovery from waste.

Contrary to their name, most lanthanides are not rare. For example, Ce, the most abundant of the group, has a natural abundance that is comparable to that of Ni. With the exception of radioactive Pm, even the least abundant lanthanides (Tm and Lu) are more abundant than Ag and Au. However, their chemical properties are very similar to each other, which makes their separation difficult.

The distinguishing feature of the lanthanides is that it is the 4f-orbitals that are filled. These orbitals are well-shielded from the environment by the 6s and the 5d orbitals, therefore, they essentially do not participate in bonding. The result is that the reactivity of the lanthanides are similar. The rich f-electron configuration on the other hand gives rise to a broad range of interesting physical properties, e.g. magnetism and luminescence.[1, 4]

The dominant oxidation state of lanthanides is +3, with an electronic configuration of $[Xe]4f^n$ (n = 0–14).[1] Until recently only a handful of ions in other oxidation states were utilized, such as Sm, Eu and Yb in their +II state, and Ce(IV) (see *Table 1.1*). SmI_2 is a single-electron reducing agent and Ce(IV) compounds are excellent oxidants. In the past decade, +II complexes have been prepared and structurally characterized for all lanthanides with the exception of Pm.[5] Similarly, the importance of lanthanides beyond Ce in their +IV state is increasingly recognized.[6] The Ln(II)/Ln(III) redox potentials are given in *Table 1.1*,[7] these will be discussed in more detail in this thesis.

Table 1.1. Electronic configuration for +2, +3 and +4 lanthanide ions, and the Ln(II)/Ln(III) redox potentials ($E_{1/2}$ [V vs NHE]).

Ln	La	Ce	Pr	Nd	Pm	Sm	Eu	Gd	Tb	Dy	Ho	Er	Tm	Yb	Lu
+II						$4f^6$	$4f^7$			$4f^{10}$			$4f^{13}$	$4f^{14}$	
+III	$4f^0$	$4f^1$	$4f^2$	$4f^3$	$4f^4$	$4f^5$	$4f^6$	$4f^7$	$4f^8$	$4f^9$	$4f^{10}$	$4f^{11}$	$4f^{12}$	$4f^{13}$	$4f^{14}$
+IV		$4f^0$	$4f^1$	$4f^2$					$4f^7$	$4f^8$					
$E_{1/2}$	-3.1	-3.2	-2.7	-2.6	-2.6	-1.6	-0.3	-3.9	-3.7	-2.5	-2.9	-3.1	-2.3	-1.1	-2.7

The unique magnetic and luminescent properties of these metal ions render them indispensable in numerous applications, such as in permanent magnets (Nd), light displays (Tb, Eu), lasers (e.g. Yb, Nd), optical fibers (Er), magnetic resonance contrast agents (Gd), and in luminescent probes that can function in complex milieu (e.g. Eu, Tb), i.e. in the presence of a multitude of potentially interfering species.[4, 8] This thesis describes the investigation of such luminescent complexes, their photophysical behavior, and the evaluation of strategies for influencing this behavior.

1.1 Lanthanide luminescence

In trivalent lanthanides luminescence arises from Laporte forbidden f-f transitions.[9] Because of the forbidden nature of these transitions, direct excitation of lanthanides is inefficient ($\varepsilon < 10\ M^{-1}cm^{-1}$). To circumvent this problem a light harvesting organic chromophore ("antenna") is often installed in close proximity of the ion (see *Figure 1.1*). Upon excitation of the antenna energy can be transferred to the lanthanide ion, which can relax back to its ground state by emitting a photon. The lifetimes of these species are in the µs-ms range. The transitions between the energy levels are characteristic for each lanthanide, and are little affected by the environment. Because of this, the resulting emission peaks are sharply spiked and narrow, appearing always at the same wavelength. They serve as a readily identifiable fingerprint for the emitter. The combination of a light-harvesting antenna and a Ln emitter has the potential to yield efficiently absorbing species that possess the advantages of the unique lanthanide emission. An important parameter for describing emitters is their brightness, which is expressed according to Eq. 1:

$$B = \varepsilon \times \Phi \tag{1}$$

where ε is the molar absorption coefficient and Φ is the quantum yield of the given fluorophore.

Due to their unique emission properties, lanthanide complexes offer solutions to several challenges posed by the conventional organic fluorophores. Unlike most organic fluorophores, Ln complexes have large apparent Stokes shifts, and thus no self-quenching. Additionally, overlap between the narrow emission peaks is minimal, which results in easily identifiable signals. The

detection of the long-lived Ln emissions in time-resolved mode, i.e. after the application with an initial delay after pulsed excitation of the sample, eliminates the short-lived autofluorescence caused by the biological fluorophores, which leads to better signal-to-noise ratios.

1.2 Sensitization mechanisms

Although a great number of organic chromophores have been used as antennae, only a handful of them are truly efficient sensitizers of the Lns.
For the visible emitting Lns, the choice of antenna is restricted to UV absorbing chromophores, while the NIR emitting Ln require antennae which have singlet and triplet energies close to this spectral region. A typical Ln complex is shown in *Figure 1.1*, with the antenna attached close to the Ln coordination environment.

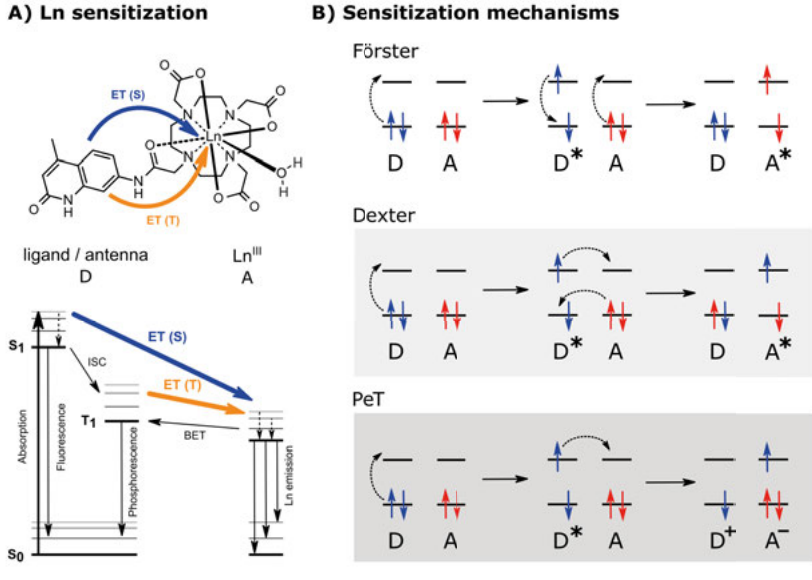

Figure 1.1 Ln luminescence sensitization by a light harvesting antenna which is attached close to the binding site. Energy diagram is shown below (left). The different sensitization mechanisms are depicted on the right: Förster EnT (top, white area), Dexter EnT (middle, light gray area) and PeT (bottom, dark gray area).

The two main types of Ln sensitization mechanisms are 1) Förster resonance energy transfer, and 2) Dexter energy transfer (electron exchange mechanism) (*Figure 1.1*).

Förster resonance energy transfer is a through-space mechanism based on a Coulombic dipole-dipole interaction between the antenna and the Ln. It is dependent on the electric field, therefore, distance is crucial for the efficiency of this process. While this mechanisms can operate over distances up to 100 Å,

it has a distance dependence of $1/r^6$.[10] It is noteworthy that no spin change can occur during this process.[11]

The Dexter energy transfer (also known as the double electron exchange mechanism) requires much shorter distances (<10–15 Å), as its distance dependence is e^{-r}.[10] The Dexter mechanism operates by through bond electronic coupling between the donor and the acceptor. The spin selectivity rules do not apply here, and the transition can either be singlet-singlet or triplet-triplet.[11]

For Yb complexes a third mechanism has been described, and consists of a photoinduced electron transfer (PeT) from the excited antenna to the Yb(III), and a back electron transfer from the transient Yb(II) to the antenna radical cation.[12] This mechanism resembles the Dexter mechanism, but the electron transfer happens only in one direction. PeT from the antenna to the Ln has been observed in Eu(III) complexes, where it has usually contribution to a diminished antenna and Ln fluorescence.[13] This will be discussed later in Chapter IV.

Luminescent lanthanide complexes can be characterized by their quantum yields (Φ_{Ln}), as defined in Eq 2.

$$\Phi_{Ln} = \eta_{sens} \cdot \Phi_{Ln}^{Ln} = \eta_{sens} \cdot \frac{\tau_{obs}}{\tau_{rad}} \quad (2)$$

In sensitized luminescence the number of emitted photons is determined by the sensitization efficiency (η_{sens}) and the intrinsic quantum yield of the lanthanide (Φ_{Ln}^{Ln}). The first of these parameters depends on the efficiency with which the feeding level of the antenna is populated by the initially formed excited state (e.g. from the singlet to the triplet through ISC), and the efficiency of the energy transfer to the lanthanide. When Φ_{Ln} is known, the sensitization efficiency can be calculated from the radiative and the observed lifetimes, as shown in Eq. 2. For most lanthanides, this is not trivial.[14] For Eu however τ_{rad} can be calculated from the emission spectrum.[15]

1.3 Quenching

Unlike organic fluorophores and phosphorescent transition metal complexes, the excited states of lanthanide ions are usually not sensitive to atmospheric oxygen.[16] In aqueous solutions the major quenching mechanism is vibrational coupling of the lanthanide excited state to X-H overtones (X = O, N, C). For Eu and Tb, which have relatively large energy gaps (12300 cm^{-1} and 14800 cm^{-1}, respectively) between their emissive states and ground states, X is O, and to a smaller extent N.[17] In the case of ions with small excited state-ground state gaps even C-H oscillators are detrimental. For example, the near infrared emitting Er, which has an energy gap of < 3100 cm^{-1}, is appreciably sensitive to C-H oscillators within 20–30 Å.[14] Usually, coupling is weaker to

X-D oscillators, which vibrate at lower frequency, and therefore more overtone is needed for coupling to the Ln excited state. Deuteration has found two applications. First, the number of water molecules in the lanthanide coordination sphere (q) can be calculated using Eq. 3 from the luminescence decay values in water (k_{H2O}), and deuterated water (k_{D2O}).

$$q = A(k_{H2O} - k_{D2O} - \Delta k_{corr}) \quad (3)$$

Second, ligand deuteration can improve the lanthanide luminescence quantum yield in many cases, although for Tb the effect may be the opposite.[17a] C-H fluorination can have a similar effect, as demonstrated by the widespread use of perfluorinated diketonate ligands.[4b]

Lanthanide luminescence can be diminished by processes that quench the antenna excited states. The antenna triplet state can have a long lifetime due to either slow energy transfer to the lanthanide, or back energy transfer from the lanthanide excited state.[16, 18] Such emitters can be sensitive to the presence of atmospheric oxygen.[16, 18a]

The antenna can participate in electron transfer with various reductants. The presence of a proximal amine can quench the antenna excited state.[19] Electron transfer to environmental reductants, such as ascorbate and urate is well established. Both processes have been used to design responsive probes.[19-20] Finally, electron transfer is possible to the lanthanide in case the metal ion has a +II state accessible through reduction by the excited state antenna.[12, 21] The latter process has been often invoked in Eu complexes to explain diminished quantum yields.[13]

1.4 Structural features of macrocyclic lanthanide complexes

Lanthanides ions exhibit a large variation in their coordination geometries. Depending on first and second order (steric) effects, complexes are known with coordination numbers as low as 2,[22] and as high as 12.[23] The f-orbitals of the Ln(III) ions are shielded from the environment by the empty 5d and 6s orbitals, therefore they do not participate in directional bonding.[1] Instead, they prefer to bind to hard donor atoms (such as O, F) through Coulombic interactions. The coordination number of the positively charged metal ion is determined by how many ligands can be accommodated while also minimizing repulsion, and is thus influenced by the size of both the Ln and the donor ligands. Due to the lanthanide contraction earlier Lns have larger ionic radii which decreases with increasing atomic number. As a result, Ln-hydrates are either 9- (La-Eu) or 8-coordinate (Dy-Lu) in water.[1]

Due to the increased charge density of smaller lanthanides, their electrostatic attraction toward ligands increases which in turn results in stronger binding. The lanthanide complex stabilities can further be improved with the use of multidentate ligands. The pendant arms of a multidentate ligand dynamically coordinate to the lanthanide. De-coordination of one arm does not result in the dissociation of the complex. Greater denticity in multidentate ligands induce larger entropy change upon complex formation, thus yielding more stable complexes. The highest thermodynamic and kinetic complex stabilities are observed for lanthanide complexes of macrocyclic ligands.

Stability is an important aspect of using lanthanides for biomedical applications. For example the widely used Gd-MRI contrast agents are toxic if the Gd(III) leeches out. Ln(III) ions are similar in size to Ca^{2+} and Zn^{2+} and can disrupt cellular processes through the transmetallation of enzymes. An additional motivation for stable complexes comes from the fact that the dissociation of the Ln from the ligand results in the loss of emission. This eventually shortens the available timeframe for the experiments, which in turn limits the utility of these tools.

Saturation of the coordination environment with multidentate ligands is not just advantageous for complex stability, it also shields the Ln from the environment. The O-H oscillators (found in polar solvents) are effective quenchers of the excited state of the lanthanide and their direct coordination to the metal lowers the emission intensity.

In terms of stability and saturation, the best performing ligands are all octa- and nonadentate macrocycles. In *Figure 1.2* a collection of these complexes is presented.

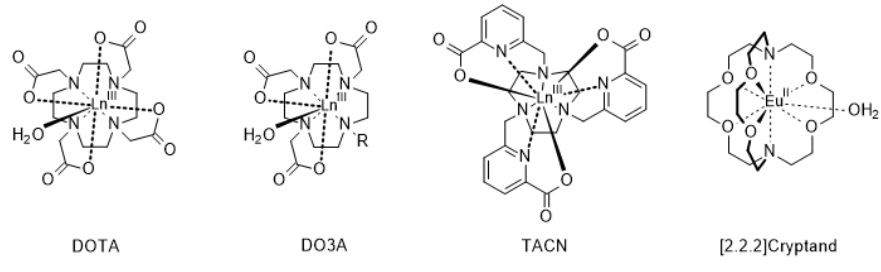

Figure 1.2 Selected macrocyclic ligands which result high stability +III and +II lanthanide complexes.

DOTA and DO3A are polyaminocarboxylate ligands that have a cyclen (1,4,7,10-tetrazadodecane) core.[24] TACN based ligands are the macrocyclic version of the popular tridentate dipicolinic acids.[25] Several years ago Eu(II) received much attention because of its potential use in MRI imaging; recently, this attention has intensified.[26] Cryptands with larger cavities and softer donor atoms (e.g. N and S vs O) are better ligands for complexing the softer Ln(II) ions.[27]

Most lanthanide complexes have coordination geometries which can be categorized into two main groups: 1) square antiprism (non-capped, or monocapped) and 2) trigonal tricapped prism.[24] Top and side views of these geometries are depicted in *Figure 1.3*.

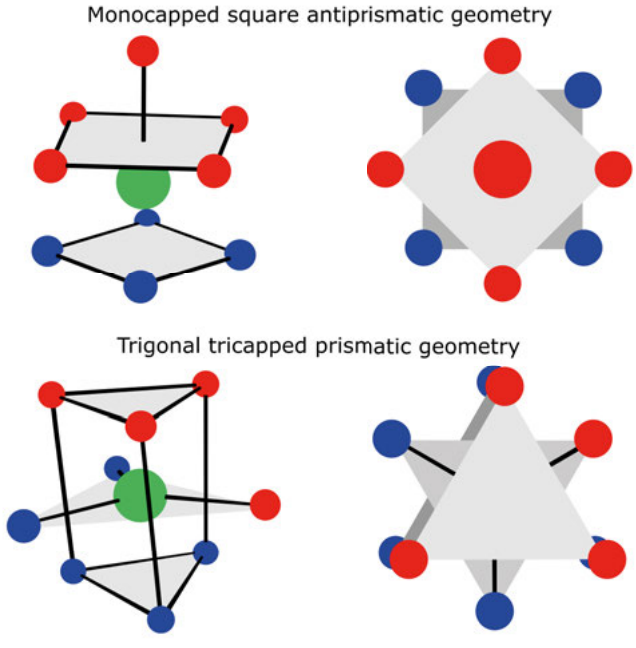

Figure 1.3 Monocapped square antiprismatic coordination geometry (upper row, sideview – left, topview – right) and trigonal tricapped prismatic geometry (bottom row, sideview – left, topview – right). Blue spheres represents N, red spheres O and green spheres the Ln ions.

According to the literature cyclen-based complexes exhibit square antiprismatic geometry.[24] When the encapsulated Ln is large, there is room for a water molecule to occupy capping position of one square of the antiprism. On the other hand, triazanonane based complexes have trigonal tricapped prismatic coordination geometry.[25d]

1.5 Fluorescent dyes and their use in microscopy

Fluorescent microscopy has greatly contributed to the development of chemical biology in the past few decades. This technique utilizes luminescence which is the spontaneous emission of a photon when an excited molecule returns to its ground state.[10] The fluorescent molecules are used to detect and localize biological entities while leaving the studied tissues and cells alive and functional. In fluorescent microscopy the samples are usually measured on a dark background, and the dyes can be visualized in very low concentrations

making this a highly sensitive method. There are several classes of organic chromophores with varying brightness and colors.[28] The core structure of most of these compounds can be easily modified to fine-tune their properties. With the installation of reactive groups, targeting biomolecules can be labelled and the localization of the fluorophores in cells becomes possible. Another possibility is to turn the dyes analyte-responsive, which enables the investigation of dynamic biological processes, and the quantification of cellular components.[29] .

A wide variety of dyes can be excited with UV light and emit in the near UV-blue region.[28a] **Endogenous fluorophores** such as tyrosine, tryptophan, NADH and flavin mononucleotide belong to this class of compounds. Cellular autofluorescence originates from these natural emitters which is often disturbing during fluorescent microscopy measurements. **Polycyclic aromatics** such as the EDANS are widely used in FRET experiments,[30] and pyrenes have been used to study protein conformations[31] and RNA folding.[32] There are several dyes which can selectively interact with DNA in cells. For staining the cell nucleus, DAPI is commonly used as it only becomes fluorescent upon binding to DNA.[33] Ethidium bromide is a different and widely used nucleic acid stain, which is an intercalating **phenanthridine** derivative.[34] Another well-established DNA-binding chromophore family is based on transition metal complexes, with prominent examples that include the ruthenium polypyridyls.[35] Fluorescein and rhodamine belong to the **xanthene** family. These compounds are among the best organic emitters with high quantum yields (> 90%) and molar absorption coefficients. They are readily rendered analyte-responsive, and have thus often been used as indicator fluorophores (e.g. of pH, Na^+, Ca^{2+}, Zn^{2+}).[36]

The **BODIPY** core is common to family of dyes with a difluoroboron moiety in its structure. Probes which utilize the lipophilicity of these compounds have been successfully developed.[37] The photophysical properties of the BODIPY dyes can be tuned by extending the conjugated system, through the replacement of the fluorides on the boron with other ligands, and by peripheral substitution.[38] There are only a handful of established chromophores which emit in the red and the near infrared. **Cyanine** dyes are popular red emitting compounds. They turned out to be powerful in gene expression studies for labeling DNA and RNA.[39] Recent reports on new fluorophores emitting in this region have highlighted their utility for biological work.[29h, 40]

While widely used, organic dyes have several disadvantages. They have broad absorption and emission spectra, and usually have small Stokes shifts. This can be a problem in microscopy because a minimal Stokes shift lowers the brightness by self-quenching. The emission lifetimes of most organic fluorophores are short, usually in the ns range. This is similar to the emission lifetime of the autofluorescence. Most organic fluorophores are prone to photobleaching, and the degradation products can be cytotoxic.

Despite all their beneficial properties Ln complexes are not widely used. There are two main reasons for that. First, Lns have high energy receiving levels. Therefore, high energy excitation is needed. Excitation in the UV requires quartz optics which increases the price of the instrument. Furthermore, UV light excites not just the Ln complex but most biological chromophores, which may damage the sample. In recent years two-photon absorbing lanthanide complexes were developed which provides a solution to this problem.[41] The second, and maybe even more important reason for the reluctance to use Ln complexes is their low brightness in aqueous media.

For comparison, the best emitting organic fluorophores (analogues of fluorescein and BODIPY) have brightness values close to 100 000 $M^{-1}cm^{-1}$, while that of the commercially available state-of-the-art Lumi4 Tb complex is only ~10 000 $M^{-1}cm^{-1}$.

In fluorescent microscopy the resolution of the collected images depends on the photon output of the fluorophore. Organic chromophores have ns lifetimes, therefore the number of photons that they emit in a short timeframe is high. Ln complexes that already suffer from lower brightness, have low photon output rates due to their μs-ms-range lifetimes. This translates to less than 10 000 photons/s.[42] Together, the low number of photons produced by Ln complexes with the strong background fluorescence of the UV excited biological sample make steady-state fluorescence microscopy inconvenient with Ln emitters. Their weak emission intensity only becomes detectable if the local emitter concentration is high and the background fluorescence is eliminated. This has been achieved with NIR emitting Yb containing metal organic frameworks[43] and Sm containing dendrimers.[44]

Time-resolved fluorescent microscopy allows the collection and accumulation of long-lived Ln emissions in the NIR[45] as well as in the visible region.[46] The widespread adaptation of this method is probably hampered by the lack of commercial availability of the instrumentation. However, there are numerous studies which demonstrate the potential of this technique. Live cells have been successfully stained with the lanthanide helicates developed by Bünzli.[47] Analogues of the exceptionally bright EuroTracker Eu series could stain mitochondria.[46a] Maury demonstrated the intracellular distribution of a triazanonane-based Sm complex using two photon microscopy simultaneously in the visible and the NIR spectral range.[48]

When Ln luminophores are used in combination with bright fluorescent dyes that have absorptions overlapping with the emission of the Ln emitter, time-resolved detection of the dye becomes possible. The concept is based on luminescence resonance energy transfer (LRET), and relies on a process wherein the Ln complex (donor) can populate the emissive levels of the fluorophore (acceptor). The lifetime of the fluorophore is thus governed by the lifetime of the long-lived Ln excited state.[49] The method has enabled the deciphering of biological processes such as ligand binding[50] or conformational changes of receptors.[51]

1.6 Lanthanide based luminescent probes

There is a bewildering number of responsive probes created from common organic dyes that have been used to detect biological species and to follow cellular processes. In a similar vein, lanthanide complexes can be made responsive. Lanthanide-based responsive probes enable time-resolved detection and better signal-to-noise ratio, by virtue of their large Stokes shifts and the narrow, bar code-like emission peaks.

There are three main strategies to create responsive lanthanide complexes.[52] The first approach is analogous to what is used for organic fluorophores. As the majority of lanthanide complexes are sensitized by organic fluorophores, one can render the sensitizing antenna analyte-responsive, and in many cases a change in the antenna photophysical properties will translate into a change in lanthanide luminescence. Commonly used approaches include triggering antenna formation by the analyte,[53] or controlling the antenna electronic properties with the target analytes.[54] The Ln complex specific approaches involve analyte triggered modifications on the Ln coordination environment,[55] as well as the distance variation between Ln and its sensitizing antenna as displayed in *Figure 1.4*.[56]

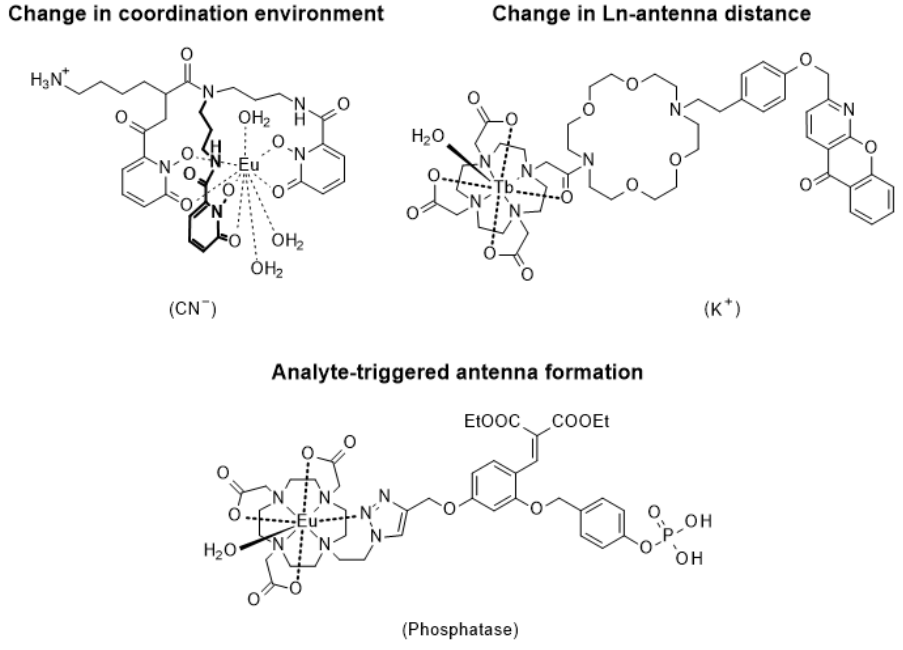

Figure 1.4 A selection of responsive Ln probes.[55b, 56b] The triggering analyte is given in parentheses.

1.7 Aims of this thesis

There have been numerous Ln-based emitters reported in the past decades. However, only a few antennae in a handful of coordination environment yield bright complexes. The de novo design of bright emitters still requires extensive optimization. Because of this reason the chemical space of Ln complexes is small and developments are usually done on the already well performing complexes. However, if we better understand the photophysical processes that impact lanthanide luminescence, the design of emissive complexes would become more rational.

The aim of this thesis was to evaluate the quenching processes that take place in Ln emitters. The role of the antenna electronic properties was studied in a focused library of coumarin- and carbostyril-sensitized Ln (Eu, Tb, Sm, Dy, Nd, Yb) complexes (Paper I). Our hypothesis was that the antenna excited states could be modulated through the antenna substitution pattern. This in turn would affect the efficiency of the energy transfer from these states.

In Paper II we prepared analogues of some of the complexes reported in Paper I by alkylation of the amide linker connecting the metal binding site and the carbostyril antenna. We expected that the removal of the N-H oscillator would improve the Ln luminescence quantum yields.

During the course of the work in Paper I we noticed that the quenching of the antenna singlet excited states correlated with the Ln(II)/Ln(III) redox potentials. We proposed that this was due to a photoinduced electron transfer from the excited antenna to the Ln(III) center. In Papers III and IV we investigated whether the electron transfer could be controlled by modulating the Ln(II)/Ln(III) redox potentials. This way, we aimed to increase the luminescence quantum yields of Eu emitters, and change the sensitization mechanisms of Yb emitters.

Finally, in Paper V we aimed to render some of our brightest emitters bioconjugatable through the introduction of reactive handles. We explored the possibility to eliminate a quenching Ln-bound water molecule from our complexes by encapsulating the Eu(III) and Tb(III) ions in a nonadentate ligand.

2. Photophysics of coumarin and carbostyril-sensitized luminescent lanthanide complexes (Paper I)

Coumarins have been used extensively in our group for multiplex detection.[53a, 53c] They possess a number of advantages, such as the ease of synthesis and modification,[57] and that they can be rendered responsive to a large variety of analytes. The probes were shown to have a large dynamic range (linear) and could enter bacterial cells; however, they had very poor quantum yields, and worked only with two lanthanides (namely Eu and Tb), which limited further extension of the strategy to more colors. Therefore, we decided to do a structure-photophysics relationship study on 7-hydroxy and 7-aminocoumarins (2H-chromen-2-ones) and the related 7-aminocarbostyril (2-quinolone) chromophores to better understand the processes that were diminishing the Ln luminescence.

2.1 Ligand design and synthesis

Our library of complexes have DO3A binding sites, which have been widely used for metal complexation.[24] This macrocyclic chelator contains a cyclen ring (1,4,7,10-tetraazacyclododecane), which is substituted with three methylcarboxylate arms installed on the nitrogen atoms. This metal binding site is connected to the sensitizing chromophore either through a triazole or an amide linker. According to the linker structure our complexes can be divided into two groups. Where the antennae are bound through the triazole (**Lc** ligands, first group, **6**), a relatively soft aromatic nitrogen might coordinate to the Ln, forming a six-membered ring. In the second group (**Ld** ligands, **17**), an amide was used for connection. Here the amide O coordinates to the metal ion, forming a more favored five membered ring.[24] Distances between the organic chromophore and Ln ion differ in the two groups, which impact the sensitization mechanism.

The preparation of the **Lc** ligands is summarized in *Scheme 2.1.* In the first step of the synthesis 7-oxycoumarin (umbelliferone) derivatives (**1**) are *O*-alkylated with propargyl bromide in the presence of potassium carbonate base. The resulting alkylated coumarins (**2**) were reacted with the azide (**8**) in

^{t}BuOH:H_2O (1:1) mixture by using copper(II) sulfate with sodium ascorbate as reductant. The critical step of the synthesis was the alkylation of the ^{t}Bu-protected DO3A core (**9**). The hindered secondary amide can only be alkylated under forcing conditions, by extensive heating in the presence of potassium iodide catalyst and potassium carbonate base. The expected product (**4**) was formed in a low yield and was difficult to purify. The deprotection of the *tert*-butyl ester groups was performed in a 1:1 solution of TFA and DCM. The free acid ligands (**5**) were purified on silica gel using acetonitrile and aqueous ammonium hydroxide solution (28%) as eluents. Complexation required the use of excess Ln salts (2.4 equiv) and reflux conditions in MeOH to lead to **Ln6a-f**.

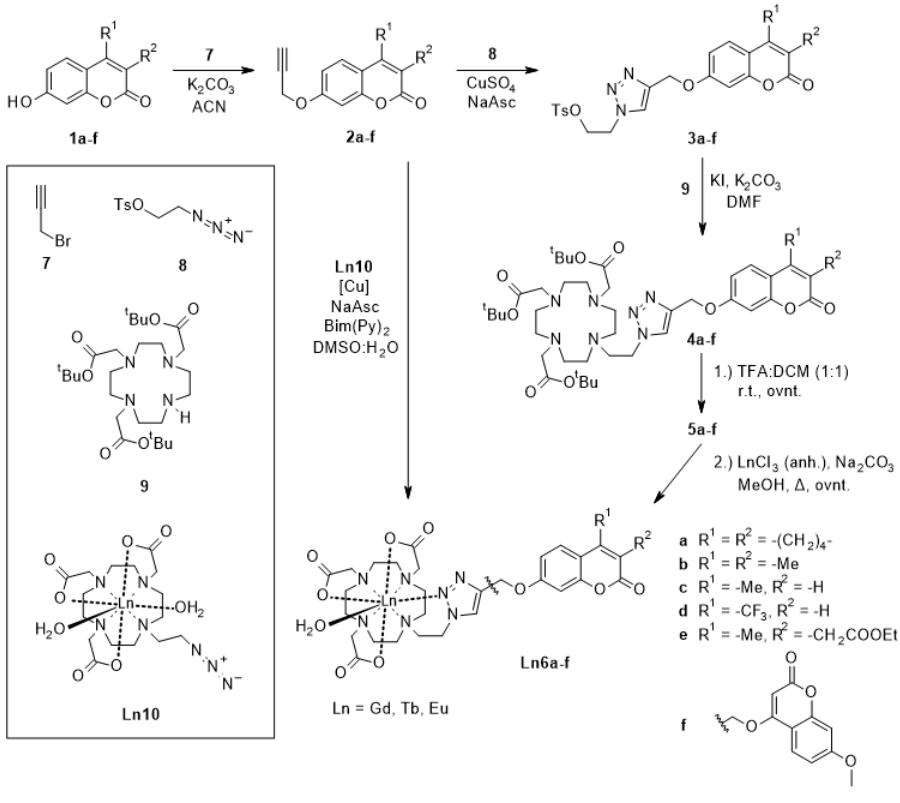

*Scheme 2.1 Synthesis of the triazole linked lanthanide complexes (**Lc**).*

We have previously established an alternative route for the same triazole linked ligands.[53c, 58] The overall yield of this approach is improved, owing to the better yields achieved in the intermediate steps. A late stage Cu-catalyzed cycloaddition allows the introduction of sensitive groups in moderate yields. To compare the two routes, we have prepared one of the complexes using a late-stage triazole formation between **2b** and **Ln10**. The linear synthetic approach and this new convergent route provide the same quality complexes based on LC-MS analysis, and absorption and emission spectroscopy.

The synthesis of the **Ld** series is shown on *Scheme 2.2*. Here both coumarin and carbostyril antennae were used. The differently substituted starting materials (**11**) were either purchased, or prepared using literature methods.[59] Chloroacylated aromatic amines (**12**) were prepared through their reaction with chloroacetyl chloride in the presence of Et_3N base. Initially, the reaction must be cooled in an ice-water bath to minimize side product formation. Subsequently, the mixture has to be allowed to warm up to room temperature. Often an additional amount of reagent was required to drive the reaction to completion. Monoalkylation of cyclen with the carbostyril chloroacetates (**12**) was executed in chloroform using minimal amount of DMF as co-solvent.[60] Polar solvents promote overalkylation,[61] but their use was inevitable because of the poor solubilities of **12** in chloroform. Trialkylation with *tert*-butyl bromoacetate was initially done by refluxing **14** in ACN with an inorganic base (K_2CO_3). The reaction was difficult to control because exact amounts of alkylating agent were needed to produce the desired product (**15**) selectively. Less than 3 equiv of reagent resulted the mixture of di- and trialkylated cyclens which were difficult to separate. The use of excess reagent caused the unselective formation of overalkylated species, with substitutions taking place both on the N and O atoms of the carbostyril. These side products were separable, but their formation diminished the yield. Replacing the base with DIPEA and performing the reaction at room temperature prevented overalkylation. However, analytically pure samples of the product were hard to obtain because of the co-elution of DIPEA·HBr on silica gel. Acidic deprotection of the ligands by TFA proceeds slowly and requires overnight stirring. Purified ligands (**16**) were used for the complexation and in this case no forcing conditions (inorganic base, reflux) were needed to acquire the corresponding complexes (**Ln17**).

Complexes of both **Lc** and **Ld** were prepared using 2.4 equivalents of $LnCl_3$. The excess unreacted Ln salt can either be removed by column chromatography on aluminum oxide, or by sequestration onto chelex 100 chelating resin. The resin had successfully been used to purify Gd-based MRI contrast agents,[62] and was also applicable for the purification of our complexes. However, while the resin bound the excess Ln salt, it also retained significant amounts of the product, greatly diminishing the isolated yield.

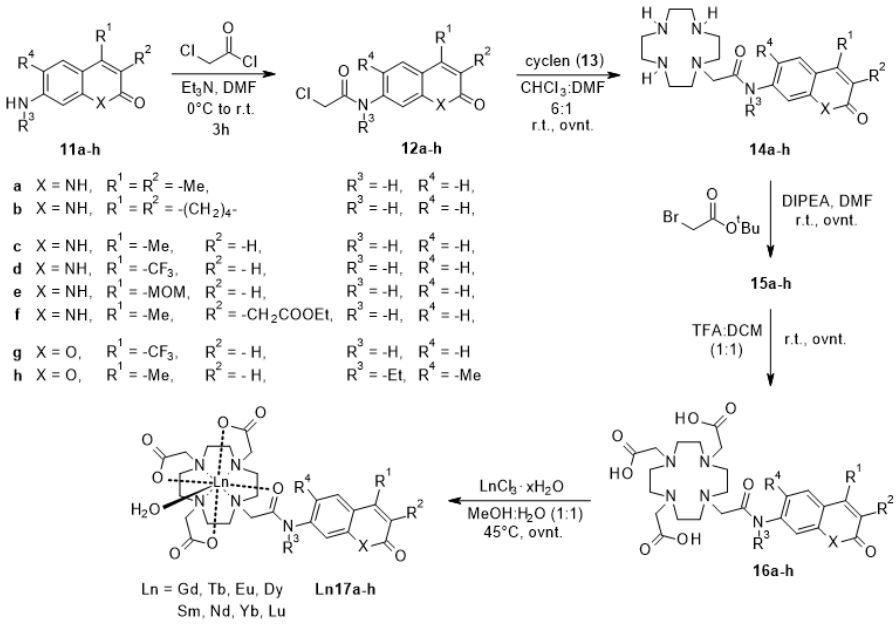

*Scheme 2.2 Synthesis of the amide linked lanthanide complexes (**Ld**).*

Control experiments proved that there were no notable differences in the photophysical properties of the analytically pure complexes and Ln salt-contaminated samples. As a result, and because of the size of the library, it was reasonable to measure just the ether washed, precipitation-purified complexes. HPLC-MS analysis confirmed that each complex had a single absorbing species with the corresponding mass spectrum matching the expected protonated or sodiated molecular ion. Complex purities were estimated by measuring the ^{1}H NMR spectra of their diamagnetic Lu analogues.

2.2 Photophysical characterization

2.2.1 Triazole linked complexes (**Lc**)

Lc complexes were analyzed in 0.1 M HEPES buffered aqueous solution at pH 7.0. Complex concentrations were adjusted to 10 μM. These complexes only have triazole-linked 7- or 4-oxycoumarin sensitizers. Typical absorption and emission spectra are shown in *Figure 2.1.*

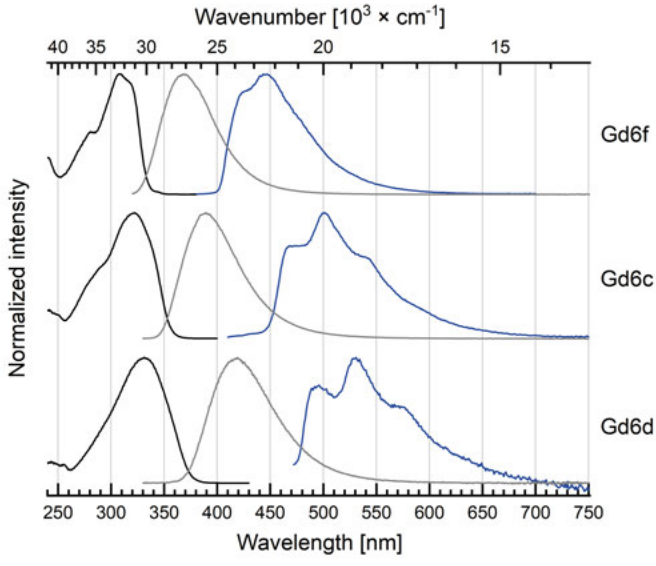

*Figure 2.1 Excitation spectra (298 K, black lines, left, λ_{em} = 400, 410, 450 nm), steady-state fluorescence emission (298K, gray lines, middle, λ_{ex} = 320, 330 nm) and time-resolved phosphorescence emission (77K, blue lines, right λ_{ex} = 320, 330 nm) spectra of selected GdLc complexes. [**Gd6**] = 10 μM, HEPES-buffered aqueous solutions 0.1 M, pH 7.0.*

Coumarin containing complexes exhibit large Stokes-shifts (>60 nm) and have broad, ill-defined absorption and emission peaks. Functional groups at the 4-position impact the photophysics: a general bathochromic shift is observed in both absorption and emission peaks going from an electron donating (-OMe) to the strongly electron withdrawing CF_3 group. Triplet energy levels follow the same trend: the highest value of 25 000 cm^{-1} (-OMe) decreases to 21 100 cm^{-1} (CF_3) along the series. Extinction coefficients are fairly high, and fall in the range of 17 000–25 000 $M^{-1}cm^{-1}$.

Typical fluorescence emission spectra of three Ln ions (Gd, Tb, Eu) with a selected **Lc** ligand (**Ln6e**) are presented in *Figure 2.2* . The photophysical data for the **Lc** series are collected in *Table 2.1*. Coumarin antennae have moderate to high ligand quantum yields (Φ_L) and dominate the steady-state emission spectra. The highest Φ_L values were found for Gd complexes that have electron donating groups in both 3- and 4-positions of the coumarin scaffold (**Gd6a,b**). We used Gd complexes as references, because the Gd has inaccessible energy levels in this ligand system. Gd is assumed to have a similar heavy atom effect as the emissive Tb and Eu. A minimal ligand fluorescence drop was observed in Tb complexes, which increased in the Eu complexes. Higher ligand fluorescence results from slower nonradiative deactivation rates. Amongst these ligands Φ_L exponentially increased with increasing S_1-T_1 energy gap, which is in accordance with an energy gap law behavior.

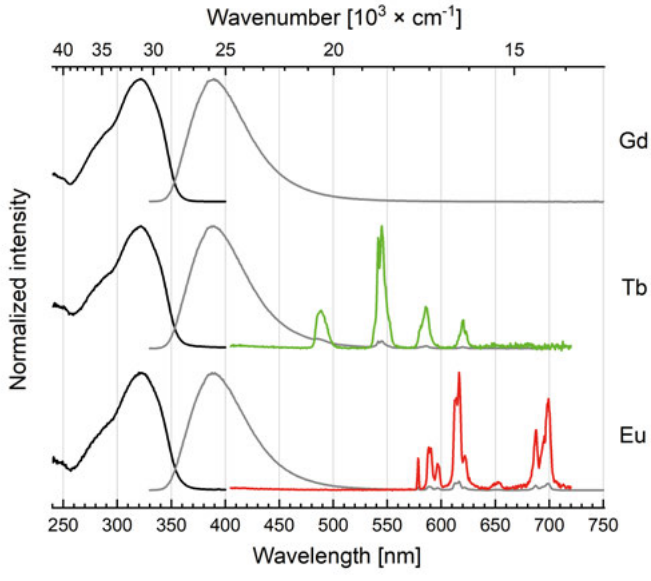

*Figure 2.2 Excitation spectra (black lines, left, λ_{em} = 389 nm (Gd), 545 nm (Tb), 616 nm (Eu)), steady-state emission spectra of **Ln6e** at 298 K (gray lines, right) and time-resolved emission spectra showing the Ln-centered emissions (Tb (green), Eu (red), 298 K, colored lines, right). Excitation at λ_{ex} = 322 nm, **[Ln6e]** = 1.0 × 10^{-5} M, HEPES-buffered aqueous solutions 0.1 M, pH 7.0.*

Upon antenna excitation, metal centered emissions were observed for the emissive lanthanides. Tb and Eu quantum yields were in all cases low (below 1%).

We found that in Eu complexes the quantum yield of the Eu is linearly correlated to the quantum yield of its sensitizer (Φ_L).

It was previously reported that Förster type sensitization occurs if the energy transfer rate is inversely proportional to the radiative lifetime to the donor.[63] Because of the large distance between the antenna and the Ln ion, we can assume that only Förster-type sensitization is operational in this system. For an electron exchange (Dexter) sensitization shorter distances are required between the donor and acceptor (<10–15 Å).[64]

Low temperature measurements on **Eu6c** revealed that the coumarin has a long lived (1.5 s) phosphorescence emission, which is another observation supporting the singlet mediated sensitization in the **Lc** complexes. The long lifetime of the triplet state suggests that it does not participate in the sensitization of the Eu.

Table 2.1.

Compound	Φ_L [%]	Φ_{Ln} [%]	τ_{H2O} [ms]
Gd6a	48	/	/
Tb6a	46	0.89	0.91
Eu6a	31	0.72	0.41
Gd6b	49	/	/
Tb6b	48	0.36	0.45
Eu6b	35	0.76	0.43
Gd6c	25	/	/
Tb6c	23	0.64	1.3
Eu6c	19	0.57	0.47
Gd6d	17	/	/
Tb6d	16	0.11	0.13/1.4
Eu6d	17	0.29	0.43
Gd6e	46	/	/
Tb6e	35	0.61	1.0
Eu6e	44	0.83	0.43
Gd6f	6.0	/	/
Tb6f	5.2	0.34	1.5
Eu6f	5.3	0.14	0.44

The sharp f-f transition bands in most **Lc** species could only be observed in the time-gated mode after pulsed excitation into the antenna at λ_{ex} = 320 nm. Phosphorescence lifetimes of **Eu6a-f** and **Tb6a-f** were in the high µs to low ms range: τ_{H2O}^{Eu} = ~0.44 ms, τ_{H2O}^{Tb} = 0.13–1.5 ms. After measuring the lifetimes in D_2O, we obtained q = 1.5 for the Eu complexes. This means that the soft N-donor in the triazole linker is not strongly coordinating to the Ln. As a result, two species probably exist in solution: the closed form has one, and the open form has two metal-bound water molecules.

2.2.2 Amide linked complexes (**Ld**)

The amide linked complexes (**Ld** series) have both coumarin and carbostyril sensitizers. The photophysical characterization was carried out on nominally 30 µM complex solutions. The concentration is an upper estimate because of the presence of NMR-silent contaminants, e.g. excess Ln salt or silica. This time the aqueous solutions were unbuffered; however, the pH of all the solutions was in the 6.0–7.0 range.

We analyzed the spectral changes and emission intensities of different **Ld** complexes between pH 1–10. Under acidic and neutral conditions, there was no variance on the measured fluorescence spectra. When the pH was raised above 7.4, both ligand- and metal-centered emissions decreased. The signal was almost completely lost above pH 10 in all complexes, except for **Tb17h**. Since the process was reversible, and because **Tb17h** has no acidic NH groups, we attribute this to a deprotonation step.

The emission spectrum of the Eu complex (**Eu17g)** showed no pH-dependent variation in its shape and the relative intensities of the transitions. This result suggests that no structural changes occur around the metal center. The fluorescence intensity (at λ_{em} = 545 nm (Tb), 700 nm (Eu)) was plotted against the pH. The data were fitted using a single proton equilibrium model to yield pK_a values 7.7 and 9.5 for **Tb17d** and **Tb17c**, respectively. The substituent in the 4-position clearly has a significant effect on the pK_a, therefore we initially thought that the proton from the heterocyclic NH was lost. To test this, we repeated the experiment with **Eu17g**, which has only one NH (in its linker). A pK_a value similar to that of **Eu17d** (8.4) was obtained. Presumably the electron withdrawing effects of both the CF_3 group in the antenna and from the Lewis acidic Ln(III) make the linker amide very acidic. It has also been reported that redox positive lanthanides can act as a charge sink, allowing even easier deprotonation of the linker NH.[65] Based on these data and additional literature support,[66] we can identify the deprotonation of the 7-amido NH as responsible for the diminished Ln-sensitization in basic conditions.

The ligand-centered photophysics were slightly different for carbostyril than for coumarin containing ligands. Carbostyrils have more well-defined transitions in both their absorption and emission peaks. Their Stokes shifts were smaller by approximately 2 300 cm^{-1}. In **LnLd** molar absorption coefficients were ε = 11 000–16 000 $M^{-1}cm^{-1}$, with the exception **Ln17h** which had only ε = 5 000 $M^{-1}cm^{-1}$. These values were similar to those previously reported for similar complexes.

In *Figure 2.3* excitation and emission spectra are compiled for Gd complexes with ligand **17c**, **17d** and **17h**. The measured quantum yields (ligand, Ln) and lifetime values are summarized in *Table 2.2.* for all the **LnLd** complexes prepared in this study.

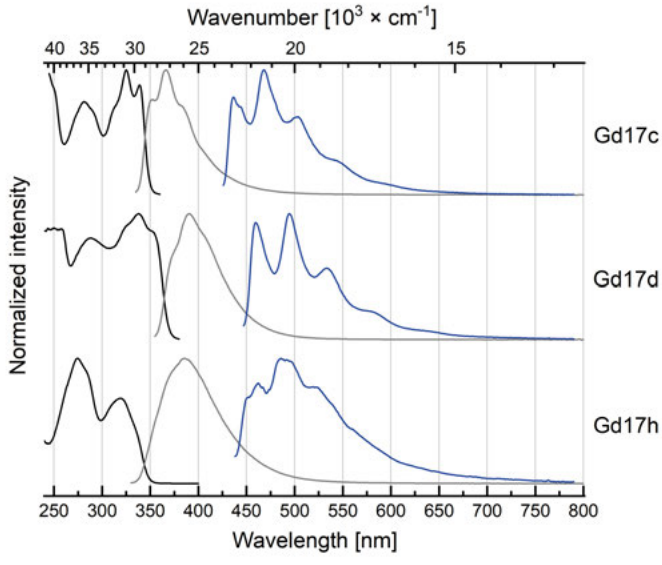

*Figure 2.3 Excitation spectra (298 K, black lines, left, λ_{em} = 405 nm), steady-state fluorescence emission (298 K, gray lines, middle, λ_{em} = 330 nm) and time-resolved phosphorescence emission (77 K, blue lines, right, λ_{em} = 330 nm) spectra of selected GdLd complexes. [**Gd17**] = 30 μM, HEPES-buffered aqueous solutions 0.1 M, pH 7.0.*

Ligand quantum yields are considerably lower than those found in the 7-oxycoumarin (**Lc**) containing ligands. The 7-amidocoumarins have the lowest ligand quantum yields (< 2%), while the 7-amidocarbostyrils have moderate values with Φ_L < 10%. The diminished quantum yields might be caused by an effect which involves specific hydrogen bonding between the amide NH and the solvent, as well as the small electron-donating ability of the 7-amide compared to a 7-oxo substituent. We found an interesting trend within each series of carbostyril complex: the highest ligand fluorescence arose from the Gd-complexes and its intensity decreased in the order Tb > Dy > Sm > Eu. This quenching effect is so pronounced that the Eu-complexes lost more than 70% of the Φ_L compared to their Gd analogues.

Several factors could lower the ligand fluorescence: singlet mediated EnT from the antenna to the Ln; altered intersystem crossing rate caused by the different heavy atom effects of the Lns; or photoinduced electron transfer from the antenna to the metal. The former two are less likely to have such a dramatic effect on the ligand fluorescence. The different lanthanide ions are often assumed to have similar heavy atom effects. Singlet ET has been shown in several coumarin-sensitized complexes,[63, 67] and was a contributor to sensitization in **LnLc**. However, in **LnLc** higher Φ_L correlated with higher Φ_{Ln}, and a large decrease in Φ_L yielded in general more emissive Ln. Here, there was no such trend, although singlet mediated EnT is still contributing to some extent, as seen from the analysis of antenna reducing powers (*vide infra*). Further-

more, the order of retained Φ_L for the different Ln within the same ligand corresponded to the stabilities of their +3 ions. As PeT had not been quantified before in this context, its contribution to quenching was difficult to estimate. Therefore, we decided to further look into this process.

Table 2.2.

Compound	Φ_L [%]	Φ_{Ln} [%]	τ_{H2O} [ms]
Gd17a	5.7	/	/
Tb17a	4.6	4.4	0.51
Dy17a	3.5	n.d.	0.009
Sm17a	2.7	0.11	0.009
Eu17a	1.3	1.1	0.58
Gd17b	7.7	/	/
Tb17b	5.9	1.9	0.14
Dy17b	4.6	0.07	0.11
Sm17b	3.7	0.12	0.009
Eu17b	1.7	1.6	0.62
Gd17c	7.7	/	/
Tb17c	5.6	35	1.4
Dy17c	4.6	0.67	0.012
Sm17c	3.9	0.16	0.009
Yb17c	4.8	n.d.	n.d.
Eu17c	0.50	3.1	0.59
Gd17d	4.9	/	/
Tb17d	4.5	3.0	0.14
Dy17d	3.6	0.13	0.008
Sm17d	3.1	0.18	n.d.
Eu17d	1.7	7.9	0.62
Gd17e	6.9	/	/
Tb17e	5.5	23	0.96
Dy17e	4.1	0.67	0.009
Sm17e	3.2	0.16	0.010
Eu17e	0.57	3.9	0.61
Gd17f	8.9	/	/
Tb17f	6.4	10	0.52
Nd17f	4.2	n.d.	n.d.
Dy17f	3.9	0.29	0.005
Sm17f	3.2	0.15	0.008
Yb17f	5.2	n.d.	n.d.
Eu17f	0.42	2.8	0.60
Gd17g	1.5	/	/
Tb17g	1.4	0.04	0.48
Dy17g	0.68	n.d.	n.d.
Sm17g	1.5	0.06	0.010
Eu17g	1.5	1.5	0.61
Gd17h	0.63	/	/
Tb17h	0.64	2.2	0.52
Dy17h	0.65	0.13	0.010
Sm17h	0.60	0.06	0.010
Eu17h	0.63	1.9	0.65

In an early study by Parker and Williams, ligand to metal PeT was proposed in a carbostyril-sensitized Eu complex.[68] Their proposal was based on a very low antenna quantum yield for the carbostyril-Eu complex compared to the Tb analogue.

An electron-rich antenna is more reducing in its excited state than an electron-deficient one. Our carbostyrils have a variety of substituents in their 3- and 4-positions. These groups are inductively changing the electron density of the aromatic system. Methyl groups are donating, while CH_2COOEt, MOM and CF_3 are withdrawing electrons from the sensitizer. Accordingly, in Eu complexes the electron poor antennae should retain more of their fluorescence emission compared to the Gd complexes. If we have a look at the Φ_L results in *Table 2.2*, we can see that the previous statement is true for **Eu17d**, but not for **Eu17f**. This is because the quenching of the ligand fluorescence is influenced by both PeT and singlet-mediated EnT.

To calculate the driving force for PeT, first we needed to determine the oxidation potentials of the antennae. We prepared model compounds having 4-Me and 4-CF_3 groups in the carbostyril. The cyclic voltammogram of **AcCS^{Me}** gave an anodic peak potential (E_{pa}) of 1.65 V vs NHE, and a cathodic peak potential (E_{pc}) of –2.09 V vs NHE. For **AcCS^{CF3}**, E_{pa} was not observed within the solvent window. Since this antenna is electron deficient, it was easier to reduce: E_{ca} was at –1.56 V vs NHE.

The free energy change of electron transfer (ΔG_{ET}) can be calculated according to Eq. (4) where E_{ox} is the oxidation potential of the donor, E_{red} is the reduction potential of the acceptor (here $E_{Ln(III)/Ln(II)}$), E_S is the excited state energy of the antenna and e_o^2/ε_a is the Coulombic attraction between the resulting ion pair.

$$\Delta G_{ET} = (E_{ox} - E_{red}) - E_S - \frac{e_o^2}{\varepsilon_a} \qquad (4)$$

All values were converted to eV. Because we only observed the E_{pa} for **AcCS^{Me}**, we used 1.65 V vs NHE in our calculations as a lower estimate of the antenna oxidation potential (E_{ox}). The redox potential of the Eu(III)/Eu(II) redox pair was at –0.35 V in water according to the literature.[69] This value is shifted to more negative values in the **Ld**-type ligand, because of the stabilizing effect of the three negatively charged carboxylates. Based on the literature, $E_{1/2}$ values of EuDOTA complexes were found between –0.92 and –1.02 V vs NHE.[70] The singlet excited state energy level of **Ln17c** is at 28 800 cm^{-1}, which equals 3.57 eV. Coulombic attraction (e_o^2/ε_a) was determined for exciplexes (≈ 0.15 eV), but in our case, the Coulombic interaction between the formed ion pair is expected to be lower (no usual charge separated form: Ln(II)-antenna$^{+\cdot}$). Now, a 'worst case scenario' approximation for ΔG_{ET} in our systems yields:

$$\Delta G_{ET} = (1.65 - (-1.02)) - 3.57 - 0.15 \text{ eV}$$
$$\Delta G_{ET} = -1.05 \text{ eV} = -101 \text{ kJ/mol}$$

A negative ΔG_{ET} means that PeT is thermodynamically favored in these Eu complexes. This process would only be disfavored if the oxidation potential of the antenna was high (E_{ox} > 2.8 V vs NHE) or if the Ln(III) was hard to reduce (E_{red} < –2.1 V vs NHE). This calculation shows that in our system Yb and Sm could also be reduced via PeT ($E_{YbIII/YbII}$ = –1.15 V; $E_{SmIII/SmII}$ = –1.55 V vs NHE.). Depending on ligand structure (strongly reducing antenna and a soft coordination environment) Dy and Nd might also be susceptible to PeT ($E_{LnIII/LnII}$ = –2.5, –2.6 V vs NHE, respectively). We can exclude any PeT for Tb and Gd as they both have redox potentials below –3.6 V vs NHE.

The donor-acceptor distance is crucial for both EnT and PeT. Within a certain distance where the electron exchange mechanism can occur, both processes could be fast. At larger distances – when PeT is thermodynamically favored – competition between the EnT and PeT should depend on the kinetics of the system.

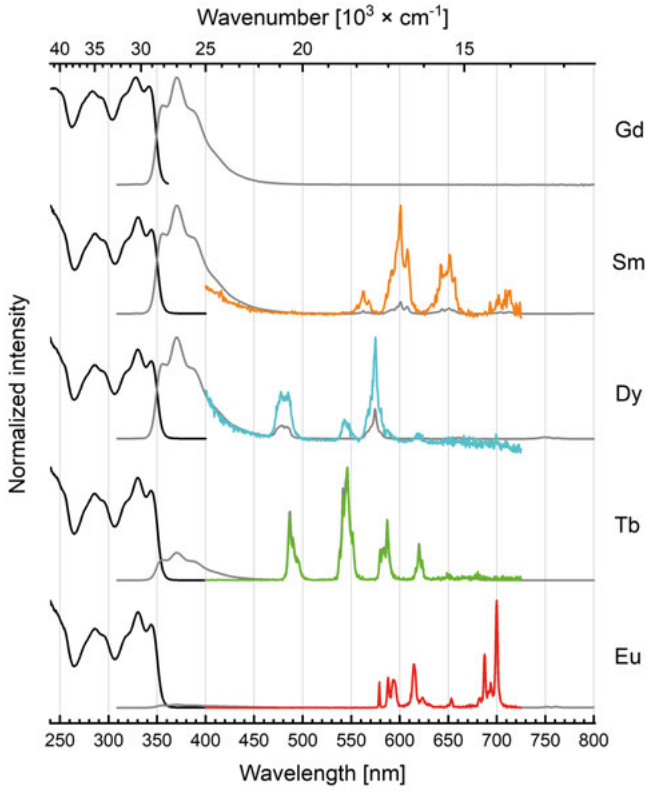

*Figure 2.4 Excitation spectra (black lines, left, λ_{em} = 370 nm (Gd), 545 nm (Tb), 575 nm (Dy), 601 nm (Sm) 616 nm (Eu)), steady-state emission spectra (gray lines, middle, λ_{ex} = 344 nm) and time-resolved emission (in color, right, λ_{ex} = 344 nm) spectra of **Ln17f** complexes in unbuffered water at 298 K. [**Ln17**] = 30 µM, unbuffered aqueous solutions, pH 5–7.*

We could record emission spectra for six different lanthanides (Eu, Tb, Dy, Sm, Nd, Yb) using the **Ld**-ligands (*Figure 2.4*). All emission arose from the

antenna excitation as proven by the excitation spectra. The steady-state emission intensity of the lanthanides are comparable to the residual ligand fluorescence, which was not the case for the previously mentioned **Lc** complexes. There are two reasons for this: 1) The intensity of the residual ligand fluorescence decreased by an order of magnitude. The previously 40-50% antenna fluorescence quantum yields dropped down below 10%. 2) The quantum yields of the Lns increased by several orders of magnitude, and are no longer below 1%.

The following transitions were found to be intense for the different Lns: Tb $^5D_4 \rightarrow {}^7F_J$ (J = 6, 5, 4, 3) at wavelengths 487, 545, 587 and 620 nm; Dy $^4F_{9/2} \rightarrow {}^6H_J$ (J = 15/2, 13/2) at wavelengths 479 and 574 nm; Sm $^4G_{5/2} \rightarrow {}^6H_J$ (J = 5/2, 7/2, 9/2) at wavelengths 563, 601 and 650 nm; Eu $^5D_0 \rightarrow {}^7F_J$ (J = 0, 1, 2, 4) at wavelengths 579, 588, 615 and 700 nm, respectively. The same transitions could be observed in time-resolved mode; however, the weaker emitting Dy and Sm spectra were often "contaminated" by Tb and Eu peaks. Initially, we thought that the samples got contaminated either during workup or sample preparation. Control experiments showed that the source of the Tb and Eu was the $LnCl_3$ reagent itself. The levels of Tb in $DyCl_3$ was up to 180 ppm, while $SmCl_3$ contained ~10 ppm of Eu as determined by ICP-MS analysis.

The hydration numbers were also calculated for the **Ld** complexes using the lifetime differences in H_2O and D_2O (Eq. 3). For all Eu complexes the formula gave q = 1. However, unreasonable values were obtained for the Tb complexes, indicating that back energy transfer to the antenna makes this q-value determination unreliable for these complexes. These data are consistent with those of found in the literature.[24]

As previously mentioned, Eu and Tb quantum yields increased several folds compared to those of **LnLc**. The best Φ_{Tb} was obtained with the Me (**Tb17c**, 35%), MOM (**Tb17e**, 23%) and 3Es (**Tb17f**, 10%) ligands. CF_3 containing coumarin and carbostyril have too low-lying triplet levels which allow for BET to occur, resulting in quenching by $^3O_2$. Despite this, **Tb17d** still performed twice as well as the best emitting **TbLc** complexes. On the other hand, these low-lying triplet levels make the CF_3 antenna a more efficient Eu sensitizer (Φ_{Eu} = 8%). For Eu, the other ligands have lower quantum yields, ranging between 1–4%.

Dy and Sm are not as bright as Tb and Eu, but they have distinct emission peaks, which could provide a nice addition to the already existing luminescent probes. The problem is that they have lower intrinsic quantum yields and their lifetimes fall in the low μs range. Since we found a promising Dy quantum yield with a **Lc** ligand, we decided to prepare the whole **Ld** series with Sm and Dy. Our best results for Dy were obtained with the 4-Me and 4-MOM antennae (0.67%). In these complexes the Dy peak intensity (J = 13/2) almost surpassed the height of the residual ligand fluorescence. Sm gave higher in-

tensities when carbostyril antennae were used than with coumarins. Differences between the results were minimal, and all Φ_{Ln} values ranged between 0.11–0.18%.

To extend the scope of our study, we attempted to record Nd and Yb emissions in the NIR region with **Ln17f**. We could obtain the metal centered emissions at 875 nm and 980 nm for Nd and Yb, respectively (*Figure 2.5*). These emission channels are desired in bioimaging as they are in the so-called biological window. Even weakly emitting probes can be used in this region. The metal emissions we found were indeed very low, and unfortunately our setup did not allow us to measure any Ln quantum yields or lifetimes for the Nd and Yb complexes.

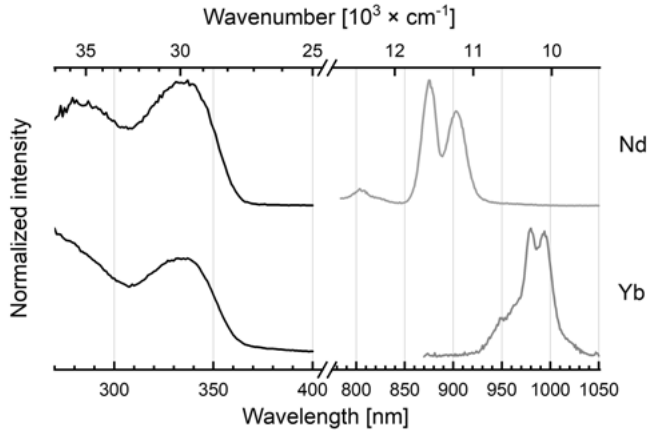

*Figure 2.5 Excitation spectra (black lines, left, λ_{em} = 875 nm (Nd), 980 nm (Yb)) and steady-state emission spectra (in color, right, λ_{ex} = 344 nm) of **Ln17f** in H_2O at room temperature. [**Ln17f**] = 30 μM, unbuffered aqueous solutions, pH 5–7.*

Yb has a single spectroscopic level at 10 300 cm^{-1} and has no spectral overlap with the singlet of the antenna. Therefore, the observed ligand fluorescence decrease in Yb complexes could only be caused by PeT. The opposite can be said about Tb. Here, the lowered ligand quantum yield is only due to singlet EnT and PeT can entirely be excluded, since Tb(III) is the second hardest lanthanide to reduce with a redox couple of –3.7 V.

When plotting the ligand fluorescence quantum yields against the redox potentials of the different Lns Yb and Tb can be used as the two anchoring points. Assuming that all Lns have the same singlet EnT efficiencies with the exception of Yb, the obtained trend in Φ_L quenching follows the redox potential of the Lns.

To conclude, in the **Ld** complexes wherein the antenna is in close proximity of the Ln, both singlet and triplet mediated EnT occur, and contribute to the lanthanide sensitization. Depending on the redox potential of the Ln, electron transfer from the antenna to the metal is possible, and it is often detrimental to Ln luminescence. Yb is the only exception, because sensitization of this metal with UV absorbing antennae should only be possible by PeT.

2.3 Cellular imaging

As a proof of concept, we wanted to demonstrate the potential of our complexes in multiplex imaging. An ideal situation would be if a single ligand could efficiently sensitize several lanthanides at the same time. Then the structure of the complexes would be identical (there would be only minor changes depending on the size of the Ln) and important factors such as cellular uptake, localization and interactions within the cell would be similar across the series. There would be no spectral cross-talk between the different Ln complexes, as they are all excited in the UV region by the antenna, and the metals have distinct emission peaks that are specific to the metal. Often wavelengths where only one lanthanide emit can be selected.

To test the limits of our complexes in a multiplex spectroscopy experiment, we selected the **17f** ligand, which was able to sensitize up to six lanthanides. A cocktail solution was made which contained Tb (2.7 nM), Eu (46 nM) together with the less emissive Dy and Sm complexes (15 μM each). All lanthanide emissions were observed in both the steady-state and in time-resolved mode. Additionally, time-resolved mode allowed us to selectively record Dy and Sm next to the Eu Tb pair, based on their different luminescent properties (shorter lifetimes, lower emission intensities). Upon the addition of the NIR emitting Nd and Yb complexes (100 μM each), the cocktail provided seven different colors both in the visible and near infrared region. A limitation of this approach could be the increasing amount of chromophore that is introduced to the system. At higher complex concentrations the output signal decreased; this was probably caused by an inner filter effect.

In cellular experiments photostability is an important parameter. Under continuous irradiation organic molecules tend to degrade, which limits the time available for experiments. Moreover, the products of photobleaching are often cytotoxic.

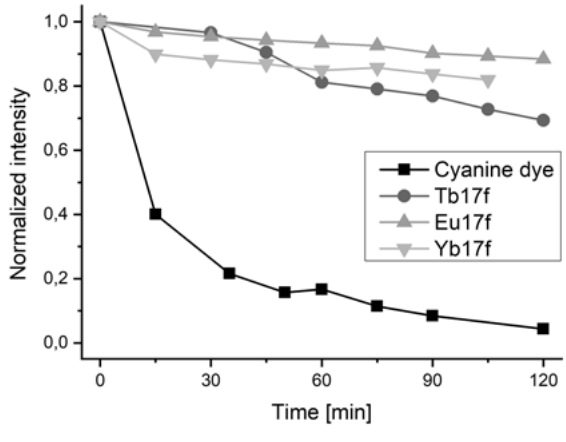

*Figure 2.6 Photostability comparison between **Ln17f** (λ_{ex} = 344 nm) and a NIR emitting dye (3,3´-diethylthiadicarbocyanine iodide, λ_{ex} = 646 nm) in water.*

We tested the photostability of our complexes against a commercially available and widely used cyanine dye (*Figure 2.6*). The organic fluorophore lost more than 90% of its emission intensity over the course of 3 h. The complexes performed better and retained 70%+ of their luminescence over the same period under identical conditions. The Tb complex had the highest photosensitivity. This is not surprising as this lanthanide can repopulate the triplet state of the organic sensitizer.

After measurements in solution, we were ready to test our complexes in living cells. *E. coli* cell cultures were incubated in buffered complex solutions [**Ln17f**] = 5–500 μM. The complexes penetrated the cells even after a few hours of incubation and were non-toxic towards the bacteria as confirmed by LB agar plating. After incubation, the cells were harvested by centrifugation, the pellet was washed 5 times with TRIS buffer to remove the excess Ln complexes. Before fluorescent measurements, the number of cells was estimated by measuring the optical density of the samples. Steady-state and time-resolved fluorescent measurements proved the presence of the more emissive complexes in the living bacteria. **Tb17f** and **Eu17f** could be detected separately as well as in a mixture (*Figure 2.7*). The steady-state spectra are dominated by strong background fluorescence due to the presence of biological fluorophores. Ln emissions are very low, but the characteristic fingerprints can already be identified. Time-resolved mode can eliminate the unwanted background fluorescence, providing exclusively the long-lived, narrow emission peaks of Eu and Tb.

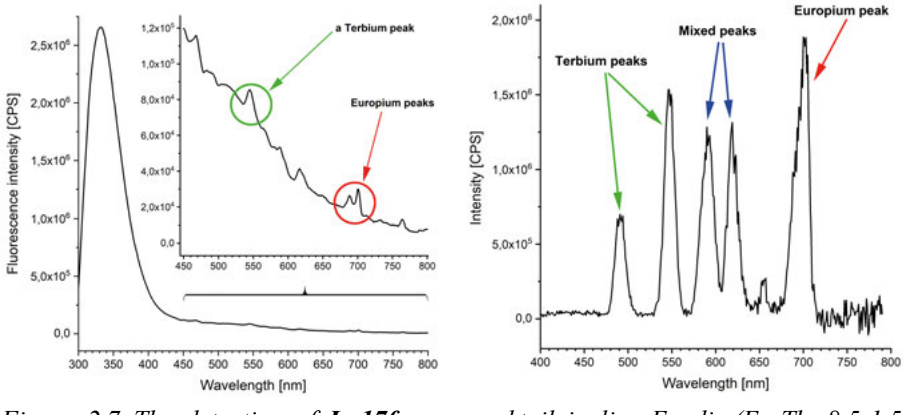

*Figure 2.7 The detection of **Ln17f** as a cocktail in live E.coli. (Eu:Tb=8.5:1.5, OD_{600}=6.647). Left spectra shows the steady-state mode, where the distinct Ln peaks were highlighted with green (Tb) and red (Eu). Right: time-resolved mode, showing only the long living Ln luminescence. Blue arrows point on peaks which are the result of both Eu and Tb emission.*

We also performed cell fractionation studies. The complex treated cells were lysed with beat beating and the insoluble parts were separated from the cytosol. Both the supernatant and membrane fractions contained the complexes,

but lower intensity signals were obtained from the latter. This experiment confirmed that the Ln-complexes penetrate inside the cells.

Finally, we moved from the simpler bacteria to the more complex mammalian cells. Here only cell viability tests were done on a preosteoblastic cell line (MC3T3-E1). Results show slight reduction in cell viability. Cells maintained 80%+ of viability with most **LnLd** complexes, and showed signs of recovery after 72 h.

We also wanted to record fluorescent images of the **LnLd** complex dyed mammalian cells. Unfortunately we did not have access to a fluorescent microscope with a UV laser, thus we turned to a two-photon microscope (Zeiss 710 NLO) that had a Nd:YAG laser. The cells were treated with both the complex and DAPI, and after fixation the samples were irradiated between λ_{ex}=700–750 nm. On the obtained fluorescent images we could only observe the cell nucleus which was stained by DAPI. We could not detect luminescence from Ln complexes. The carbostyril antennae have very low two-photon cross section (GM) values,[71] and are therefore not likely to be efficiently excited. Therefore, we did not pursue this experiment further.

2.4 Conclusion

A library of 61 complexes was synthesized and photophysically characterized. Small and systematic changes on the ligand structures contributed to the better understanding of the Ln sensitization and quenching mechanisms. We found that in complexes with distant antenna Förster type sensitization is the most probable dominant mechanism. Here, the Ln quantum yields were generally low (below 1%). Both FRET and Dexter type sensitization were observed for complexes having a close antenna, which resulted in significantly higher Ln quantum yields. In these latter complexes electron transfer from the antenna to the lanthanide was found thermodynamically possible. Our findings show that the reduction to the +II metal oxidation state via PeT is important in Eu and Yb, and possible in Sm, Dy, and Nd complexes. PeT resulted the quenching of both ligand and Ln fluorescence with the exception of Yb. Within each complex series the degree of ligand fluorescence quenching matched with the reduction potential of the Lns.

In solution, multiplex imaging was tested with one of our ligand which was able to sensitize up to 6 different Lns. Signals on seven different channels were observed: one in the UV (antenna), four in the visible (Tb, Eu, Dy, Sm) and two in the NIR region (Nd, Yb). The complexes gave sharp signals with minimal overlap and displayed excellent photostabilities. The complexes were taken up by *E. coli*, as shown by fractionation of the cells. Intracellular detection was done with the more emissive Eu and Tb complexes, which was greatly enhanced with the use of time-resolved mode. Complexes were found to be non-toxic to bacteria, and tests on mammalian cells showed more than 80%+ cell viabilities.

Our future goal is to develop brighter complexes by improving the sensitization efficiency and cancelling out the quenching mechanisms. We intend to create systematic studies to further study the role of PeT. We would also like to find ways to turn the brightest complexes responsive in order to develop more efficient probes.

3. Highly luminescent lanthanide complexes sensitized by tertiary amide-linked carbostyril antennae (Paper II)

To better understand the sensitization mechanism in Ln-complexes, studies that investigate relations between structural variations and luminescent properties are in great demand. In the literature, and in the previous chapter most carbostyril sensitized Ln complexes possess the same secondary amide linker. This exocyclic amide was only modified in one example before,[68] but no detailed investigations into its behavior were done. We were intrigued to see what effect an extra pendant arm will have at this position. We expected small changes in photophysics, mostly due to the removal of the quenching N-H oscillator in the linker arm, but we were clearly mistaken.

3.1 Ligand design and synthesis

To investigate the effect of exocyclic N-alkylation in DO3A-carbostyril complexes, we decided to use antennae from our previous project. We selected the 4-Me, 4-MOM, 4-CF_3, as well as the 4-Me and 3-CH_2COOEt substituted carbostyrils. The 4-Me substituted carbostyril (cs124) has been widely used, and is the only example where we can refer to a tertiary amide linked literature analogue.[68] The 4-CF_3 is well known and proved to be the best sensitizer for Eu in the carbostyril series. The MOM and ester functionalized carbostyrils carry the possibility for further functionalization, and in Chapter II they seemed to be the best sensitizers for a wide variety of lanthanides based on the lanthanide luminescence quantum yields and their ability to sensitize Dy, Sm, Nd and Yb with efficiencies that were comparable to previously reported antennae.

Before determining our synthetic strategy towards tertiary amide linked complexes, we analyzed a side-product isolated during the work described in Chapter II. We discovered that overalkylation both on the linker, and on the amide of the heterocyclic core is possible, using K_2CO_3 as a base during macrocycle alkylation (*Scheme 3.1*). This mixture of overalkylated ligands (**19a, 19b**) were studied with 2D NMR techniques. The results indicated that exocyclic amide alkylation is favored under these conditions. Further studies on

this reaction (based on UV-Vis absorption and mass analysis) revealed that it is rather the amide in the heterocyclic ring that reacts, resulting in both N- (**19a, 19b**) and O-alkylated (**20a, 20b**) ligands. The unselective formation of amides and the difficulty of their separation, encouraged us to abandon this route.

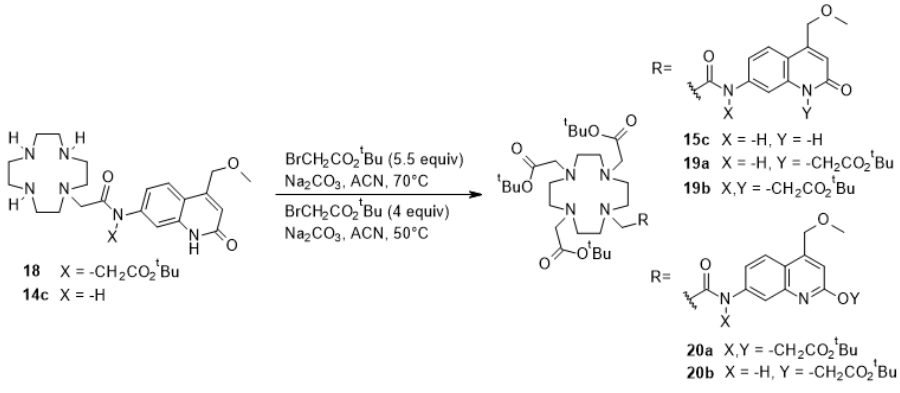

Scheme 3.1 Attempted synthetic route towards the tertiary amide linked products.

To improve the selectivity for linker alkylation, we decided to attach the carboxymethyl arm on the linker amine at the beginning (*Scheme 3.2*). We expected the primary amine to be much more nucleophilic than the carbostyril amide. Alkylation of the 7-aminocarbostyrils with *tert*-butyl bromoacetate was performed in DMF in the presence of DIPEA base. This sluggish reaction provides the N-alkylated products (**21**) in good yields only when a large excess of alkyl bromide is used. In the subsequent acylation step we had to replace the originally used Et_3N base with a less nucleophilic and more sterically hindered one (2,6-di^{t}BuPy) in order to obtain the tertiary amide products (**22**). When other nitrogen bases were used (DIPEA, DBU, 2,6-lutidine) either no reaction occurred, or significant amounts of side products were observed. During the mono-alkylation of cyclen less di- and tri-alkylated side-product formation was observed compared to the same reactions with the secondary amide analogues. This is due to the better solubilities of **22** in chloroform, which meant that less DMF co-solvent was needed to solubilize them, which in turn improved the selectivity of the reaction. Column chromatography on silica gel allowed the isolation of the pure products (**23**) in good yield. For the alkylation of the cyclen secondary amines with *tert*-butyl protected carboxymethyl arms, *tert*-butyl bromoacetate was used in DMF with DIPEA. K_2CO_3 base in refluxing ACN gave two side-products, alkylated on the heterocyclic amide (**19b**, **20a**). The only drawback to using DIPEA is that the separation of DIPEA·HBr from the product (**24**) is difficult on silica gel columns. The removal of the *tert*-butyl protective groups was done by overnight stirring in a TFA:DCM (1:1) mixture. The completion of the reaction was confirmed by LC-MS analysis. Complexation was complete after 18 h at 45 °C in EtOH:H_2O (1:1) solvent mixture. The complexes were purified on a silica gel

column. Here, it was important to keep the stationary phase short, otherwise the complex was retained on the column. The use of NH_4OH had to be avoided, because it caused the partial loss of the lanthanide ion from the complex.

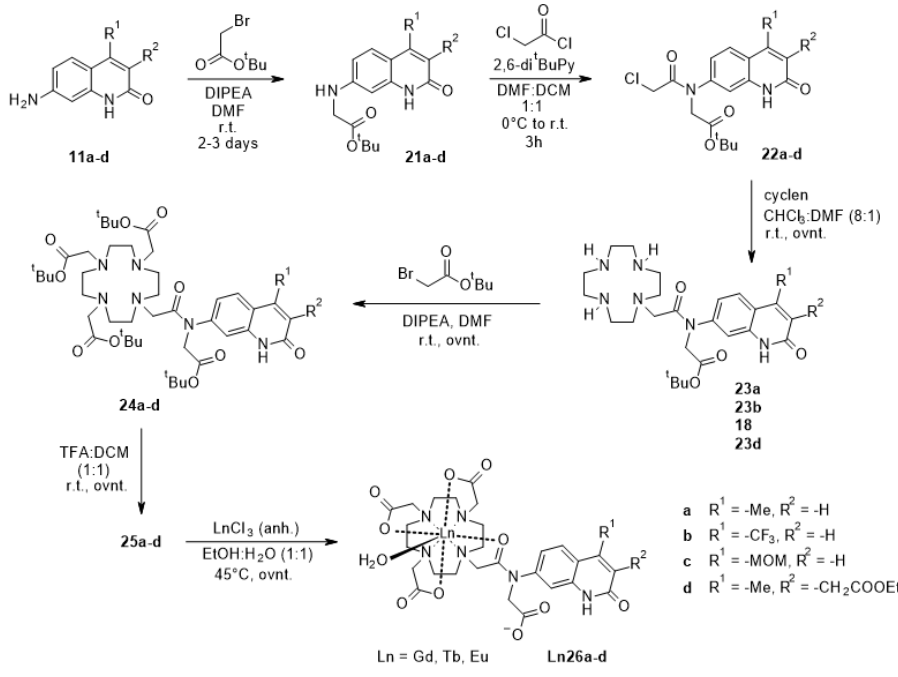

Scheme 3.2 Synthesis of the Ln complexes having and extra carboxymethyl arm on their linker amide.

3.1.1 Crystal structures

To understand the reason for the improved photophysical properties of the *N*-alkylated compared to the non-alkylated complexes, we wanted to compare their structures. Such studies can reveal differences in the antenna-lanthanide distances, antenna orientations, and complex geometries. Unfortunately, we could not obtain single crystals of the final tertiary amide linked complexes. However, the crystal structure of a precursor that already contains the antenna in the macrocycle (**23a**) might give us some insights into the antenna conformation in the final complexes. **23a** grew from a concentrated DMSO-d6 solution in an NMR tube, while **Dy17f** was grown purposefully by using the vapor diffusion method (glyme vapors into the concentrated aqueous complex solution.)

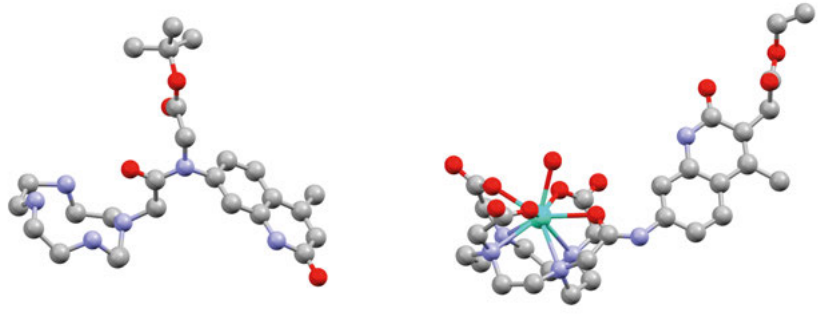

*Figure 3.1 X-ray structures of the tertiary amide linked ligand (**23a**) and the secondary amide linked Dy complex (**Dy17f**). Oxygen atoms are represented in red, nitrogen atoms in light blue, carbon atoms in gray and dysprosium in pale green.*

As shown in *Figure 3.1*, the antenna orientation differs between the Dy complex (**Dy17f**) and the tertiary amide-linked ligand (**23a**). We assume that some of the photophysical properties may be influenced by this conformational change.

The molecular geometry around the Dy ion is capped square antiprismatic. Cyclen based ligands are expected to form this type of coordination environment. The two planes formed by the four nitrogen and four oxygen donor atoms are parallel to each other. The capping oxygen atom belongs to the coordinating water molecule. The Dy-N distances were found to be between 2.600(2) and 2.657(2) Å. The negatively charged carboxylates have shorter Dy-O bond-distances (2.300(2)–2.332(2) Å) compared to the amide (2.423 Å) and the capping water (2.433 Å).

3.2 Photophysical characterization

Measurements were performed on nominally 30 μM aqueous complex solutions. Previously we found basic conditions responsible for the reversible loss of the luminescence intensity. The pH at which this occurred varied with the antennae. We suspected that an NH deprotonation on the ligand could cause such effect. With the linker alkylation we removed one of these acidic NHs, however we were wary of the acidity of the core NH (pK_a ≈ 11.6 (2-Hydroxypyridine)),[72] which is probably further lowered by the EWG in the 4-position). As a result, we decided to measure our complexes at a pH where deprotonation does not occur. Thus, the pH of the complex solutions were set to 6.5 with PIPES buffer.

During UV-Visible absorption measurements no variations of the ligand absorptions were observed with different lanthanides. Absorption spectra of

the new tertiary amide linked complexes showed a hypsochromic shift compared to their non-*N*-alkylated analogues. The electron donating ability of the negatively charged carboxymethyl group may account for the 5–6 nm change in all cases (*Table 3.1*). Similar blue-shift was observed on the ligand (residual) fluorescence of the complexes, with the exception of the 4-CF_3 substituted antenna.

Low temperature phosphorescence measurements on the Gd-complexes unveiled the antenna triplet energy levels. The summarized antenna properties of various Gd complexes are shown in *Table 3.1*.

Table 3.1

Compound	λ_{max} [nm]	λ_{em} [nm]	$E_{00}(S_1)$ [cm^{-1}]	$E_{00}(T_1)$ [cm^{-1}]	$\Delta(S_1\text{-}T_1)$ [cm^{-1}]
Gd26a	323 (–6)	364 (–2)	29 200 (+400)	23 900 (+400)	±0
Gd26b	337 (–5)	393 (+3)	27 550 (+50)	23 100 (+700)	–650
Gd26c	326 (–6)	374 (–1)	28 700 (+400)	23 900 (+400)	±0
Gd26d	326 (–5)	368 (–2)	28 900 (+300)	23 400 (+400)	–100

Tb has excited states at 20 400 cm^{-1} ($^5D_4$) and Eu at 21 500, 19 000, and 17200 cm^{-1} ($^5D_2$, $^5D_1$, $^5D_0$). The principle for achieving efficient energy transfer is to have the antenna triplet about 5 000 cm^{-1} above the receiving level in Tb. For larger gaps, the energy transfer becomes less efficient. In the case of Eu the ideal triplet level is less clear-cut, as there are several receiving levels. Furthermore, the triplet should be at least 2 500–3 500 cm^{-1} above the Ln receiving levels. If the gap is below 2 500 cm^{-1}, then thermal back energy transfer can occur to the triplet, which can result in quenching (e.g. by atmospheric oxygen) and therefore diminished lanthanide emission.

The measured triplet energies just fall into the ideal range for Tb (*Table 3.1*). The triplet energy of the CF_3 substituted antenna is close to the border, therefore we cannot exclude BET completely.

The antenna singlet and triplet energy levels increased for all new ligands, while the energy gaps between S_1-T_1 states were essentially unchanged, except for **Ln26b**. This trifluormethylated ligand now has a higher energy triplet level, compared to the non-alkylated analogue, which later turned out to be advantageous for Tb luminescence.

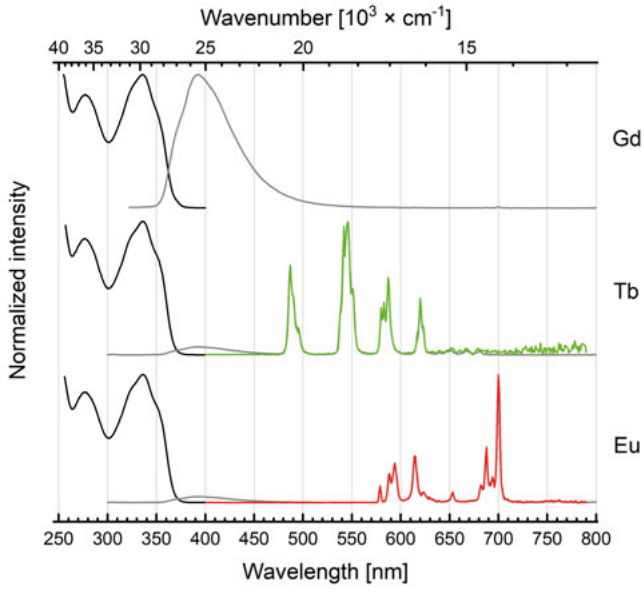

Figure 3.2 Excitation spectra of the ligand- and metal-centered emissions (black lines, left, λ_{em} = 410 (Gd), 545 (Tb), 700 nm (Eu)). Steady-state emission spectra of ***Ln26c*** *at 298K (gray lines, right, λ_{ex} = 337 nm) and time-resolved emission spectra showing the Ln-centered emissions (Tb (green)), Eu (red), colored lines, right, λ_{ex} = 337 nm). [**Ln26c**] = 30 μM, in 10 mM PIPES buffered aqueous solutions at pH 6.5.*

Different steady-state and time-resolved emission spectra are compiled in *Figure 3.2*. For complexes which contained the non-emissive Gd only typical carbostyril fluorescence was observed. The emissive Tb and Eu complexes displayed residual antenna fluorescence, along with robust Ln-centered emission. $^5D_4 \rightarrow {}^7F_J$ (J = 6-0) transitions were detected for Tb at 490, 545, 580, 620, 650, 667 and 680 nm; and the $^5D_0 \rightarrow {}^7F_J$ (J = 0-6) transitions were located at 580, 590, 615, 655, 700 nm for Eu. Excitation spectra were recorded at fixed emission wavelengths (λ_{em} = 410, 545, 700 nm). All collected excitation spectra from the residual ligand fluorescence and Ln emissions well matched with the complexes' absorption spectra. This confirms that what we see is indeed antenna sensitization.

In *Table 3.2* the obtained ligand and Ln quantum yields are compared to their secondary amide linked analogues. The measured lifetimes in H_2O and D_2O are also given, along with the calculated q values.

The ligand quantum yields in Gd complexes have slightly decreased compared to the non-*N*-alkylated analogues. We reason that a charged transfer excited state is involved in carbostyril fluorescence. Based on the crystal structures presented in 3.1.1, we can say that the tertiary amide group is less coplanar with the chromophore. Because of the worse orbital overlap, a less polar emitting state is formed upon excitation, resulting weaker antenna fluorescence.[73]

Table 3.2

Compound	Φ_L [%]	Increase X fold	Φ_{Ln} [%]	Increase X fold	τ_{H2O} [ms]	τ_{D2O} [ms]	q
Gd26a	6.8	0.88	/	/	/	/	/
Tb26a	5.9	1.1	43	1.2	1.91	3.11	0.7
Eu26a	1.5	3.0	6.0	1.9	0.65	2.18	1.0
Gd26b	3.2	0.65	/	/	/	/	/
Tb26b	3.1	0.69	16	5.3	0.7	1.34	-*
Eu26b	2.7	1.6	12	1.5	0.66	2.16	1.0
Gd26c	5.1	0.74	/	/	/	/	/
Tb26c	4.5	0.82	45	2.0	1.81	2.92	0.8
Eu26c	2.5	6.3	8.9	1.9	0.66	2.17	1.0
Gd26d	7.7	0.87	/	/	/	/	/
Tb26d	7.1	1.11	42	4.2	1.56	2.47	0.9
Eu26d	1.7	4.1	5.9	2.1	0.65	2.16	1.0

In Tb complexes singlet mediated EnT further decreases the ligand quantum yield, although this drop was at best 13%. Both Gd and Tb are among the lanthanides that are least susceptible for reduction, therefore we can exclude PeT as the cause of the reduced antenna fluorescence.

This cannot be said for Eu, which is the most reducible lanthanide. We expect the singlet energy transfer to be a minor cause for the greatly diminished ligand fluorescence. The decrease (up to 78%) should be mainly due to PeT from the antenna to Eu(III) ion. This opens up a non-radiative deactivation pathway, which will be further discussed in Chapter IV. It is worth mentioning that the Φ_L is still higher compared to the non-alkylated analogues. Probably, the extra negatively charged pendant arm has a stabilizing effect on Eu(III) resulting in less efficient PeT quenching, or the altered conformation promotes EnT over PeT.[74]

In every case the tertiary amide linked carbostyrils led to increased Tb and Eu luminescence. Tb quantum yields all surpass 40%, with just only one exception. The 4-CF_3 substituted antenna is known for being a weak sensitizer for Tb, but here as high as 16% metal quantum yield was achieved. This is a 5.3 times higher value than in the non-N alkylated analogue. The Eu quantum yields doubled compared to the secondary amide linked analogues, however the highest value still barely exceeds 10%, making Eu less emissive than Tb in this ligand system.

The coordination environment has not changed with the addition of the extra carboxymethyl arm. There are multiple pieces of evidence which support this statement: CV measurements, the unchanged Eu spectral fingerprint, and the calculated q values. The latter was determined using the measured luminescence lifetimes. For the hydration numbers in the Eu complexes we obtained q = 1.0, and in the Tb complexes q = 0.7-0.9. The slightly smaller q value in Tb complexes can be explained by its smaller size compared to Eu ($r_{Ln^{3+}}$ = 0.947 Å (Eu) vs 0.923 Å (Tb)).[75] 4-CF_3 antenna has a low lying

triplet energy level, which allows back energy transfer from the excited Tb, therefore the calculated q value in this case is meaningless.

Intrinsic quantum yields were determined from the Eu observed and radiative lifetimes the. Within the experimental error of the quantum yield and lifetime measurements (10%), the same intrinsic quantum yields were obtained for all Eu complexes (12%). This value is slightly higher compared to what was found in the non-alkylated analogues. The removal of one NH oscillator from the proximity of the Ln could have this effect.

The intrinsic quantum yields can give further information about the sensitization efficiencies. With the alkylation η_{sens} became 1.4–1.9 times higher, which explains the higher quantum yields in the tertiary amide linked complexes. To find the responsible parameter, η_{sens} has to be further analyzed. It has two main components: the population of the triplet state and the efficiency of the energy transfer process. Presumably the intersystem crossing which populates the triplet state was only marginally affected by heavy atom effects (larger N-alkyl group), while the S_1-T_1 energy gap seemed to be largely unchanged (*Table 3.1*, with the exception of **Gd26b**). For these reasons we cannot significantly attribute the large fluorescence enhancement to the change in ISC. The energy transfer process might have been influenced by the blue shift, which allows better overlap between the antenna and Ln energy levels. It is hard to draw reliable conclusions about the orientation factors and donor-acceptor distance in solution. However, the orientation factors are likely influenced by the tertiary amide linker, since it has larger rotational energy barrier around the C-N bond. We also observed orientation differences in our crystal structures, but as it was mentioned, static and dynamic conditions are clearly different.

3.3 Conclusion

We have prepared 12 new DO3A based lanthanide complexes with four different carbostyril antennae. The linker was structurally modified by attaching an extra carboxymethyl arm. This small intended change resulted in tertiary amide linked complexes, which were readily compared with their secondary amide analogues. The new structure greatly enhances both Tb and Eu luminescence, while keeping the same hydration state.

There are several factors which could contribute to the improved photophysics. Detailed analysis of the Eu complexes revealed that the sensitization efficiency drastically increased in the new complexes. Removal of an NH oscillator from the close coordination sphere increased the intrinsic quantum yield. Better overlap was achieved with the higher energy triplet levels, which was beneficial for energy transfer, especially in the case of Tb. The intersystem crossing is likely to be slightly promoted by the extra methyl-carboxylate group. This substitution also altered the antenna orientation in the solid state, however factors like distance and orientation are hard to predict in a dynamic environment.

4. Photoinduced electron transfer in Europium and Ytterbium complexes (Paper III)

Based on the result in Chapter II and a literature overview, we propose that PeT indeed plays an important role in the luminescence of redox positive ($E_{1/2}$ > –2.0 V vs NHE) lanthanide ions. In this chapter an in-depth study is discussed, which tries to estimate the contribution of PeT in Europium and Ytterbium complexes, and the evaluation of strategies for eliminating its detrimental effects.

4.1 Literature overview of photoinduced electron transfer in lanthanide complexes

PeT can appear in different contexts when Ln complexes are discussed.[11] Most literature examples describe the quenching of the antenna excited state by an external quencher,[20, 76] or by a remote quencher on the antenna.[19] These electron transfer phenomena form the basis of responsive Ln probes. Another PeT mechanism was identified in 2-(2-pyridyl)benzimidazole-bound Nd complexes that were decorated with an anthracene pendent group.[11, 77] Anthracene excitation was followed by electron transfer to the electron-poor pyridylbenzimidazole. Charge recombination yielded anthracene in its triplet excited state, which sensitized Nd emission. The alternative mechanism involving rapid intersystem crossing of the anthracene in the Nd complex, followed by energy transfer to the lanthanide could be ruled out, as anthracene fluorescence was quenched in the presence of all tested metal ions, including those of Zn^{2+} and Gd^{3+}.

The ligand to metal electron transfer was experimentally confirmed by Horrocks.[12] Upon exciting tryptophan residues at 289 nm in an Yb containing protein, Yb-centered NIR emission was detected. The quenching of tryptophan fluorescence was seen only in proteins loaded with redox positive Yb and Eu, while other lanthanides had no such effect. An LMCT band was neither seen for Yb, nor Eu in that system. This led to the recognition of the electron transfer process.

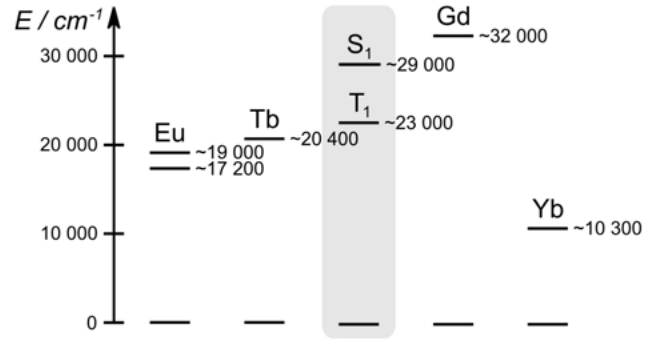

Figure 4.1 Energy level diagram of the sensitizer carbostyril (gray area, middle) and of four Lns: Eu, Tb, Gd, Yb.

The energy level diagram of Eu, Tb, Gd, and Yb is represented in *Figure 4.1*. In the middle the singlet and triplet energy levels of the UV absorbing chromophore (in this case carbostyril) are depicted. The spectral overlap between the chromophore and lanthanide is essential for energy transfer, and directly proportional to its efficiency. Singlet and triplet-mediated EnT is possible for both Eu and Tb. Gd on the other hand has too high-lying energy levels, which therefore are inaccessible in this system. Yb has a single spectroscopic level at around 10 300 cm^{-1}, which is too low for spectral integral overlap with any states of the given chromophore (lowest energy triplet transition was found for **Gd17d** at 15 700 cm^{-1}).

The driving force towards Ln(II) formation in any given antenna-Ln pair can be calculated by using Eq. 1 in Section 2.2.2. The resulting charge separated state consists of a strongly oxidizing antenna radical cation and a fairly reducing Ln^{2+}. A fast recombination is very plausible, for which Horrocks's calculations show that in his system.[12] the ΔG value is higher than the $^2F_{5/2}$ state in Yb and lower than the $^5D_0$ state in Eu. Back electron transfer ultimately returns the initial antenna-Ln ground state in both cases. However in the case of Yb, a fraction of the back electron transfer first yields the excited state Yb, from where the ground state is reached through radiative or non-radiative decay. Calculations for Horrocks's tryptophan- and our carbostyril-Ln systems suggest that PeT quenches Eu, and promotes Yb luminescence (*Figure 4.2*).

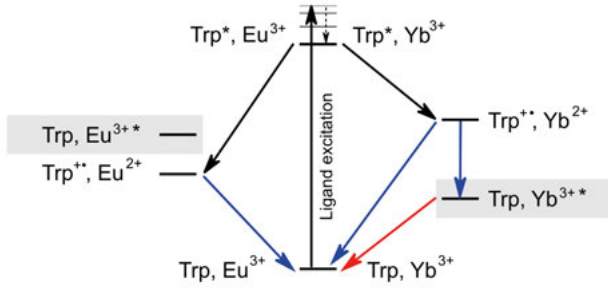

Figure 4.2 Proposed electron transfer mechanism between tryptophan and two Lns (Eu, Yb). Black arrows: electron transfer, blue arrows: back electron transfer, red arrow: Yb emission. Picture was redrawn from reference [12].

The contribution of PeT in Ln complexes, can be controlled either by changing the Ln-antenna distance, by tuning the redox properties of the antenna, or by modulating the Ln(III)/Ln(II) redox potential values.

The feasibility of the first approach is supported by results presented in Chapter II. When longer triazole linked antennae were used for the sensitization of Lns, PeT was not playing a role; however, a longer distance will result in less efficient EnT. PeT and energy transfer have different distance dependencies,[10] therefore, there may be a "sweet spot" when the contribution of PeT is minimal but the EnT is reasonably effective. This approach necessarily results in less emissive Ln complexes, and is thus not suitable for obtaining bright emitters.

Modulating the redox properties of the antenna could minimize PeT. An electron poor chromophore is less likely to give up an electron, therefore it would not participate in PeT. The redox properties can be adjusted by the installation of electron donating or withdrawing groups on the chromophore. By doing so the antenna singlet and triplet energy levels are also likely to be shifted, and the difficulties in predicting the effect of these changes complicates the design.[59c] A good example is Williams' study, wherein phenanthrolidine sensitized complexes were studied. A small structural change on the antenna (N-protonation) decreased the electron density of the sensitizer. The triplet and singlet energies were slightly lowered but were still considerably higher compared to $^5D_0$ receiving level. Eu lifetimes were unaffected, while both ligand residual and metal fluorescence increased threefold in the protonated complex. This increase was attributed to the suppressed PeT from the ligand singlet to the Eu.[78] The disadvantage of this approach is that it alters the singlet and triplet energy levels of the antenna, therefore the energy transfer may be affected.[78]

The third way to modulate PeT is to tune the redox properties of the metal center. This strategy has not yet been explored purposefully, presumably because Ln(III) ion redox potentials are not considered consequential in the luminescent lanthanide community. Due to the shielded valance shells from the

surrounding ligand environment in f-elements, variations in redox values are expected to be small. The development of MRI active Eu(II) complexes pushed the Eu(III)/Eu(II) redox potential further to more positive values.[26a, 26c, 26e, 79] With this, a 1.4 V difference was achieved compared to the most negative reported value.[80] The stabilization of the less stable +II state was accomplished by the installation of soft donor atoms in the ligand framework, and by the adjustment of the ligand cavity size. For Ce(IV)/Ce(III), the same effect was observed: soft donor ligands favor the softer +III state.[81] It is noteworthy that recently the opposite strategy, i.e. by encapsulation into a negatively charged ligand displaying hard donor atoms enabled the isolation and study of Bk(IV).[82]

In *Figure 4.3* a selection of Eu(III)/Eu(II) redox couples with different multidentate ligands are compiled. The harder Eu(III) cation is better stabilized by polyaminocarboxylate ligands. Highly negatively charged ligands are better at stabilizing Eu(III). Even though the overall charge is the same in **29** as in **30**, the directly coordinating softer amide oxygens in **30** have a less stabilizing effect on Eu(III) compared to the harder carboxylate oxygens in **29**. The same rules apply to cryptands. Additionally, the smaller cavity stabilizes the +III oxidation state as it has a smaller ionic radius (r = 0.947 Å (Eu^{III}) vs 1.17 Å (Eu^{II})).[75] This is represented by the differences between the redox couples of **32** and **33**.

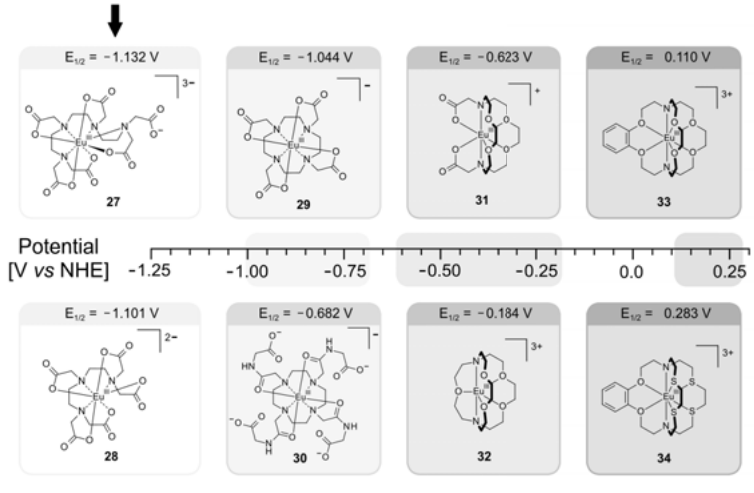

Figure 4.3 Eu(III)/Eu(II) redox potentials in different multidentate ligand environments in water. The originally determined values were calculated versus NHE to enable comparison.

There are only a few examples in the literature where redox potential differences can be correlated with luminescent properties. However, in these complexes changes in the luminescence were not explicitly linked to changes in redox potential, and because of the lack of electrochemical data such correlations are tentative. In Selvin's study, where a soft amine N-donor was replaced

with an anionic O-donor in the macrocyclic framework, correlations might be found.[83] DTPA and DOTA frameworks were equipped with the same carbostyril antenna and linker. It is important to mention that in these complex pairs the sensitization mechanism and efficiency must have been identical because of the identical Ln-antenna distances and orientations, and they possess the same number of O-H, N-H oscillators around the binding site (q = 1). This was supported by the same lifetime and quantum yield for Tb in these ligands. However, in the case of Eu while the lifetime remained unchanged, the quantum yield almost doubled for the overall negatively charged complex. This result supports a PeT quenching in the less charged Eu complex.

In order to observe and evaluate PeT, we designed complexes relying on the third approach. Complexes with the same hydration state and antenna were needed. The distance between the metal and the sensitizer was kept constant using the same linker. For chelation, cyclen and triazanonane were used, yielding two sets of complexes which are discussed based on the macrocyclic part.

4.2 Preliminary results

Encouraged by our literature findings we decided to carry out a quick study of 3 complex pairs. In one pair the Eu is either chelated with the hard donor carboxylates (from Chapter II) or soft donor carboxamides, while having the same carbostyril antenna (*Figure 4.4*). It is important to mention that the complexes keep their donor-acceptor distance and hydration states.

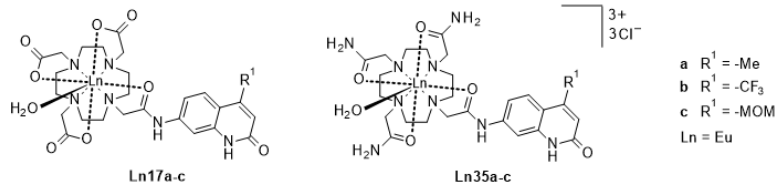

Figure 4.4 Structure of the hard and soft donor chelated lanthanide complex pairs.

4.2.1 Photophysics and electrochemistry of Eu complexes

The photophysical measurements were performed in unbuffered and PIPES buffered (10 mM, pH 6.5) aqueous solutions. Cyclic voltammetry was done in aqueous solutions (pH 6.5) using LiCl (0.1 M) as an electrolyte. The scan rate was 0.05 V/s. Results are shown in *Table 4.1*.

The voltammograms show a single redox event in all cases. Sometimes we observed an additional redox event, which was identified as free $EuCl_{3(aq)}$ by control experiments. This additional free Eu comes from the complexation reaction where excess Ln salt was used. Purification by column chromatography

did not always completely remove the excess Ln salt, which explains the variable amounts of this contaminant in each sample. There are minor differences between the $E_{1/2}$ values within the triamide complexes, but they are in the same range. Thus, changes of substituent on the antenna do not affect the half-wave potential. For this reason, only one triacid complex was measured. Its half-wave potential is –852 mV vs NHE, and is ~0.3 V more negative than for the triamide complexes, indicating the stabilization of the Eu(III) redox state.

Table 4.1.

Compound	Φ_L [%]	Φ_{Eu} [%]	$E_{1/2}$ [mV vs NHE]	ΔE [mV]	q
$EuCl_3$	-	-	-380	155	-
Eu17a	0.5	3.1	n.d.	n.d.	1.0
Eu35a	0.1	0.3	-562	316	0.7
Eu17c	0.6	3.9	-856	185	1.0
Eu35c	0.1	1.2	-551	160	0.9
Eu17b	1.7	7.9	n.d.	n.d.	1.0
Eu35b	0.4	3.1	-576	316	0.8

PeT quenches both ligand and Eu fluorescence emission. The diminished ligand fluorescence is probably solely caused by PeT in these complexes. Φ_L decreased drastically in each complex pair upon going from the triacid to the triamide framework. A slightly larger drop was found for the 4-Me substituted antenna (80%) than for the less reducing 4-CF_3 substituted antenna (75% drop). Eu luminescence was not only quenched by PeT, but also by the newly introduced NH oscillators in the proximity of the Eu. However, their overall effect can be expected to be comparable in the triamide complexes (identical number of NH in each complex). Only 10, 30 and 40% of the original Eu emission was retained in the triamide complexes (Me (**Eu35a**), MOM (**Eu35c**), CF_3 (**Eu35b**) respectively). This trend follows the reducing power of the antenna, but quantification is not possible while NH quenching is present.

4.2.2 Results with external fluoride

The addition of an external fluoride anion is the most straightforward way of proving the PeT quenching of the ligand. Upon addition of 100 mM KF to the **Eu35c** containing solution, the capping water molecule is replaced by the better coordinating, hard and compact F^- anion. This yields only a minor change in the structure but has significant effect in the luminescent properties. The coordinating fluoride shifts the Eu redox potential more to the negative,[84] and changes the overall complex charge from +3 to +2.

We have more than one piece of evidence that F^- coordinates. First, the Eu emission spectra changed when fluoride was added. Both the shape and intensity varied among the different transitions, involving the hypersensitive peak (J = 2). These changes imply an alteration of the inner coordination sphere. Then, we could grow single crystals of the fluoride-bound complex (*Figure 4.5*).

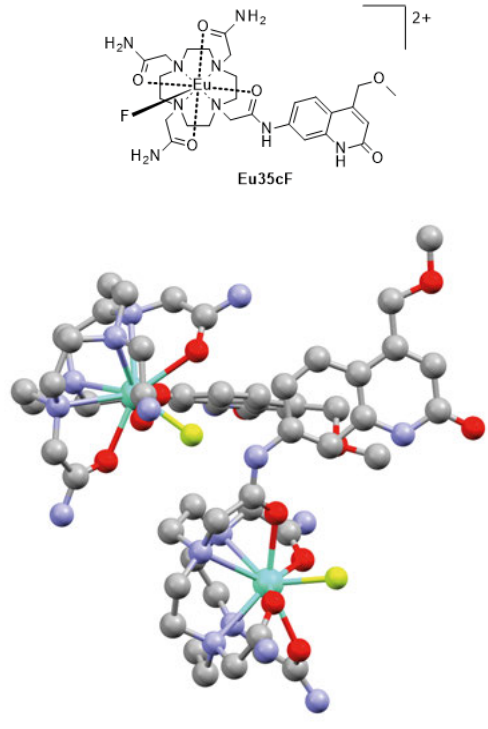

Figure 4.5 Crystal structure of the fluoride containing Eu-complex. The chemical structure is shown above for clarity. Oxygen atoms are represented in red, nitrogen atoms in light blue, carbon atoms in gray, europium in pale green, and fluorine atoms in yellow.

Since we have crystal structures of a Eu complex coordinating to a water (*Figure 5.1*), we can compare the bond distances between the Eu and the capping atoms. The Eu(III)-F distance was 2.221–2.234 Å, while the Eu(III)-OH_2 distance was significantly longer, 2.467 Å.

By comparing the results in *Table 4.2*, we can see that upon addition of fluoride the ligand quantum yield doubled from 0.18% to 0.36%. At the same time Φ_{Ln} increased 7-fold, due to a combination of two effects. First, the coordinating fluoride removed the water with its two OH oscillators. Second, the harder donor lowered the Eu(III)/Eu(II) redox potential, thus stabilizing the Eu(III) state, which became less prone to take an electron from the excited antenna. Fluoride also raised the Eu lifetime in water from 0.5 ms to 0.98 ms.

Table 4.2

Compound	Φ_L [ms]	Φ_{Ln} [ms]	τ_{H2O} [ms]
Gd35c	6.3	/	/
Eu35c	0.18	1.1	0.50
Eu35c + 100 mM F^-	0.36	7.1	0.98

4.3 Cyclen based complexes

Changing the chelating arms on the macrocyclic ligand alters the Lewis basicity of the coordinating O-atoms. Replacing carboxylate with an amide increases the overall charge of the complex, which is expected to make the Ln(III) more likely to accept an electron. In this section, the synthetic routes towards the neutral, +1, +2 and +3 complexes are presented. Later, their photophysical characterization is described.

4.3.1 Synthesis

The synthesis of the neutral complexes has already been discussed in Chapter II (see *Scheme 2.2*).

The overall +1 charged complexes have two carboxylic acid and two amide arms. Their synthesis (*Scheme 4.1*) starts with the preparation of 1,7-bis(t-butoxycarbonylmethyl)-1,4,7,10-tetraazadodecane (DO2A-t-Bu ester, **38**). This compound is a widely used building block for metal complexes, and its synthesis is well established.[85] Allen reported an optimized procedure in 2014, which provides this key intermediate in shortened reaction times compared to the existing methods.[86] The trans-protection of the cyclen is the first step, and remains selective even under reflux conditions. In the second step, the amount of base turned out to be crucial to drive the reaction towards completion. In Allen's report the third deprotection step is carried out under microwave irradiation; however, when large quantities are handled the reaction must be set up in several batches. Therefore, we decided to perform the transfer hydrogenation under conventional thermal conditions. The desired product formed overnight in very good yields, but column chromatography was needed to ensure good purity.

Attaching only one antenna to the cyclen works when only up to 0.5 equivalents of **12c** is used. This step usually requires multiple chromatographic steps to separate the excess unreacted starting material from the product (**39**). The final alkylation step is conducted using a slight excess of the alkyl bromide. When larger excess and longer reaction times are used alkylation on the amide nitrogen in the carbostyril core may occur, making purification tedious.

The deprotection in TFA:DCM mixture forms the free ligand **41**. The replacement of the carboxylate arms with amides exclude silica stationary phases from the purification options, therefore alumina or reversed phase columns can only be used at this step. Complexation provides the overall +1 charged complex with chloride as a counteranion (**Ln42**).

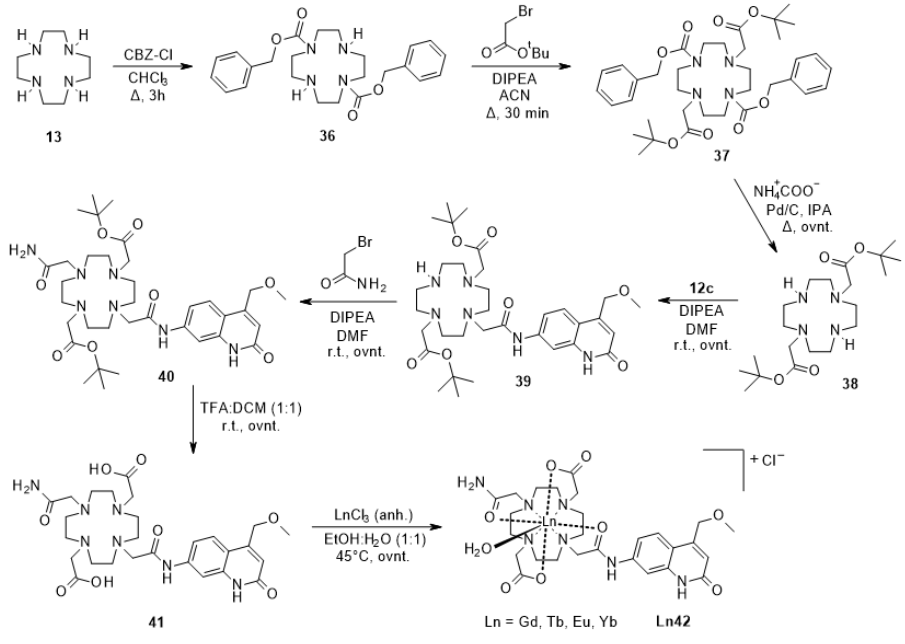

Scheme 4.1 Synthesis of the +1 charged cyclen complexes.

For the charged complexes (*Scheme 4.2*) we prepared another key intermediate as we were unsure if we could remove the CBZ protecting groups while keeping the antenna intact, and if the DO2-Amide analogue **38** could be prepared and purified. Thus, we chose diBoc-cyclen as the starting point (**43**). Initially, we tried to prepare **43** using 2 equivalents of Boc-anhydride, but only small quantities of **43** were isolated, together with the tri- and monoprotected cyclen. Literature methods rely on the use of Boc-OSu,[87] which exclusively delivers the trans-protected **43**. These literature procedures do not mention chromatographic purification. However, we observed the cleavage of one Boc group upon extraction of the reaction mixture with 3M NaOH solution. **43** was monoalkylated with **12c** to give **44**. It is noteworthy that already 0.4 equivalents of the chloroacetylated antenna yields substantial amounts of the fully alkylated cyclen. A lengthy purification on a silica column enabled the separation of the product from the excess starting material and the dialkylated side-product. Alkylation with ethyl bromoacetate gave **45**. Selective deprotection of the macrocyclic amines was achieved by TFA:DCM (1:1) mixture (**46**). A second alkylation with 2-bromoacetamide afforded **47**. Deprotection under basic conditions (3 equiv. NaOH in ACN:H_2O (1:1)) gave the free ligand (**48**), which

was then treated with lanthanide chlorides to give the +2 charged complexes with 2 chloride anions (**Ln49**).

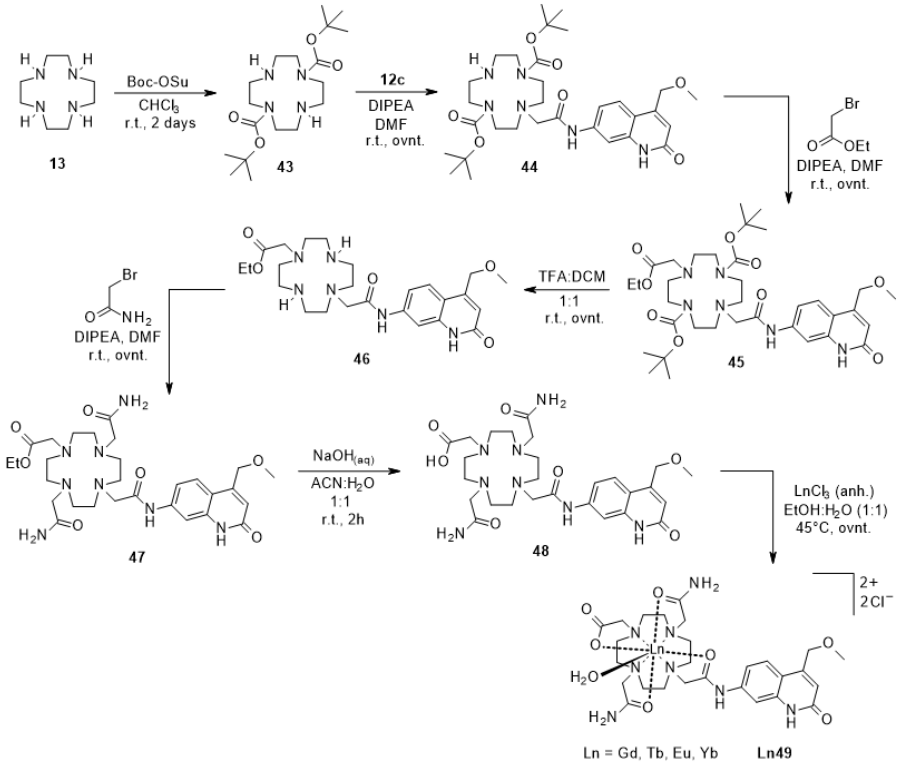

Scheme 4.2 Synthesis of the +2 charged cyclen complexes.

The preparation of the +3 charged complexes is shown in *Scheme 4.3*. The synthesis is analogous to those of the neutral complexes. Monoalkylated **14c** is alkylated with arms carrying different (primary, secondary, tertiary) amides. After purification these amide containing ligands (**50a**, **50Me**, **50diMe**) can be readily used for chelation.

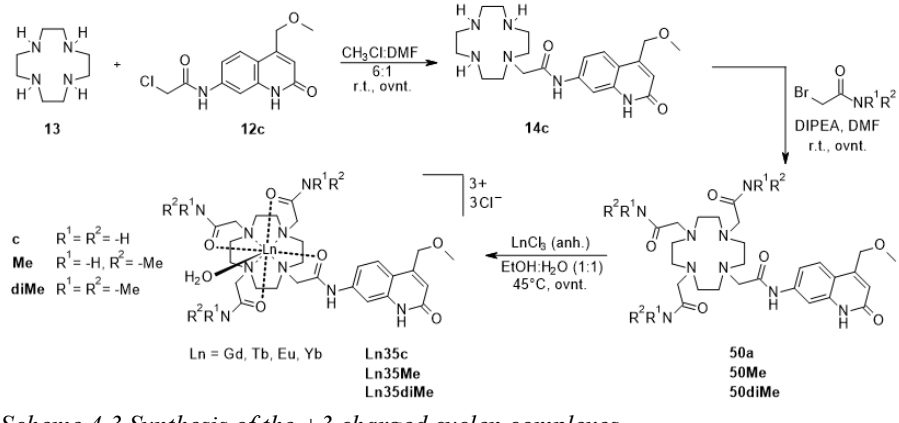

Scheme 4.3 Synthesis of the +3 charged cyclen complexes.

4.3.2 Photophysical characterization

Measurements were performed on 10 μM complex solutions in 0.01 M PIPES buffered aqueous solution at pH 6.5. The absorption spectra were identical for all complexes. Only a small absorption growth was observed in the region from 270–315 nm, which was increasing with the increasing number of amide arms on the complexes. Because of this, for fluorescence measurements λ_{ex} > 320 nm was used.

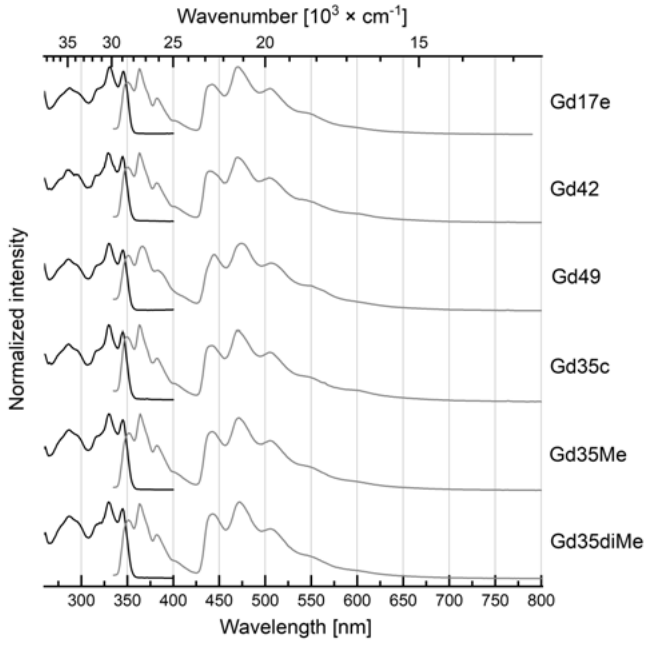

Figure 4.6 Excitation spectra of the ligand centered phosphorescence emissions (black lines, left, λ_{em} = 442 nm). Steady-state emission spectra (gray lines, right) at λ_{ex} = 330 nm of the Gd-complexes (30 μM) at 77K with 10% glycerol added to the 10 μM, PIPES buffered aqueous solutions 0.01 M, pH 6.5.

Low temperature phosphorescence measurements on the Gd-complexes revealed the antenna triplet states. Energy levels were identical in all cases, which is expected, as they carry the same antenna (*Figure 4.6*). Only minor differences were observed, such as shifts in peak maxima by 1–2 nm and small intensity changes between transitions. The former can be ascribed to instrumental error. The latter is probably due to thermal irregularities during the measurement. The antenna triplet is at 22 600(±100) cm^{-1}.

The stepwise replacement of the carboxylate arms by amides in the Gd complexes resulted in changes in the ligand fluorescence (*Table 4.3*). With the increasing number of amides the antenna quantum yields were decreased gradually (by ~0.2% for each new amide). A possible explanation could be vibrational quenching of the excited chromophore via NH oscillators. If this hypothesis was true then the emission intensity should recover upon replacement

of the hydrogens with methyl groups in the amides. However, very similar Φ_L values were obtained for all amides (non-, mono-, and dimethylated) which suggest that this explanation is not sufficient. Another possibility could be the altered electronics of the antenna which would be caused by the changed Lewis acidity of the metal. The amides increase the Lewis acidity of the Ln, which therefore withdraws electrons through the 7-amido group of the antenna. Because of the smaller push-pull effect the photophysics of the antenna slightly changes.

The degree of singlet energy transfer was equal for the differently charged Tb complexes, and resulted in a 25% decrease in the ligand fluorescence compared to their Gd analogues. The relative Φ_L ratios of the Tb complexes showed the same trend as seen in the Gd complexes. The increasing amount of carboxamide groups gradually diminished the Φ_L.

Table 4.3

Compound	Overall charge	Abs. Φ_L [%]	Rel. Φ_L [%]	Abs. Φ_{Ln} [%]	Rel. Φ_{Ln} [%]	τ_{H2O} [ms]	τ_{D2O} [ms]	q
Gd17e	0	7.21	100	/	/	/	/	/
Gd42	+1	7.01	97.2	/	/	/	/	/
Gd49	+2	6.81	94.5	/	/	/	/	/
Gd35c	+3	6.52	90.5	/	/	/	/	/
Gd35Me	+3	6.36	88.2	/	/	/	/	/
Gd35diMe	+3	6.45	89.5	/	/	/	/	/
Tb17e	0	5.39	100	27.6	100	1.07	1.49	1.02
Tb42	+1	5.25	97.4	27.2	98.6	1.04	1.50	1.17
Tb49	+2	5.06	93.9	26.4	95.7	0.972	1.43	1.35
Tb35c	+3	4.84	89.7	26.0	94.1	0.956	1.33	1.17
Tb35Me	+3	4.87	90.4	25.7	93.1	0.983	1.41	1.24
Tb35diMe	+3	4.87	90.4	27.7	100	1.01	1.32	0.86
Eu17e	0	0.32	100	5.07	100	0.605	2.16	1.04
Eu42	+1	0.20	62.4	3.64	71.8	0.572	2.01	0.93
Eu49	+2	0.10	32.3	2.59	51.1	0.522	1.79	0.88
Eu35c	+3	0.15	45.5	1.03	20.3	0.439	1.25	0.84
Eu35Me	+3	0.09	29.4	1.63	32.1	0.498	1.45	0.92
Eu35diMe	+3	0.20	63.0	2.89	57.0	0.549	1.40	0.94
Yb17e	0	5.92	100	/	/	/	/	/
Yb42	+1	5.48	92.6	/	/	/	/	/
Yb49	+2	4.36	73.6	/	/	/	/	/
Yb35c	+3	3.03	51.2	/	/	/	/	/
YbMe	+3	3.39	57.3	/	/	/	/	/
YbdiMe	+3	4.35	73.5	/	/	/	/	/

Eu complexes show larger differences in their ligand fluorescence. First of all, these data need to be analyzed carefully because of the larger error in the low quantum yields (smaller S/N ratio). On the other hand, it is clear that the previous relative Φ_L ratios (which were identical within the Gd and Tb series) now have changed for the Eu series. Φ_L drastically decreases when the charge

of the complex increases. There are also large differences depending on amide substitutions. This means that in comparison to Tb and Gd there is an additional ligand fluorescence quenching which is due to the Eu. When Eu is compared to Tb and Gd, the most significant difference is in their redox potential. The reduction of Eu(III) by the excited antenna being easier, PeT from the antenna to the Eu ion may be involved here and would explain the lower ligand fluorescence observed.

The absolute Φ_{Tb} suffered a 1–2% drop because of the weak quenching effect of NH oscillators; this effect was largely additive. The only exception was **Tb35Me** for which the lowest value was obtained. Both non-NH containing ligands (**Tb17e** and **Tb35diMe**) resulted identical Tb quantum yields. This could reflect the relative insensitivity of the Tb excited state to NH quenching.

Eu luminescence underwent a more pronounced diminution because of the NH oscillators. The **Eu35c** exhibits only 20% of the **Eu17e** luminescence, which is not surprising as it has 6 more amide NH oscillators in the first coordination sphere of the Eu. For Tb, the elimination of NH-s by substitution with methyl groups yielded the same Tb luminescence as in the triacid analogue. Here Φ_{Eu} in **Eu35diMe** is only 60% of the Φ_{Eu} in **Eu17e**. The quenching by the newly introduced CH oscillators should be small. Experiments with deuterated complexes show that only sufficiently close (3.5–4.5 Å) C-H vibrations can quench the excited state of Eu.[88] In our complexes the dimethylamide CHs are at least 7 Å from the metal. Therefore, the 40% decrease in Φ_{Eu} in **Eu35diMe** compared to **Eu17e** cannot come from CH quenching (Note: the relative Φ_{Eu} difference is also 40% between the **Eu35c** and **Eu35diMe**). Thus, we attribute the 40% difference between **Eu17e** and **Eu35diMe** to more efficient PeT in the +3 charged complexes.

The correlation between the number of NH oscillators and Tb luminescent lifetimes follows the trend expected based on the NH quenching effect. The Tb excited state on the other hand couples better with the overtone of the O-D frequency, and instead of considerably longer luminescent lifetimes only a slight increase can be observed. There are a few examples when X-H deuteration to X-D does not result improved photophysics. For example, Tb (which has a large energy gap between its $^5D_4$ emissive and $^7F_0$ ground level) is quite insensitive to ligand deuteration.[89] It has been suggested that C-H deuteration may accelerate quenching Tb complexes, although this effect would be within the experimental error.[88] C-D oscillators in Pr cryptates however have proven to be better quenchers than the C-H ones.[90]

Europium on the other hand couples well with X-H vibrational modes and also has smaller energy gap between its emissive and ground state. The more pronounced X-H quenching results in larger differences in the measured Eu lifetimes in water for the differently charged complexes. A 3-4 fold increase in lifetimes was recorded in heavy water, due to the inefficient coupling of the $^5D_0$ level with the O-D modes.

The hydration state of the complexes was calculated according to the refined Horrock's method, which takes NH vibrations into account.[88] Lifetime measurements have 10% experimental error, furthermore, the equations were calibrated for hydrophilic complexes. Therefore, q should be handled with caution, and is usually considered to carry 20% error.[24] If the calculated numbers are fractions, that suggests the presence of differently hydrated species.

Each lifetime was measured at least 3 times and an average value was used for calculation. In the case of Tb the calculated q numbers are around q = 1, and in some cases the obtained values differ by more than the experimental error. We found previously (in Chapter II) that in some cases antenna-dependent quenching processes can cause large deviations and render the model inapplicable. In Eu complexes the q values were closer to 1.0, and mostly within the limits given by the experimental error. Overall, we can conclude that hydration states are similar in all complexes, and the major species in solution are the ones wherein the lanthanide coordinates to 1 water molecule.

Table 4.4.

Compound	Overall charge	τ_{rad} [ms]	τ_{obs} [ms]	Φ_{Eu}^{Eu} [%]	η_{sens} [%]
Eu17e	0	5.14	0.605	11.8	43.0
Eu42	+1	5.14	0.572	11.1	32.8
Eu49	+2	4.93	0.522	10.6	24.4
Eu35c	+3	4.96	0.439	8.85	11.6
Eu35Me	+3	5.11	0.498	9.75	16.7
Eu35diMe	+3	4.91	0.549	11.2	25.8

The Eu radiative lifetimes were calculated for each Eu complex according to ref. [15] (*Table 4.4*). Values were found to be around 5 ms and quite similar in all complexes. The observed lifetimes on the other hand varied to a larger degree. The NH and other quenching effects are influencing the observed lifetimes, and therefore we expect to see their effect in the intrinsic quantum yields and sensitization efficiencies, too. While the intrinsic quantum yields suffered an up to 3% decrease while going from the neutral to the +3 charged complexes, the removal of the NH quenchers in the +3 charged complexes almost brought back the intrinsic quantum yield to its initial value, which differed by only 0.6%. The sensitization efficiencies gradually decreased with increasing overall charge of the complex. A 30% difference was found between the triacid and the triamide complex. Again, η_{sens} can be restored to some extent by removing the NH quenchers from the first coordination sphere.

We further investigated the effect of fluoride on the Eu complexes, because we were interested in how well and at which point the fluoride coordinates to the Ln. In neutral complexes the positive charge of Eu(III) is well balanced by the three negatively charged carboxylates, and one could expect only limited interaction with the fluoride. We compared the emission spectra of **Eu17e** in the presence and absence of F^- anion. Indeed, only minor changes were found on the Eu spectral fingerprint, which suggests very weak interaction with fluoride (*Figure 4.7*). On the other hand, recently we obtained crystal structures of neutral Ln complexes from a solution containing F^-. The complexes have a capping F^- rather than the more abundant water oxygen.

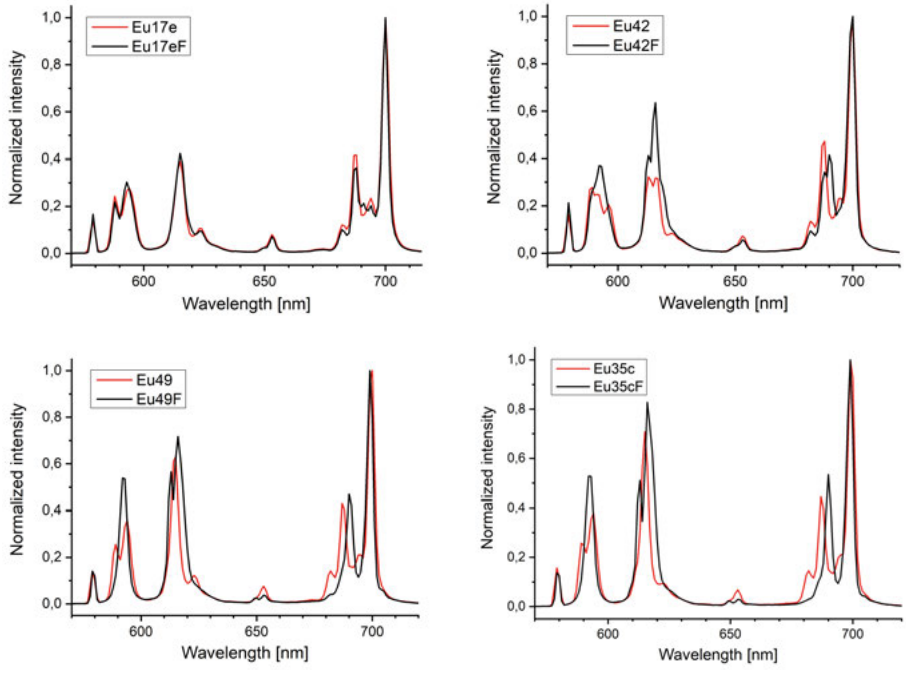

Figure 4.7 Eu spectral changes in the differently charged Eu-complexes upon fluoride addition. (neutral – top left, +1 – top right, +2 – bottom left, +3 – bottom right.

With the increasing overall charge of the complexes, the coordination becomes stronger with fluoride. This is supported by the spectra in *Figure 4.7*, where intensity changes were observed in the $J = 2$, 4 transitions. Also, the splitting of the Eu ($^5D_0 \rightarrow {}^7F_1$) transition gives useful information about the symmetry of the system.[91] If the $J = 1$ transition displays 1 peak (no splitting) the symmetry is high. In complexes having axial symmetry splits the transition often into 2 peaks, and low symmetry complexes give a splitting of 3. Our Eu complexes have axial symmetry, except for the +1 charged one, which shows the highest number of splitting suggesting a different coordination mode. It is clear from the spectra that when fluoride replaces the capping water the symmetry increases (decreased splitting of the $^7F_1$ level).[91]

Fluoride coordination could further be probed by measuring the Eu emission lifetimes. An increase in luminescent lifetime is in accordance with a lower number of directly coordinating OH oscillators.
Both ligand and Eu quantum yields were measured in the presence of 100 mM fluoride concentration (*Table 4.5*). Comparison of the results to the water capped Eu complexes reveals that fluoride has a general fluorescence enhancing effect. The largest increase in ligand fluorescence was calculated for the +2 and +3 charged complexes, which can be explained by the reduced PeT quenching of the antenna. Before, we reasoned that X-H vibrations might have a detrimental effect on the ligand fluorescence, but this effect cannot be strong. Even though we are analyzing small quantum yield values here, it would be surprising if a 2–3 fold increase in Φ_L was caused by the partial removal of a coordinated H_2O.

Table 4.5.

Compound (charge)	Φ_L	Φ_L +F^-	Increase X fold	Φ_{Eu}	Φ_{Eu} +F^-	Increase X fold
	[%]	[%]		[%]	[%]	
Eu17e (0)	0.32	0.39	1.22	5.07	5.80	1.14
Eu42 (+1)	0.20	0.36	1.80	3.64	6.20	1.70
Eu49 (+2)	0.10	0.34	3.40	2.59	8.35	3.22
Eu35c (+3)	0.15	0.31	2.07	1.03	7.58	7.34

The opposite can be said about the Φ_{Eu} where both the removal of the OH oscillator and the likely redox potential shift were advantageous for the metal luminescence. An exponential increase of Φ_{Eu} was observed upon fluoride addition going from the neutral complex toward the +3 charged. To have better understanding, experiments such as cyclic voltammetry, and luminescence lifetime measurements are needed to further evaluate these data. Another possibility could be the use of ^{19}F NMR. The fluoride NMR signal would shift upon the coordination to the paramagnetic Eu, and by following the signal while continuously increasing the F^- concentration even binding constants could be determined for each complex.

4.4 Triazanonane based complexes

Pyridine is a common structural motif in ligands. Perhaps the best examples are the widely used transition metal based photoredox catalysts for organic synthesis and for water splitting (e.g. $[Ru(bpy)_3]^{2+}$).[92] Pyridines are also used for chelating lanthanides. In the past two decades the archetypal dipicolinic acid complexes have further been developed into the more stable azamacrocyclic derivatives. Recent highlights include one and two photon excitable brightly luminescent bioprobes,[93] and circularly polarized light emitting protein affinity probes.[94]

Many of these Ln probes utilize antennae with ILCT states, where the acceptor pyridine unit is para substituted with an electron-donating group. Through the modification of the para position either bioconjugation or the fine-tuning of the pyridine electronics become possible. To modulate the Lewis basicity of the donor nitrogen atom via inductive and mesomeric effects within the pyridine ring, we decided to install both electron donating (-OMe) and withdrawing substituents (-Cl, $-CF_3$) in the para-position of the aromatic ring. This way the distant structural modifications allow us to change the redox potential of the Ln, while leaving its first coordination sphere intact. As the overall charge of the complexes would remain unchanged, we expected the effect of the ligand changes to be quite subtle.

4.4.1 Synthesis

The synthesis of the triazanonane-based ligands consist of two main parts: the construction of the substituted pyridine-carboxylic acids and the preparation of the chloroacetylated antenna (**12c**). The latter had been discussed previously (see Chapter II.).

The first step of the synthesis is the formation of the pyridine-dimethylesters, where the introduction of the para substituents occurs simultaneously (*Scheme 4.4*). As starting materials dipicolinic acid (**51**) and chelidamic acid (**52**) were used. Fischer-Speier esterification can yield the diesters, but this reaction requires long reaction times and cannot introduce the chloro substituent. Esterification with thionyl chloride and methanol can provide **52Cl, 52OH, 52OMe** in one pot depending on the reaction procedure. Direct quenching of thionyl chloride with methanol results in the formation of **52Cl** and **52OMe**, but in poor yield. If the thionyl chloride is first removed and methanol is added to the acyl chloride in dry DCM, **52Cl** and **52OH** are obtained in good yield. **52OH** can be converted to **52OMe** if necessary by refluxing in acetonitrile in the presence of large excess of MeI and K_2CO_3 base. The reaction needs to be followed in order to minimize quaternerization of the aromatic nitrogen.

To install CF_3 group in the para position, two more reaction steps were needed. The aryl chloride (**52Cl**) is not active enough in the Pd-catalyzed trifluormethylation, therefore an aryl iodide (**52I**) is first prepared. Replacement

of the chloro substituent occurs in dry acetonitrile with acetyl chloride and NaI upon sonication of the reaction mixture. At last, Pd-promoted nucleophilic trifluormethylation of **52I** resulted **52CF3** in good yield.

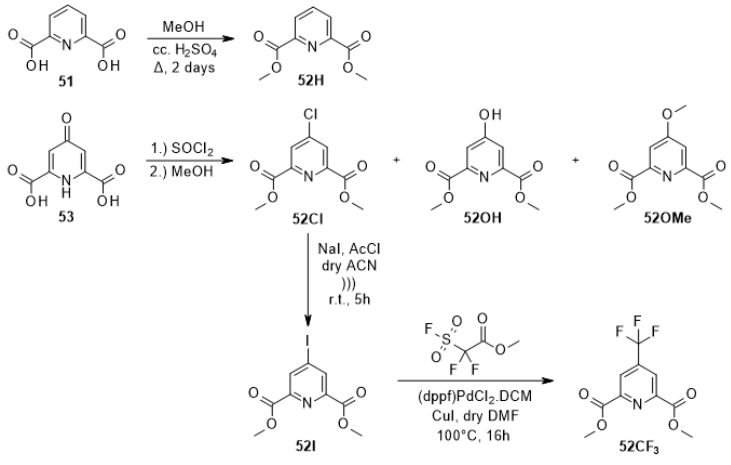

Scheme 4.4 Synthesis of the differently substituted pyridine dimethylesters.

With the pyridine derivatives in hand, a common synthetic route delivers the Bromobenzyl pyridines (*Scheme 4.5*). Controlled reduction with $NaBH_4$ gives rise to the formation of the mono-alcohol (**54**). This alcohol is further reacted with PBr_3 to produce an alkyl bromide (**55**), which can be later appended to the macrocycle.

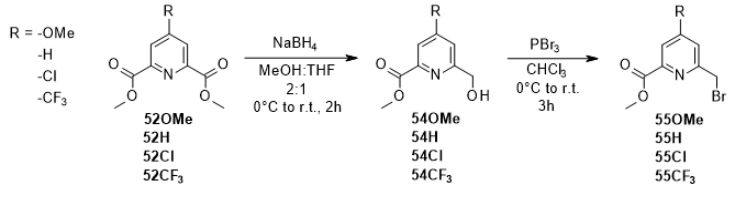

Scheme 4.5 Synthesis of the Bromobenzyl pyridines.

The pendant arms are attached on the macrocycle (*Scheme 4.6*) by alkylation of **57** in an unusual $CHCl_3$:MeOH (1:1) mixture. This is needed because of the appalling solubility of **57** in DMF, yielding a gel like material without delivering the product. In the new solvent mixture the final ligand architecture is easily built up. Purification is crucial at this step to avoid any organic contaminants in the final complexes. Multiple chromatographic steps were needed, and solely alumina columns could be used. Hydrolysis of the methyl esters in ACN:H_2O (1:1) mixture is instantaneous in the presence of only 3 equivalents of hydroxide. For lanthanide complexation the previously established conditions were used. Upon chelation a white precipitate was formed, which could be removed by column chromatography, along with the excess lanthanide salt. Column chromatography provided complexes (**Ln60**) with varying purity in

moderate to good yields, while most of the inorganic by-products were successfully removed. The major contaminants were excess $LnCl_3$ and NaCl.

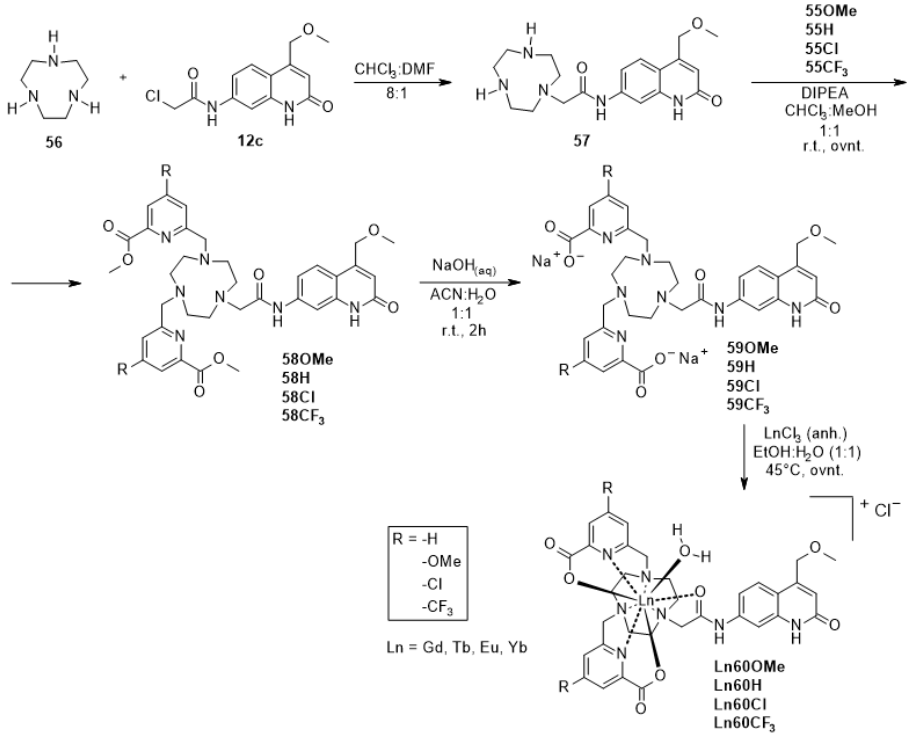

Scheme 4.6 Synthesis of the triazanonane based complexes.

4.4.2 Photophysical characterization

The photophysical measurements on the trizanonane based complexes were done similarly as before: in buffered 10 mM aqueous PIPES with complex concentrations in the 10–15 μM range. The absorption spectra differed between the ligands depending on the substitution pattern of the pyridine pendant arm. Changes were found between 250–310 nm, and above 310 nm only the carbostyril antenna absorbs.

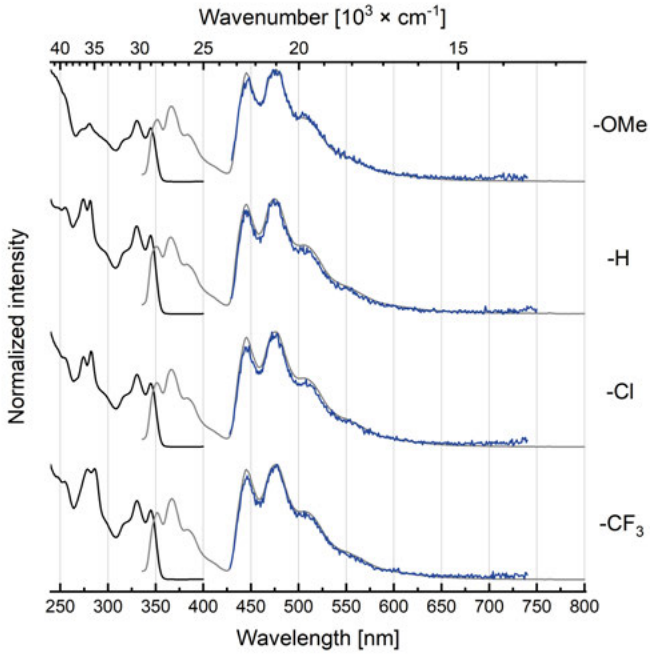

*Figure 4.8 Excitation spectra of the ligand centered phosphorescence emissions (black lines, left, λ_{em} = 442 nm). Steady-state emission (gray lines, middle) and time-resolved phosphorescence spectra (blue lines, right) at λ_{ex} = 330 nm of the Gd-complexes (**Gd60**) at 77 K with 10% glycerol added to the 10 μM, PIPES buffered aqueous solutions 0.01 M, pH 6.5.*

Emission spectra in all cases were recorded at λ_{ex} = 330 nm or above to have exclusively carbostyril-based sensitization. First, steady-state and time-resolved emission spectra of the Gd-complexes were recorded at low temperatures (*Figure 4.8*). The energy levels of the antenna singlet and triplet states were found to be exactly alike, as well as the ratio between them, which means that they undergo ISC to the same extent. This suggests that identical sensitization mechanisms can be expected in all complexes. The excitation spectra of the fluorescence emission matched only with the carbostyril antenna absorption. On the other hand, the excitation spectra of the phosphorescence peaks matched with the UV absorption of the entire complex. This means the pyridine pendant arms have observable triplet energy levels in this region. To

solely detect these pyridine triplet states we would need to measure model compounds without the carbostyril antenna.[95]

Table 4.6.

Compound	Abs. Φ_L [%]	Rel. Φ_L [%]	Abs. Φ_{Ln} [%]	Rel. Φ_{Ln} [%]	τ_{H2O} [ms]	τ_{D2O} [ms]	q
Gd60OMe	7.03	100	/	/	/	/	/
Gd60H	6.70	95.3	/	/	/	/	/
Gd60Cl	4.66	66.3	/	/	/	/	/
Gd60CF$_3$	2.17	30.9	/	/	/	/	/
Tb60OMe	5.35	100	32.3	100	0.764	1.01	1.29
Tb60H	4.93	92.1	29.0	89.8	0.817	1.08	1.19
Tb60Cl	3.68	68.8	26.6	82.4	0.730	0.987	1.48
Tb60CF$_3$	1.77	33.1	12.9	39.9	0.598	0.939	2.74*
Eu60OMe	0.157	100	3.75	100	0.506	1.34	1.09
Eu60H	0.148	76.6	2.49	66.4	0.496	1.33	1.13
Eu60Cl	0.120	62.8	1.39	37.1	0.489	1.20	1.06
Eu60CF$_3$	0.105	49.6	0.761	20.3	0.481	1.14	1.05
Yb60OMe	4.86	100	/	/	/	/	/
Yb60H	3.71	76.3	/	/	/	/	/
Yb60Cl	1.99	40.9	/	/	/	/	/
Yb60CF$_3$	1.03	21.2	/	/	/	/	/

We obtained remarkably varied antenna quantum yields (Φ_L) for the Gd complexes at room temperature (*Table 4.6*); Φ_L decreased drastically upon the introduction of electron withdrawing pyridine substituents. The ligand emission was only a third in CF_3 substituted ligands compared to the Φ_L of the OMe analogues. In section 4.3.2 we saw a slight reduction in Φ_L when amide pendant arms were introduced. In that case either the increasing amount of NH oscillators or the increasing Lewis acidity of the lanthanide could cause the up to 10% drop in ligand fluorescence. It is worth emphasizing that in those complexes the overall charge changed from 0 to +3, but this time the triazanonane complexes all have +1 charge. We can expect a slight Ln-N(Py) distance increase when EWG groups are in the para position. However, as long as we do not have crystal structures, this remains a hypothesis. For all complexes but one q = 1 was obtained (*vide infra*), therefore there are no significant changes around the close coordination environment. For these reasons we expect that the difference must come from the different electronics of the pyridines.

Our current hypothesis is that there is an electron transfer between the excited carbostyril chromophore and one of the pyridine arms. In complexes wherein the antennae have ILCT excited states pyridine acts as an electron acceptor within the same antenna unit. We have not yet performed electrochemical measurements on our triazanonane complexes, therefore we do know the redox potentials of the pyridines. Literature data suggest that electron deficient N-containing aromatics (e.g. quinoxalines) are easily re-

duced.[96] Katakis and co-workers successfully reduced pyridinecarboxilic acids with the weak reductant Eu(II) in acidic conditions.[97] Our pyridines are very similar to the protonated ones found in those studies: coordination to the Lewis acidic lanthanides might have similar electron withdrawing ability as protonation. In addition, in our pyridines the Cl and CF_3 substituents lower the electron density on the aromatic ring even further (*Scheme 4.7*).

Through the extended conjugated system involving the lanthanide orbitals the electron from the antenna could end up on one of the pyridine units. This would cause charge separation within the complex, thus quenching the singlet excited state of the sensitizer.

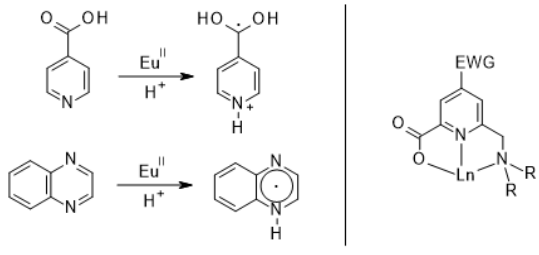

Scheme 4.7 N-heteroaromatics and their reduction (left), electron poor pyridine unit in our triazanonane Ln complexes (right).

To test this hypothesis, we need to measure the redox potential of the differently substituted pyridine fragments in suitable model compounds lacking the antenna. To simulate the electron withdrawing ability of the Lewis acid, the lanthanide should be preferably retained. The cyclic voltammetry should be performed in water. Another possibility would be to add increasing amounts of pyridine to our complex solution and evaluate its effect on the ligand fluorescence.

A similar trend was found in Tb complexes where this putative singlet quenching mechanism and the singlet mediated energy transfer both contributed to a decrease in Φ_L. The combination of these two effects resulted in Φ_L values between 1.77–5.35%. We intended to study PeT between the antenna and Eu, but the evaluation of the results became more complicated as there is an additional ligand fluorescence quenching mechanism in operation. The Φ_L of Eu complexes are very low (below 0.2%). The trend among the Eu Φ_L did not mirror those found in Gd and Tb complexes. Probably this is the combined outcome of multiple PeT mechanisms (ligand to metal, ligand to ligand).

Antenna excitation at λ_{ex} = 330 nm resulted in Tb and Eu emission. The shape and intensity of the peaks differed from the ones obtained for ordinary in cyclen complexes (*Figure 4.9*).

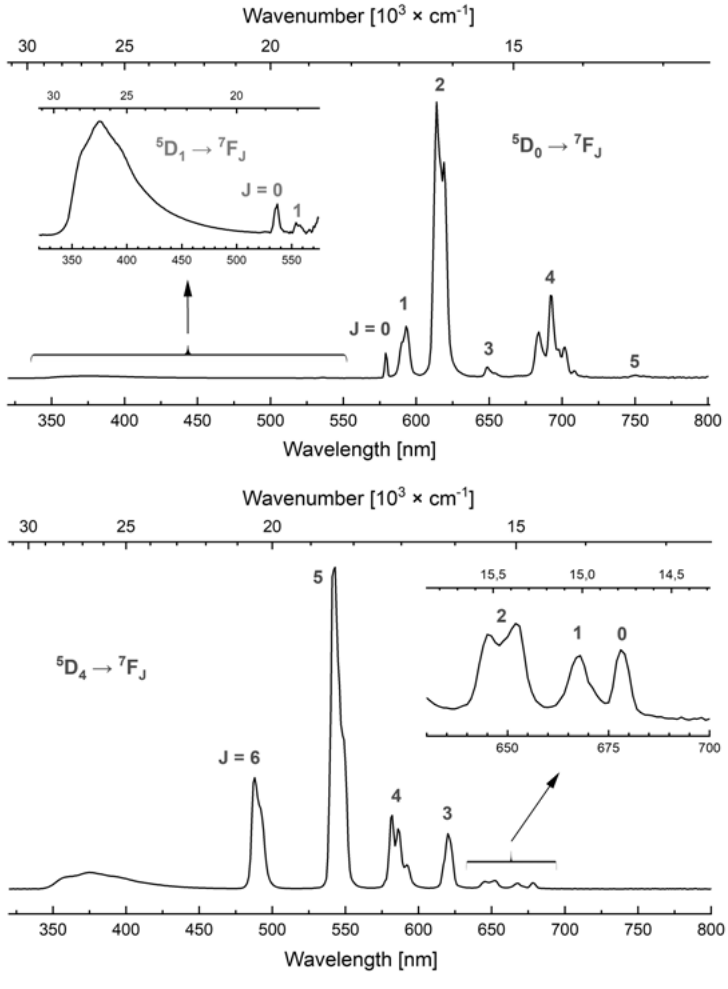

*Figure 4.9 Steady-state emission spectra of **Eu60OMe** (top) and **Tb60OMe** (bottom) with typical transitions highlighted (λ_{ex} = 330 nm, **[Ln60OMe]** = 30 μM in PIPES buffered aqueous solutions 10 mM, pH 6.5).*

The following transitions were found for Tb: $^5D_4 \rightarrow {}^7F_J$ (J = 6 – 0) at wavelengths 488, 543, 582, 620, 652, 668 and 678 nm, respectively. The J = 5 transition was found to be more than twice as high as the second most intense peak. In the Eu spectra transitions were $^5D_0 \rightarrow {}^7F_J$ (J = 0-5), with maxima at 579, 593, 614, 649, 693 and 751 nm. It is important to point out that in these Eu complexes the hypersensitive and higher energy $^5D_1 \rightarrow {}^7F_J$ (J = 0, 1) transitions were also visible (537, 554 nm, respectively). The highest intensity peak belongs to the J = 2 transition in contrast to the cyclen based Eu complexes, where the J = 4 transition is the strongest.

Tb quantum yields are relatively high in aqueous solutions for complexes having one coordinating water molecule. Φ_{Tb} slightly decreases going from the electron donating OMe (32%) towards the electron-neutral and electron-

withdrawing groups (H (29%), Cl (27%)). There is a large gap between these results and the CF_3 substituted Tb complex, where the Φ_{Tb} halved (13%).

All Eu complexes have Φ_{Eu} below 4% which is comparable to the results achieved by the same antenna sensitized Eu cyclen complexes (see before *Table 4.3*). There is a continuous decrease going from electron donating to withdrawing para substituents. The biggest difference in Eu quantum yields is between the **Eu60OMe** (3.75%) and **Eu60H** (2.49%). It is clear that an electron rich Eu environment increases both ligand and metal luminescence. Eu(III) in such surroundings is better stabilized, as well as the pyridines.

Table 4.7.

Compound	Φ_L [%]	Φ_{L+F^-} [%]	Increase X fold	Φ_{Ln} [%]	Φ_{Ln+F^-} [%]	Increase X fold
Gd60OMe	6.86	6.92	1.01	/	/	/
Gd60H	6.38	6.29	0.99	/	/	/
Gd60Cl	4.53	3.35	0.74	/	/	/
Gd60CF$_3$	2.12	1.31	0.61	/	/	/
Tb60OMe	5.35	5.22	0.98	32.3	23.4	0.724
Tb60H	4.93	4.93	1.00	29.0	21.7	0.748
Tb60Cl	3.68	2.86	0.78	26.6	17.8	0.669
Tb60CF$_3$	1.77	1.14	0.64	12.9	13.8	1.070
Eu60OMe	0.157	0.768	4.89	3.75	15.4	4.11
Eu60H	0.148	0.653	4.41	2.49	13.6	5.46
Eu60Cl	0.120	0.463	3.85	1.39	11.8	8.49
Eu60CF$_3$	0.105	0.322	3.07	0.761	9.22	12.12
Yb60OMe	4.51	6.45	1.43	/	/	/
Yb60H	3.64	5.70	1.57	/	/	/
Yb60Cl	2.03	3.13	1.54	/	/	/
Yb60CF$_3$	0.954	1.28	1.34	/	/	/

Since the triazanonane complexes have an overall +1 charge, they are likely to coordinate to fluoride. As fluoride coordination is beneficial for Eu luminescence we decided to have look at its effect on the whole set of the triazanonane complexes (*Table 4.7*). We found that Φ_L in redox-active lanthanides generally increased (Eu, Yb), and we expected stagnation of ligand fluorescence in Tb and Gd complexes. While this was true for the OMe and H substituted complexes, in complexes substituted with electron withdrawing Cl and CF_3 the already low antenna fluorescence further decreased. At the moment we do not know how to explain this phenomenon. Upon fluoride coordination the emission spectra of both Tb and Eu changed, and both splitting and intensity changes were observed (*Figure 4.10*).

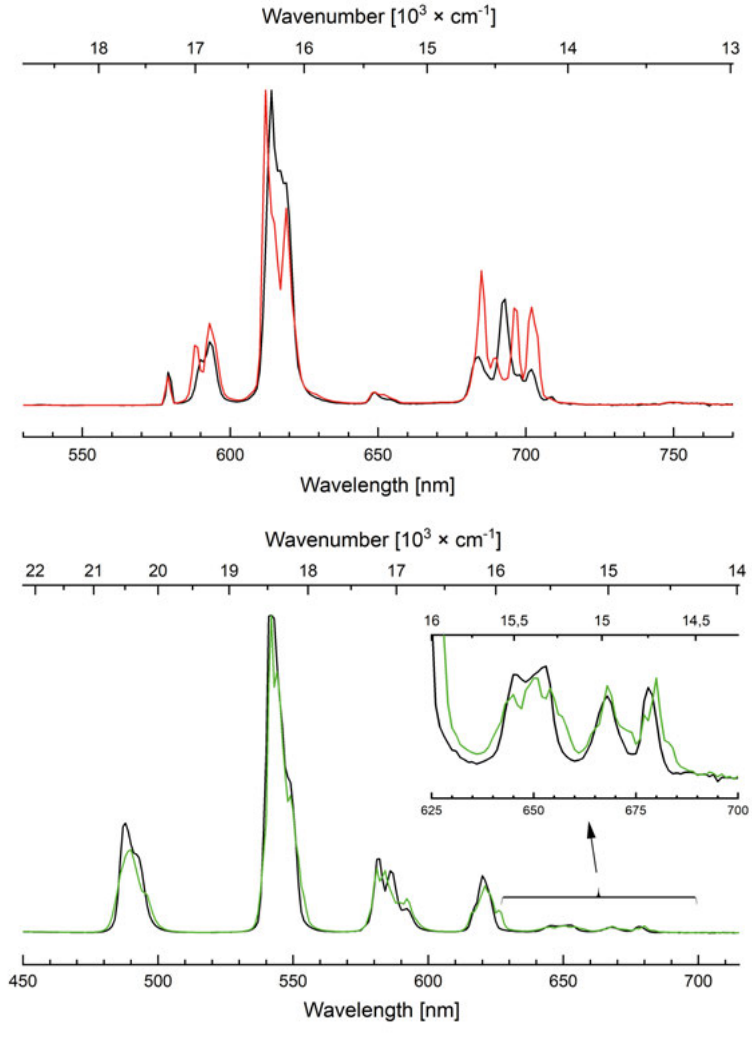

*Figure 4.10 Emission spectra of **Eu60OMe** in the absence (black line) and in the presence of 100 mM fluoride (red line) on the upper spectra. In the lower spectra **Tb60OMe** is displayed in the absence (black line) and in the presence of 100 mM fluoride. (λ_{ex} = 330 nm, **[Ln60OMe]** = 30 μM in PIPES buffered aqueous solutions 10 mM, pH 6.5).*

As we replaced the coordinating water with fluoride we expected to see an increased Φ_{Tb}. However, all Tb complexes (except CF_3) suffered an approximately 30% luminescence drop. This may be due to the altered electronics around the coordination environment, which negatively impacts the sensitization, although other reasons are conceivable. In the Eu complexes the removal of the OH oscillator from the first coordination sphere and the stabilized Eu(III) strongly enhanced the Φ_{Eu}. The new quantum yields were quite high, between 10–15%. The trend in the enhancement followed that of the electron withdrawing ability of the para substituent.

Table 4.8.

Substituent	τ_{rad} [ms]	τ_{obs} [ms]	Φ_{Eu}^{Eu} [%]	η_{sens} [%]	Φ_{Eu}^{Eu} ratio	Φ_{Eux}^{Eu} ratio	η_{sens} ratio
Eu60OMe	2.67	0.506	19.0	19.7	1.54	4.11	2.68
Eu60OMe+F^-	3.70	1.079	29.2	52.7			
Eu60H	2.86	0.496	17.3	14.4	1.66	5.46	3.29
Eu60H+F^-	3.72	1.069	28.7	47.4			
Eu60Cl	2.69	0.489	18.2	7.64	1.61	8.49	5.27
Eu60Cl+F^-	3.63	1.063	29.3	40.3			
Eu60CF$_3$	2.85	0.481	16.9	4.50	1.72	12.11	7.04
Eu60CF$_3$+F^-	3.67	1.068	29.1	31.7			

The calculated radiative lifetimes (*Table 4.8*) are similar in the triazacyclononane complexes (~2.75 ms). This is on average half of what was found in the cyclen derivatives. Because of the shorter radiative lifetime and very similar observed lifetimes these triazanonane complexes have higher intrinsic quantum yields (17–19%) than the cyclen complexes. The sensitization efficiency in these complexes are found to be low, below 20%. The addition of fluoride increased all values: radiative lifetimes with 1 ms, observed lifetimes by 0.5 ms. As a result the intrinsic quantum yields almost doubled, and the observed quantum yields were 4–12 fold higher. The greatly improved sensitization efficiency in fluoride containing complexes are due to multiple factors: the removal of the OH oscillators, as well as the minimized PeT quenching in the Eu complex.

4.5 Influencing the PeT sensitization pathway in Yb complexes (Paper IV)

In fluorescence microscopy detection in the near infrared region is desired for several reasons. The absorbance of biological samples in the NIR is minimal, which results in lower autofluorescence and deeper light penetration of tissues. This means that even very weak emitters can be observed. Further improvements can be achieved by utilizing the Lns long-lived and sharp emission peaks. The best candidate among the NIR emitting lanthanides is Yb, which has the highest intrinsic quantum yield of this series.

Yb can be sensitized by an antenna in two different ways: either via triplet mediated EnT or through an electron transfer-back electron transfer mechanism (*Figure 4.11*).

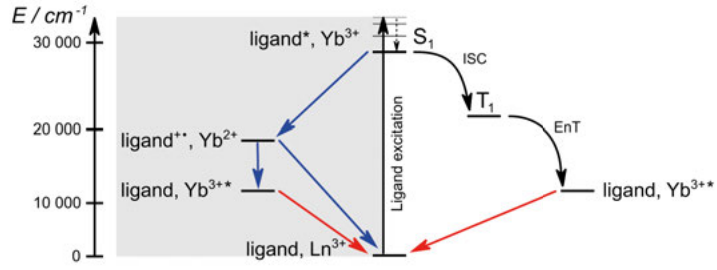

Figure 4.11 The two sensitization pathways of Yb: triplet mediated EnT (right), electron transfer mechanism (gray area, left). Curvy black arrows: intersystem crossing and energy transfer, blue arrows: forward/back electron transfer, red arrows: Yb emission.

Efforts to obtain bright Yb emissions have focused on improving the triplet mediated EnT or shielding the Yb from X-H quenchers. We propose that by changing the redox potential of the Yb the electron transfer mechanism can be controlled. This would provide a new approach to obtain bright Yb complexes and open new ways to create responsive probes.

The cyclen and triazanonane ligands described in this chapter were complexed with Yb as well. So far, we have only preliminary data of the Yb(III)/Yb(II) redox potentials in model cyclen complexes that do not bear the antenna. The cyclic voltammograms were recorded under an inert atmosphere in DMF with the electrolyte NBu_4ClO_4 (0.1 M) at a glassy carbon electrode and using ferrocene as an internal reference. There is approximately 0.9 V difference between the Yb redox potentials of the triacid and the triamide complexes ($E_{1/2}$ at 0.05 V/s for the triacid: –2.24 V vs NHE, triamide: –1.33 V vs NHE).

In *Table 4.3* and *Table 4.6* the antenna fluorescence quantum yields of Yb complexes are shown. Singlet EnT transfer from the 4-MOM substituted antenna is not probable because there is no spectral overlap the donor (28300 cm^{-1}) and acceptor (10300 cm^{-1}) levels. If we assume that the heavy atom effect of Gd and Yb to be similar, then the Φ_L decrease found in Yb complexes can only be caused by PeT. By taking each Gd and Yb complex pair we can see that reduction of the antenna fluorescence increases with overall charge of the complex. In the neutral complex there is an 18% decrease in Φ_L, in +1 charged 22%, in +2 charged 36% and in the +3 charged complexes 54% (*Table 4.3*).

Using the same antenna, the driving force for the PeT sensitization increased when the Yb(III) was destabilized with a soft donor environment. This means that during charge recombination a larger fraction of back electron transfer could form the antenna-Yb^* pair, which would result in higher Yb luminescence.

We are currently trying to measure and compare Yb emissions from our complexes. Measurements will be performed both in water and D_2O, the latter

in order to minimize the X-H vibrational quenching from the environment (ligand and solvent).

4.6 Conclusion

In this chapter the synthesis and photophysical evaluation of two types of Ln complexes were presented with the goal of studying PeT. As an antenna a 4-MOM substituted carbostyril was placed at the same distance from the Ln in all cases. This provided identical singlet and triplet energy levels, and identical sensitizations within each series of complexes. The hydration number matched in all complexes (q = 1) which minimized the differences in quenching.

We attempted to control the driving force of PeT by changing the Ln(III)/Ln(II) redox potential with different coordination environments. We destabilized the Ln(III) state by introducing soft donor atoms on the chelating arms. In cyclen complexes electrochemical measurements showed that this way we could shift the Ln(III)/Ln(II) redox potential by ~0.3 and ~0.4 V (in Eu and Yb complexes, respectively). In triazanonane complexes the same strategy was used using the inductive and mesomeric effects of the para substituent on the chelating pyridines.

Indications of PeT could be observed most easily by following the change in residual antenna fluorescence in cyclen based complexes. In Yb complexes the decrease in Φ_L can only be due to PeT, while in Eu complexes singlet mediated EnT could also contribute to the diminished antenna fluorescence. We found that there is an extra component in the quenching of the ligand fluorescence in the triazanonane based ligands. This made evaluation of these data more complicated, therefore further investigations are required.

The effect of PeT on Ln luminescence could also be investigated, on the other hand there is a significant NH quenching caused by the ligand, which complicates the picture. We are currently planning to minimize this NH quenching in our complexes by measuring the Ln quantum yields in D_2O, and replacing the amide H atoms with methyl groups.

We were able to alter the PeT mechanism by using an external fluoride anion. We found that the coordinating fluoride is beneficial for both ligand and metal fluorescence. However, further analysis is needed to determine the degree of fluoride binding, without which it is not possible to draw any conclusions.

5. Bioconjugable lanthanide complexes (Paper V)

In the past chapters a large number of lanthanide complexes were made and we better understood our DO3A based systems. We obtained several emitters with high quantum yields along with a few well emitting Sm and Dy complexes. The latter two are underutilized in imaging, but would provide an interesting complement to the widely used Eu and Tb emitters. To extend the utility of our complexes to biomolecule labelling we decided to develop clickable versions of our complexes. Some of the antenna we had been using had the potential to be easily modified by further functionalization, such as the 4-methoxymethyl and the 3-carboxymethyl substituted carbostyrils. Functionalization at a late stage is advantageous, therefore we decided to use the carbostyril with the ester functionality. A simple and selective hydrolysis, then an amide-bond formation would enable the introduction of bioconjugatable groups into our complexes.

Our approach was not new, the same scaffold has already been used to attach such lanthanide complexes to biomolecules.[98] Despite of this, we still decided to synthesize our compounds, since they contain a macrocyclic binding site, which is superior to the linear counterparts (reduced metal leaching [99]). Furthermore, we can implement our previous findings, which resulted in brighter complexes.

5.1 Synthesis

The syntheses of our potentially bioconjugatable complexes were described in detail in Chapter I (see *Scheme 2.2*) and Chapter II (see *Scheme 3.2*). There, only the 4-methyl substituted carbostyrils were synthesized with the carboxymethyl arm at position 3. The quantum yields show that this antenna is a good sensitizer for Tb (10% for **Tb17f** and 40% for **Tb26d**) and moderate for Eu (2.8 for **Eu17f** and 5.8% for **Eu26d**). We have not synthesized the same antenna having CF_3 group at position 4, but based on the literature and our previous findings, a better Eu emitter can be obtained by using that antenna. To brush up on the ligand synthesis, the whole synthetic route is shown in *Scheme 5.1*.

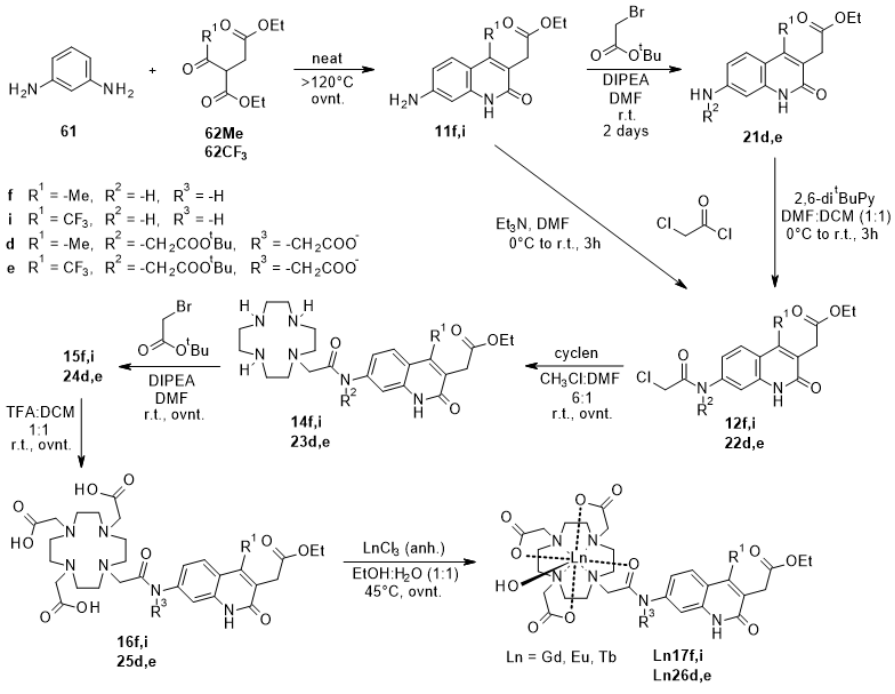

Scheme 5.1 Synthesis of the ethyl-ester functionalized complexes.

A divergent synthesis strategy was employed to increase efficiency while accessing different bioconjugatable lanthanide complexes. Having a relatively late stage key compound allows the introduction of several different reactive groups into our core structure, while keeping the overall number of synthesis steps low. Also, these reactive groups presumably cannot withstand harsh reaction conditions, which is a limiting factor in synthesis design.

First, we attempted to modify our final complexes, but these efforts were unsuccessful. However, the fully protected ligand (2 steps prior to the final complex, **15f**) seemed to be a more promising candidate for modifications. **15f** contains an ethyl and three *tert*-butyl ester groups. These protective groups can be selectively cleaved by using basic or acidic conditions, respectively. Treatment with 3 equivalents of NaOH in acetonitrile/water (1:1) mixture afforded the free carboxylic acid on the antenna (**63**) (*Scheme 5.2*). Basic ester hydrolysis is rapid unlike the acidic cleavage of the *tert*-butyl group, which usually requires an overnight stirring. In the next step, reactive groups could be installed into **63** through amide bond formation. Alkyne and azide containing amines were either purchased or synthesized following reported procedures.[100] We chose HATU as coupling agent, since it has been successfully used for structurally complex molecules,[101] and has enhanced reactivity compared to other frequently used coupling reagents, such as HOBt and EDCI (*Scheme 5.2*).[102] As HPLC-MS analysis showed, the reactions proceeded to

completion after an overnight reaction at 50 °C. The reaction had a clean profile, and the byproducts formed during the reaction were easily separable by column chromatography.

The following deprotection yielded the desired ligands, but in the case **66b** substantial amounts of side product[103] was observed which diminished the yield. The side product was identified as **66c** based on ^{1}H NMR and ESI-MS analysis.

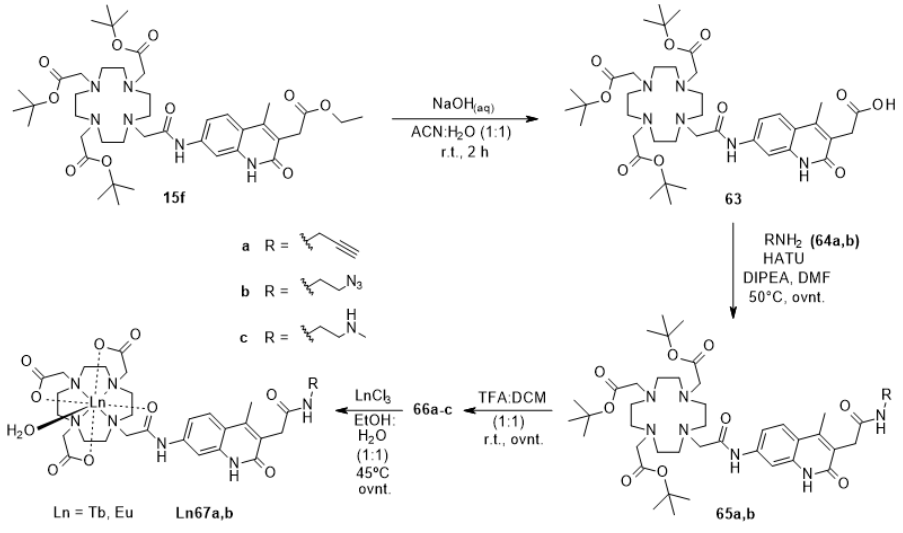

Scheme 5.2 Selective hydrolysis of the ethyl-ester group followed by amide formation with HATU as coupling agent.

In addition to the octadentate ligands, which allow water to access the lanthanide ion, we intended to synthesize nonadentate ligands as well. By excluding OH oscillators from the first coordination sphere, an enhanced brightness was expected.[104] To obtain such ligands we needed to replace one monodentate carboxymethyl arm in the cyclen with a bidentate pyridylcarboxylate. In order to do so, we used the previously synthesized DO2A-tBu ester as the starting material (**38**) (see Chapter IV) and **22d** to get **72** (*Scheme 5.4*). Only 0.5 equivalents of alkylating agent was used to prevent overalkylation; however, a small amount of dialkylated byproduct was still formed. This compound was inseparable on an alumina column from the desired product (**72**). Up to 3 chromatographic steps were also needed to remove the excess of unreacted **38**. This trialkylated cyclen was further reacted with **71** to obtain the fully alkylated cyclen (**73**). Unfortunately, we could not use the previously synthesized methyl ester protected pyridine carboxylic acids (see *Scheme 4.5*). Therefore we needed to use a different synthetic route[105] to get a *tert*-butyl ester protected pyridine derivative **71** (*Scheme 5.3*). After the deprotection of **73**, the free ligand was subjected to column chromatography on an aluminum oxide stationary phase. Regrettably, a significant amount of **74** was lost on the column even though NH_4OH (aq., 28%) was used as eluent. Using too basic conditions

might explain the formation of approximately 10% side product during the chromatographic step. HPLC analysis showed that the side product is a carbostyril based organic contaminant without the macrocyclic ring. The lanthanide complexation proceeds smoothly upon overnight stirring of the reaction mixture at 45 °C. These complexes (**Ln75**) on the other hand cannot be purified using either silica or alumina columns because they are retained on these stationary phases, therefore the ligand (**74**) must be of high purity.

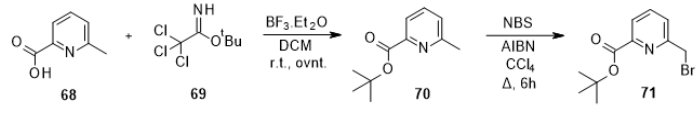

Scheme 5.3 Synthesis of tert-butyl 6-(bromomethyl)pyridine 2-carboxylate.

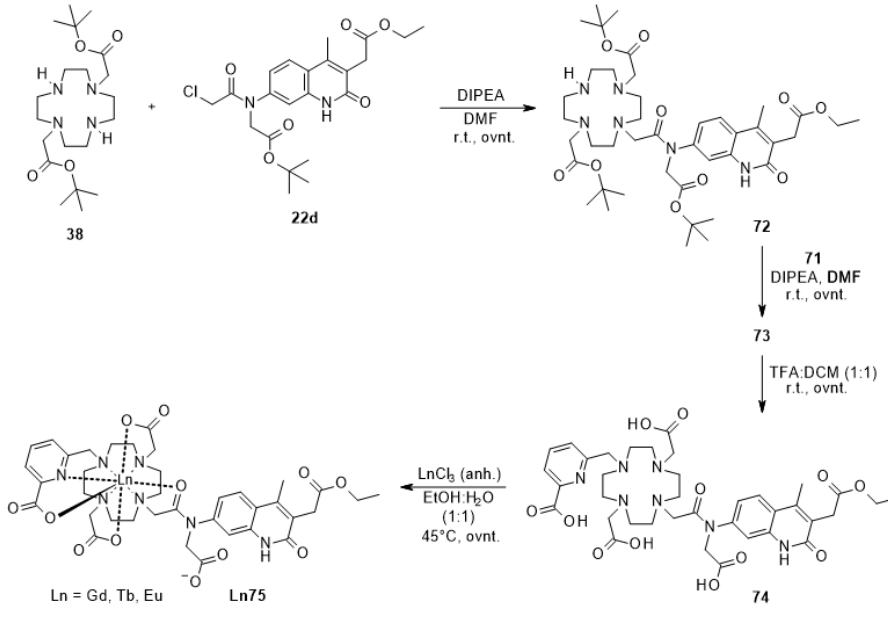

Scheme 5.4 Synthesis of the complexes having pyridine carboxylate as a pendant arm.

5.2 Crystal structures

Besides the regular chemical characterization methods, we were also able to confirm our final bioconjugatable complex structures with X-ray crystallography. Single crystals of an alkyne carrying Eu (*Figure 5.1*) and an azide group containing Tb complex (*Figure 5.2*) were grown by slow vapor diffusion of glyme into a solution of the complexes in water. Orientations of the antenna were found to be identical. The flexible side arms with the alkyne and azide clickable groups could be observed. Both complex have the same monocapped square antiprism geometry ($\Lambda(\delta\delta\delta\delta)$) in the crystal. Eu(III)-OH_2 distance is

2.467 Å, while the Tb(III)-OH_2 bond length is slightly shorter: 2.461 Å. This can be explained with the smaller size of the Tb.

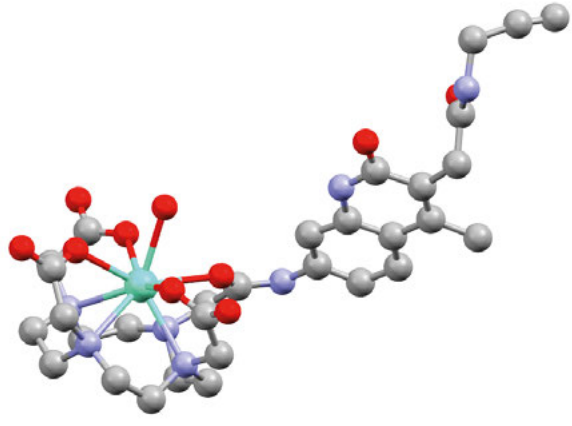

*Figure 5.1 Crystal structure of **Eu67a**. Oxygen atoms are represented in red, nitrogen atoms in light blue, carbon atoms in gray, and europium in pale green.*

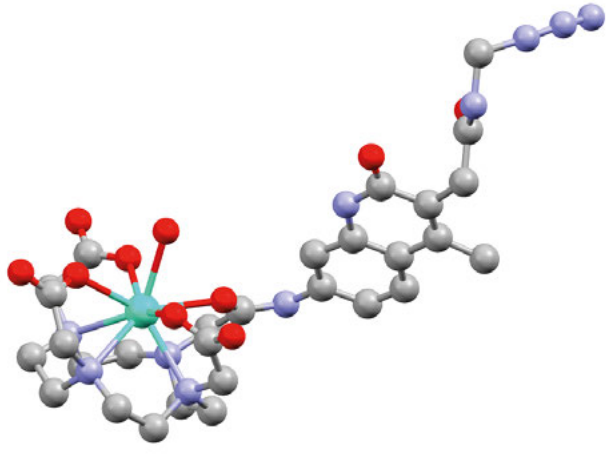

*Figure 5.2 Crystal structure of **Tb67b**. Oxygen atoms are represented in red, nitrogen atoms in light blue, carbon atoms in gray, and terbium in pale green.*

5.3 Photophysical characterization

For the sake of consistency, and to enable comparison to previous results, all complexes were measured in 10 mM PIPES buffered aqueous solutions at pH 6.5. Complex concentrations were at 10 µM. The absorption spectra were not

affected by either the amide coupled reactive groups, or the identities of the complexed lanthanide ions. However, the Me and CF_3 substituted antennae have distinct absorption maxima (λ_{max} = 330 nm (**Ln17f**) and 346 nm (**Ln17i**), respectively). The exocyclic N-alkylation has hypsochromic effect and shifts these absorption maxima more to the UV (to λ_{max} = 326 nm (**Ln26d**) and 342 nm (**Ln26e**), respectively). The pyridylcarboxylate arm only alters the absorption bands in the region below 300 nm, which is attributed to the presence of the pyridine chromophore (**Ln75**).

For complexes bearing the 4-Me substituted antenna photophysical data are collected in *Table 5.1*. Gd-complexes were prepared for the determination of the antenna quantum yields and triplet energy levels. Upon excitation into the lowest energy antenna absorption band, sharply spiked Eu and Tb emissions were observed. There was no significant difference between the Ln quantum yields once the bioconjugatable groups were introduced. This is not surprising because they are quite distant from the coordination site and likely do not impact the antenna orientation. Furthermore, they are electronically separated by a methylene bridge from the antenna. Φ_{Tb} slightly increased from 10% to 11–13%, and Φ_{Eu} from 2.8% to 3.4–3.6%. Ligand quantum yields show the opposite trend, here a consistent decrease was observed in both Tb and Eu complexes. This approximately 20% change in both directions might be coming from the different electron withdrawing ability of the amide compared to the ester group (weak effect on the antenna through CH_2). Quantum yield measurements are often assumed to carry ~10% relative error, therefore we need to treat these small changes with caution. However, while the actual error can be larger than this due to the uncertainties in the absorbance measurements, we note that this error is systematic, and applied to the entire class of complexes measured together.[106]

As it was discussed in Chapter III, mounting an extra carboxymethyl arm on the linker amide is beneficial for both Tb and Eu luminescence. With the use of the same antenna a 4-fold and 2-fold increase was achieved, respectively, compared to **Tb17f** and **Eu17f**.

The most effective vibrational quenchers of the Ln excited state, are the OH oscillators.[88] The exclusion of the directly bound water molecule from the complexes should therefore enable even higher Ln quantum yields. To saturate the coordination sphere we installed a bidentate picolinate arm on the cyclen, which was found effective removing the capping water in previous studies.[107]

Quantum yields were determined in the same manner as before, and excitation spectra confirmed that upon excitation over ~310 nm the pyridinecarboxylate arm is not involved in the sensitization. Φ_{Ln} for the Tb complex (**Tb75**) is 46%, which is slightly higher than what was found in **Tb26d**. A surprisingly low 5.8% Eu quantum yield was obtained for **Eu75**. This was rather unexpected since it is basically equivalent to the value that was obtained with the octadentate analogue (**Eu26d**). Lifetime measurements in normal and

heavy water showed that the number of coordinating water molecules was reduced from 1 to 0. This essentially means that the quenching OH-s were removed, but this effect was counterbalanced, and thus did not result in higher quantum yields. In theory it should have, especially in the case of Eu which couples rather well to the third vibrational overtone of an OH oscillator.

Analysis of the Eu spectra shows that the nonadentate complex (**Eu75**) has a different spectral fingerprint, which suggest symmetry changes around the coordination environment. Alterations were observed at the $J = 1, 2, 4$ transitions. The hypersensitive peak ($J = 2$, at 615 nm) remarkably increased compared to the magnetic dipole transition ($J = 1$, 590 nm), where the removal of the coordinating water molecule might have had an effect.[15] Tb is less sensitive to these coordination changes. Despite of this, changes were also observed on mainly the $J = 6, 4, 2$ transitions. Literature supports that the greatest sensitivity arises from these transitions.[108]

We determined the radiative lifetimes by comparing the ratio of the invariable magnetic dipole transition to the total Eu emission (see *Table 5.3*). In the new nonadentate complex the radiative lifetime decreased by approximately 30% compared to the octadentate analogues. At the same time the observed lifetime increased up to 1 ms, which was due to the removal of the OH oscillators from the first coordination sphere. Both of these results are beneficial for luminescence and contributed to a 3 folds higher intrinsic quantum yield. Since the measured Φ_{Eu} did not increase the sensitization efficiency became rather low, only 21%.

Our current hypothesis is that a different quenching pathway opened up in **Eu75**, which lowered the sensitization efficiency. This effect is probably the same quenching mechanism that was observed earlier in Chapter IV (4.4.2). A very good indication to that is the halved Φ_L in **Eu75** compared to **Eu26d**. There was no structural modification on the antenna side, therefore the ligand fluorescence decrease cannot be accounted for a change in singlet mediated EnT. The importance of complex conformation for efficient energy transfer was recently demonstrated in a coumarin-sensitized Eu complex.[109] However, less efficient energy transfer would not account for the lower antenna fluorescence either. Also, energy transfer between the antenna and pyridine arm is unlikely as the pyridine is higher in energy. Only the triplet levels of pyridine could overlap, but that would likely result in an efficient Ln sensitization, as pyridine-based ligands are known sensitizers of both Eu and Tb.[110] Therefore, we propose that the reduced Φ_L to be due to antenna-to-pyridine electron transfer.

Table 5.1.

Compound	Φ_L [%]	Φ_{Ln} [%]	τ_{H2O} [ms]	q
Gd17f	8.9	/	/	/
Tb17f	6.4	10	0.52	-*
Tb67a	6.1	13	-	-
Tb67b	5.8	11	-	-
Eu17f	0.42	2.8	0.60	1.0
Eu67a	0.15	3.6	-	-
Eu67b	0.15	3.4	-	-
Gd26d	7.7/7.3	/	/	/
Tb26d	7.1/6.5	41/39	1.56	0.9
Eu26d	1.7/1.6	5.8/5.7	0.65	1.0
Gd75	7.2	/	/	/
Tb75	6.2	46	1.83	-0.14
Eu75	0.75	5.8	1.00	0.03
Yb75	6.80	/	/	/

The previously studied 4-Me substituted antenna was proven to be an excellent sensitizer for Tb and moderate for Eu. Brighter Eu complexes were already achieved with the use of the CF_3 substituted carbostyril (see previous chapters). Previous bioconjugation studies[98] also used this chromophore extensively and their best quantum yields were in the range 20-40%. In all those cases researchers relied on open chain polyaminocarboxylate ligands (DTPA, TTHA), which suffer from kinetic instability compared to macrocyclic ligands. In most of these studies competitive challenge assays showed that the linear chelators lost most of their luminescence in the course of a few hours (2–3h). Our system with the DO3A binding site is better in retaining the Ln.[111] For this reason we decided to prepare the macrocyclic ligands with the 4-CF_3 substituted antenna and results are collected in *Table 5.2.*

Table 5.2.

Compound	Φ_L [%]	Φ_{Ln} [%]	τ_{H2O} [ms]	q
Gd17i	4.0	/	/	/
Tb17i	4.0	0.07	0.078/0.303	-
Eu17i	2.0	11	0.61	1.0
Gd26e	2.7	/	/	/
Tb26e	2.7	0.54	0.023/0.746	-
Eu26e	2.5	12	0.64	1.0

First and the most obvious result is that this antenna is incompetent for the sensitization of Tb. As low as 0.07% quantum yield was measured for this lanthanide (**Tb17i**). On the other hand, the Φ_{Eu} boosted, and an appealing 11% was recorded. The modification towards the tertiary amide linked analogues had the least enhancing effect in this case. We showed in Chapter III that several folds of Φ_{Ln} increase could be achieved with the use of the extra carboxymethyl arm on the linker. Although the several folds of increase was true for

Tb26e, its Φ_{Tb} still stayed at a low 0.5%. Φ_{Eu} increased only by 1% to give a final 12%. It was interesting to see that while most of the tertiary amide linked Eu complexes performed twice as good as their secondary amide analogues, here, there was only a minor improvement. After determining the radiative lifetimes, the intrinsic quantum yields for both Eu complexes were at 12%. This means that the already very high η_{sens} (92%) of **Eu17i** could only be slightly improved to reach an almost maximal η_{sens} (99%) in **Eu26e**. All radiative lifetimes, sensitization efficiencies and intrinsic quantum yields are summarized in *Table 5.3*.

Table 5.3.

Compound	τ_{rad} [ms]	τ_{obs} [ms]	Φ_{Eu}^{Eu} [%]	η_{sens} [%]
Eu17f	5.34	0.60	11.2	25
Eu26d	5.38	0.65	12.1	48
Eu75	3.68	1.00	27.2	21
Eu17i	5.08	0.61	12.0	92
Eu26e	5.28	0.64	12.1	99

5.4 Conclusion

Bright octa- and nonadentate bioconjugatable Ln complexes were prepared, several of these were equipped with reactive handles for click chemistry. The alkyne and azide functionalities were introduced at a late stage of the synthesis. With this, the number of synthetic steps were minimized to obtain the desired ligands. We could not observe any major differences between the ethyl ester decorated parent compounds and the clickable group containing complexes. We then attempted to further improve the brightness of the complexes by introducing small structural changes for both emissive lanthanides. In the end, we were able to increase the luminescence quantum yields up to 46% (Tb) and 12% (Eu). These values are considered to be fairly high (especially for complexes having q = 1). The commercially available FRET donor Lumi4-Tb, which represents the state-of-the-art in terms of photophysical properties and complex stability (B = 10 000 $M^{-1}cm^{-1}$)[112] is twice as bright as our Tb, and ~5 times as our Eu complex. Very high Eu sensitization efficiencies were achieved in our ligand system, but quantum yields were still not comparable to the open chain chelating ligands. A crucial finding of this chapter is that saturation of the coordination sphere does not necessarily give brighter complexes, as the benefits of removing the quenching solvent molecule from the first coordination sphere can be counterbalanced by novel quenching processes enabled by the altered architecture. Specifically, we found the introducing a pyridine coordinating arm resulted in the quenching of the antenna excited state, most likely via photoinduced electron transfer.

6. Concluding remarks

This thesis presents an in-depth analysis of the structure-photophysics relationships in focused Ln complex libraries. The systematic variation of both the antenna and the metal coordination site contributed to a better understanding of Ln sensitization mechanism and the processes detrimental to lanthanide luminescence.

By varying the substituents on the antenna we were able to tune the singlet and triplet energies of the chromophores, along with their redox potentials. The degree of quenched ligand fluorescence compared to the non-photoactive Gd reference compounds followed the reduction potential of the Ln ions. Our calculations show that photoinduced electron transfer is a viable and important quenching mechanism in a large variety of complexes. In complexes carrying a readily oxidized antenna not only Eu and Yb, with stable +II oxidation states are reduced, but even the less redox positive Sm, Dy, and Nd are susceptible to PeT. This is a crucial finding, and it should be taken into consideration when designing new luminescent Ln complexes.

With the modification of the coordination environment we were able to modulate the Eu and Yb redox potentials, which was confirmed by electrochemical measurements. It has not yet been possible to quantify the diminishing effect of PeT in Eu complexes. This is because X-H-oscillators, as well as a competitive ligand-to-ligand PeT quenching also contribute to a diminished antenna fluorescence. Current efforts focus on minimizing the effects of the X-H oscillators. The competitive ligand-to-ligand quenching will be further investigated.

We propose that by controlling the Yb(III)/Yb(II) redox potential not just brighter Yb complexes may be obtained, but with this new approach the creation of new responsive Yb probes should become possible.

Lastly, we were able to develop bioconjugatable versions of our brightest and stable macrocyclic Tb and Eu complexes. We also showed that the full saturation of coordination environment does not necessarily provide brighter complexes.

Future work will be done on cells to further investigate the cellular behavior of these emitters. We now have in hand a large number of highly emissive complexes with a range of structural variations, including overall charge and charge distribution, antenna structure and lanthanide ion. Finally, we are also planning to turn our brightest complexes analyte responsive.

Svensk sammanfattning

Lantanider, en grupp grundämnen som också brukar kallas sällsynta jordartsmetaller, finns i f-blocket i det periodiska systemet. På grund av deras delvis ofyllda 4f orbitaler, som är skyddade från omgivningen av 6s och 5d orbitalerna, har de likadan kemisk reaktivitet. Å andra sidan är deras fysiska egenskaper, t.ex. magnetism och luminescens, mycket varierade på grund av den olika mängd f-elektroner som finns i 4f-orbitalerna. Därför har lantanider vitt skilda tillämpningar, såsom i lasrar, neodymmagneter, kontrastmedel i magnetresonanstomografiska undersökningar och som luminiscenta markörer i cellbiologi och biokemi.

De flest luminiscenta markörer som används idag är baserade på organiska aromater. Fördelarna med dem är att de är lättillgängliga, relativt billiga, ofta har högt kvantutbyte och hög absorption (dvs de är ”ljusa”). Till nackdelarna tillhör att de har breda absorptions och emissionsspektra, kort emissionslivslängd, och låg fotostabilitet. Det gör att det är komplicerat att använda flera markörer samtidigt då deras signaler överlappar och blir därför svårtolkade. Experiment med simultananvändning av flera markörer är särskilt intressant i biologi där biomolekyler, joner etc interagerar och små ändringar i en jons koncentration eller ett enzyms aktivitet kan starta välorkestrerade reaktionskaskader.

De flesta lantaniders trivalenta joner är luminiscenta. Deras luminiscens har lång livslängd, ibland upp till en millisekund, vilket gör att signalerna kan detekteras utan någon bakgrundsljus från miljön. Färgen från de emitterade fotonerna är olika för de olika lantaniderna. Därför går det att skilja på signaler från olika lantanider även i en komplex blandning som innehåller många emitterade komponenter, inklusive andra lantanider och organiska fluoroforer. Till skillnad från organiska fluoroforer är lantanidkomplex icke-fotolabila. Det betyder att de kan användas i långa experiment, och de producerar heller inte fototoxiska degradationsprodukter. På grund av dessa attraktiva egenskaper är luminiscenta lantanider intressanta som markörer i biologi, särskilt i mikroskopi.

Lantanidjonerna är svagt absorberande. För effektiv excitation brukar man använda en s.k. ”antenn”, en starkt absorberande organisk molekyl som kan överföra excitationsenergin till lantaniden. Parametrarna som måste optimeras för energiöverföringen har studerats och en del tumregler finns som hjälper forskarna vid designen av nya komplex. En lika viktig aspekt av komplexde-

signen är att minimera destruktiva processer, som distribuerar excitationsenergin till omgivningen utan att producera lantanidjonens exciterade tillstånd. En sådan process är fotoinducerad elektrontransfer (FeT) från antennas exciterade tillstånd (som är kraftigt reducerande) till lantanidjonen. FeT tas sällan i beaktande då lantanidjonens redoxaktivitet, dvs. dess förmåga att ha en annan laddning än den mest stabila (+3), ofta ignoreras. Bara för de två mest reducerbara lantaniderna, europium och ytterbium, brukar man tänka på möjligheten av elektrontransfer, och även i dessa fall är FeT oftast en hypotes utan experimentell stöd.

I denna avhandling undersöktes effekterna av FeT på lantanidluminescens. Studier av ett bibliotek av strukturellt skilda lantanidkomplex har visat att FeT är utbredd bland europiumkomplex, och är möjlig i komplex av andra, mindre reducerbara lantanider, t.ex. samarium, dysprosium, och även neodym. För att FeT oftast är oönskad, med undantag för ytterbiumkomplex, där FeT kan vara produktiv, har metoder för att eliminera FeT utforskats. Vi har visat att ligandens struktur påverkar lantanidjonernas reducerbarhet, och genom att binda jonerna i ligander med flera negativa laddningar kan FeT hämmas, vilket i sin tur resulterar i ökat kvantutbyte för lantanidluminiscens.

En annan strukturell faktor som sällan diskuteras är bindningen mellan antennen och liganden. När amiden som binder ihop dessa delar är tertiär förbättras kvantutbytet anmärkningsvärt mycket. Terbiumkomplex med kvantutbyte över 40% har identifierats bland tertiäramid-länkade komplex.

Luminescenta markörer behöver ofta kopplas till biomolekyler för att kunna lokaliseras i celler. Detta sker genom selektiva konjugeringsreaktioner mellan biomolekylen och markören. Reaktionen mellan azider or alkyner är en sådan selektiv reaktion och används flitigt i biokemi och cellbiologi samt i andra kemiområden, som materialkemi. Vi har syntetiserat azid- or alkynderivat av ett europium- och ett terbiumkomplex. Vi har utvärderat de reaktiva gruppernas samt konjugeringsreaktionens effekt på luminescensen. Inga negativa effekter hittades. Vi har också syntetiserat en ligand med nio donoratomer. Komplexen med en sådan ligand förväntades ha förbättrad luminescens eftersom jonerna var bättre skyddade från vattnet i omgivningen. För terbiumet bekräftades hypotesen, och kvantutbytet var 46%. Intressant nog var europiumkomplexet inte klart bättre än det mindre skyddade komplexet. Detta kan förklaras med ökad fotoinducerad elektrontransfer som tar ut en mer skyddad jonomgivnings positiva effekter.

Acknowledgements

My PhD studies would have not been possible without the help of a great number of people throughout the years.

First of all I would like express my greatest gratitude to my supervisor, ***Dr. Eszter Borbas*** who has guided me through this 4.5 years long journey. Thank you for your trust, guidance and support that you provided me on a daily basis. You are a great supervisor and I consider myself extremely lucky that we have met.
I would like to thank my co-supervisor ***Prof. Sascha Ott*** the encouraging words and that you let me be a member of SMC.
Dr. Julien Andres. I am really happy that we could work on projects together. Your precision, knowledge and criticism always fascinated me. Thank you for taking the time to teach me about spectroscopy and for giving truly valuable suggestions for my thesis.

Dr. Emilie Mathieu. You are a fantastic co-worker both in- and outside of the lab. Thank you for encouraging and helping me out on countless occasions and for proofreading my thesis!
Salavat Kiraev. Many-many thanks for your help in finishing up my projects. Your character brought life to the lab and your enthusiasm always cheered me up (even during the hard times). Maybe I am not the best person to say this, but try to find balance in life!
Dr. Kiran Reddy Baddigam. It was a pleasure to work with you and thank you for being such a nice and sincere person.
I would really like to thank all the help to ***Dulcie Phipps***, ***Ellen Demeyere***, ***Agnes Sipos*** and ***Dimitra Sakaveli***. It was a pleasure to work with you and I hope one day you will make good use of the knowledge you had gained with me.
I thank the nice memories and working athmosphere to past members of the Borbas group: ***Dr. Ruisheng Xiong***, ***Dr. Aritz Perez***, ***Mathieu Soete***, ***Axel Lecanu***, ***Anna-Bea Bornhof***, ***Andrea Fantó***, ***Fredric Ingner***, ***Dr. Siva Rama Krishna***, ***Jan Ole Kaufmann***, ***Vic De Roo*** and ***Bastien Poinot***.

I would also like to acknowledge: ***Dr. Anna Arkhypchuk*** for the indispensable help in organic synthesis; ***Dr. Juri Mai*** for being a nice company in- and outside of the lab (lunches, pubs, St. Petersburg).

I also need to express my appreciation to: ***Dr. Andreas Orthaber*** for the help solving numerous crystal structures, and ***Dr. Jordann Wells*** for proofreading my thesis and the help with the X-ray.
Michele Bedin. I am really grateful for the invaluable help with the LC-MS. Also, thank you for being a nice company both in Lab 1 and Japan.

I am grateful to all at SMC and the department who create such a friendly and nice work athmosphere: ***Dr. Henrik Ottosson***, ***Dr. Anders Thapper***, ***Ashleigh Castner, Nicolas D´Imperio***, ***Timofey Liseev***, ***Dr. Brian McCarthy, Dr. Anna Beiler***, ***Ben Johnson, Dr. Maxime Laurans, Dr. Muhammad Anwar Shameem, Dr. Arvind Kumar Gupta, Dr. Joshua Green, Dr. Simon Calusing, Daniel Morales Salazar***, ***Dr. Wangchuk Rabten***, ***Dr. Anup Rana***, ***Leandro Cid Gomes***, ***Dr. Josene Toldo, Dr. Felix Ho, Mariia Pavliuk, Belinda Petterson.***

From the department I would like to thank ***Holly Redman*** the nice times that we spent together, and ***Manuel Boniolo*** the good talks and efficient waste handling. Köszönöm ***Németh Brigittának*** a cigizés közbeni jó kis beszélgetéseket és Dr. Mészáros Liviának a kollaborációt és a remek kávé és ebédszüneteket.

Sven Johansson, Patrick Lindahl, Peter Lundström and all ***administration members*** at the department, thank you for your day-to-day help!

I appreciate the financial support from ***C. F. Liljewalch*** and ***Åforsk foundations***, ***Kungl. Vetenskapsakademien*** and ***Smålands nation***.

Many thanks to past members of SMC for creating a familiar working environment: ***Dr. Tomas Slanina***, ***Dr. Ulrike Fluch, Dr. Biswanath Das , Dr. Keyhan Esfandiarfard, Dr. Kjell Jorner, Dr. Rabia Ayub, Dr. Alexandra Denisova, Dr. Sangeeta Yadav, Dr. Hemlata Agarwala, Dr. Souvik Roy and Gwenn Delepierre.***

Dr. Jiajie Yan & ***Dr. Jia-Fei Poon***. Thank you for being such a nice company in my first two years of PhD. I will never forget the nice trips we went on to (Kiruna, Copenhagen, Stockholm, Helsinki).
I would also like to thank ***Dr. Lukasz Pilarski*** for helping me out on several occasions.

Prof. Polly L. Arnold. I am grateful that you accepted me as an exchange student in your lab. In Edinburgh I would mainly like to thank ***Jamie Purkis, Lotte van Rees, Ryan Kerr*** and ***Megan Seymour***.

Crystal Ye. Thank you for being my guide in California and that you proofread my thesis.

Ida Morgensen. I am really grateful for the Swedish translation. Also, thank you for your patience and for having me as a guest at your place multiple times.

I would like to thank ***Dr. Hao Huang*** for being a really good friend of mine here in Uppsala. Thank you for the delicious dinners, the nice gym sessions and mostly for the great conversations we had.

Jan Kudlicka. I was really lucky that I sat next to you on the introductory course 4 years ago. I really enjoyed having lunch and nice conversations with you throughout the years. Thank you for having me as a guest at your place and for helping me out twice(!) with the moving.

Szeretném megköszönönni egykori gimnáziumi kémiatanáromnak, ***Szinetárné Márkus Teréz***nek, hogy megszerettette velem a kémiát és elindított ezen az úton. Ugyanakkor köszönettel tartozom ***Hajós István***nak is, aki vállalta különórai felkészítésemet az emeltszintű érettségire és komolyan megalapozta mostani kémiatudásomat.
Köszönöm ***Dr. Nyerges Miklós***nak, hogy engedélyezte, hogy Műszaki egyetemi éveim alatt a Servier kutatóintézetben gyakornok lehessek. Nagyon hálás vagyok ***Dr. Molnár-Tóth Judit***nak, első témavezetőmnek, aki bevezetett a gyakorlati szerves kémia rejtelmeibe és segített elkészíteni szakdolgozatomat és diplomamunkámat. Neki, ***Dr. Ligeti Melindá***nak, ***Markacz Piroská***nak és ***Szabó Alexandrá***nak köszönöm a kezdeti lökést, a jó hangulatot és, hogy a mai napig tartjuk a jó viszonyt.
Köszönöm ***Kócsi Dániel****nek*, hogy annak idején kisegített és jó útra terelt kémiai pályafutásomban. Remélem, hogy viszonozni tudtam ezt a szívességet és egy nagy kalappal szeretnék neki kívánni az elkövetkezendőkhöz.
Köszönöm két jó barátomnak ***Molnár Máté***nak és ***Eredics Béla***nak a bátorító szavakat, és hogy doktori éveim alatt náluk bármikor megszállhattam és feltöltődhedtem.
Így a legvégén szeretném megköszönni ***család***omnak, de legfőképp ***drága szüleim***nek a támogatást, a segítséget és a belém vetett hitüket. Az ő önfeláldozásuk nélkül nem tarthatnék most ott, ahol vagyok.

References

[1] S. Cotton, in *Lanthanide and Actinide Chemistry*, John Wiley & Sons, Ltd, **2006**, pp. 9-22.

[2] J.Gambogi, *https://minerals.usgs.gov/minerals/pubs/commodity/rare_earths/myb1-2015-raree.pdf* **2015**.

[3] Y. Kato, K. Fujinaga, K. Nakamura, Y. Takaya, K. Kitamura, J. Ohta, R. Toda, T. Nakashima, H. Iwamori, *Nature Geoscience* **2011**, *4*, 535.

[4] a) J.-C. G. Bünzli, *Chemical Reviews* **2010**, *110*, 2729-2755; b) S. V. Eliseeva, J.-C. G. Bünzli, *Chemical Society Reviews* **2009**, *39*, 189-227.

[5] a) W. J. Evans, G. Zucchi, J. W. Ziller, *J. Am. Chem. Soc.* **2003**, *125*, 10-11; b) M. R. MacDonald, J. E. Bates, M. E. Fieser, J. W. Ziller, F. Furche, W. J. Evans, *J. Am. Chem. Soc.* **2012**, *134*, 8420-8423; c) M. E. Fieser, M. R. MacDonald, B. T. Krull, J. E. Bates, J. W. Ziller, F. Furche, W. J. Evans, *J. Am. Chem. Soc.* **2015**, *137*, 369-382; d) M. R. MacDonald, J. E. Bates, J. W. Ziller, F. Furche, W. J. Evans, *J. Am. Chem. Soc.* **2013**, *135*, 9857-9868.

[6] Z. Lin, M. L. Shelby, D. Hayes, K. A. Fransted, L. X. Chen, M. J. Allen, *Dalton Trans.* **2014**, *43*, 16156-16159.

[7] a) L. R. Morss, *Chemical Reviews* **1976**, *76*, 827-841; b) L. J. Nugent, R. D. Baybarz, J. L. Burnett, J. L. Ryan, *J. Phys. Chem.* **1973**, *77*, 1528-1539.

[8] J.-C. G. Bünzli, *Coord. Chem. Rev.* **2015**, *293-294*, 19-47.

[9] A. de Bettencourt-Dias, in *Luminescence of Lanthanide Ions in Coordination Compounds and Nanomaterials*, John Wiley & Sons Ltd, **2014**, pp. 1-48.

[10] J. R. Lakowicz, *Principles of Fluorescent Spectroscopy*, Mir, **1986**.

[11] M. D. Ward, *Coord. Chem. Rev.* **2010**, *254*, 2634-2642.

[12] W. D. Horrocks, Jr., J. P. Bolender, W. D. Smith, R. M. Supkowski, *J. Am. Chem. Soc.* **1997**, *119*, 5972-5973.

[13] D. Kovacs, K. E. Borbas, *Coordination Chemistry Reviews* **2018**, *364*, 1-9.

[14] J.-C. G. Bünzli, S. V. Eliseeva, in *Lanthanide Luminescence: Photophysical, Analytical and Biological Aspects* (Eds.: P. Hänninen, H. Härmä), Springer Berlin Heidelberg, Berlin, Heidelberg, **2011**, pp. 1-45.

[15] M. H. V. Werts, R. T. F. Jukes, J. W. Verhoeven, *Phys. Chem. Chem. Phys.* **2002**, *4*, 1542-1548.

[16] A. Beeby, D. Parker, J. A. G. Williams, *J. Chem. Soc., Perkin Trans. 2* **1996**, 1565-1580.

[17] a) A. Beeby, I. M. Clarkson, R. S. Dickins, S. Faulkner, D. Parker, L. Royle, S. A. S. de, J. A. G. Williams, M. Woods, *J. Chem. Soc., Perkin Trans. 2* **1999**, 493-504; b) R. S. Dickins, D. Parker, A. S. de Sousa, J. A. G. Williams, *Chem. Commun. (Cambridge)* **1996**, 697-698.

[18] a) A. Beeby, S. Faulkner, J. A. G. Williams, *J. Chem. Soc., Dalton Trans.* **2002**, 1918-1922; b) J. Laakso, G. A. Rosser, C. Szíjjártó, A. Beeby, K. E. Borbas, *Inorganic Chemistry* **2012**, *51*, 10366-10374.

[19] T. Terai, K. Kikuchi, S.-Y. Iwasawa, T. Kawabe, Y. Hirata, Y. Urano, T. Nagano, *J. Am. Chem. Soc.* **2006**, *128*, 6938-6946.

[20] F. Kielar, C. P. Montgomery, E. J. New, D. Parker, R. A. Poole, S. L. Richardson, P. A. Stenson, *Org. Biomol. Chem.* **2007**, *5*, 2975-2982.

[21] D. Parker, J. A. G. Williams, *J. Chem. Soc., Perkin Trans. 2* **1996**, 1581-1586.

[22] F.-S. Guo, B. M. Day, Y.-C. Chen, M.-L. Tong, A. Mansikkamäki, R. A. Layfield, *Science* **2018**, *362*, 1400-1403.

[23] a) C. Boucher, M. G. B. Drew, P. Giddings, L. M. Harwood, M. J. Hudson, P. B. Iveson, C. Madic, *Inorganic Chemistry Communications* **2002**, *5*, 596-599; b) S. R. Daly, D. Y. Kim, G. S. Girolami, *Inorganic Chemistry* **2012**, *51*, 7050-7065.

[24] D. Parker, R. S. Dickins, H. Puschmann, C. Crossland, J. A. K. Howard, *Chem. Rev. (Washington, DC, U. S.)* **2002**, *102*, 1977-2010.

[25] a) V. Placide, D. Pitrat, A. Grichine, A. Duperray, C. Andraud, O. Maury, *Tetrahedron Letters* **2014**, *55*, 1357-1361; b) S. J. Butler, L. Lamarque, R. Pal, D. Parker, *Chem. Sci.* **2014**, *5*, 1750-1756; c) V. Placide, A. T. Bui, A. Grichine, A. Duperray, D. Pitrat, C. Andraud, O. Maury, *Dalton Trans.* **2015**, *44*, 4918-4924; d) S. J. Butler, M. Delbianco, L. Lamarque, B. K. McMahon, E. R. Neil, R. Pal, D. Parker, J. W. Walton, J. M. Zwier, *Dalton Trans.* **2015**, *44*, 4791-4803.

[26] a) L. Burai, É. Tóth, S. Seibig, R. Scopelliti, A. E. Merbach, *Chemistry - A European Journal* **2000**, *6*, 3761-3770; b) É. Tóth, L. Burai, A. E. Merbach, *Coordination Chemistry Reviews* **2001**, *216-217*, 363-382; c) L. Burai, R. Scopelliti, É. Tóth, *Chemical Communications* **2002**, *0*, 2366-2367; d) N.-D. H. Gamage, Y. Mei, J. Garcia, M. J. Allen, *Angewandte Chemie International Edition* **2010**, *49*, 8923-8925; e) L. A. Ekanger, L. A. Polin, Y. Shen, E. M. Haacke, P. D. Martin, M. J. Allen, *Angewandte Chemie International Edition* **2015**, *54*, 14398-14401; f) L. A. Basal, M. D. Bailey, J. Romero, Meser M. Ali, L. Kurenbekova, J. Yustein, R. G. Pautler, M. J. Allen, *Chemical Science* **2017**, *8*, 8345-8350.

[27] M. J. Allen, *Synlett* **2016**, *27*, 1310-1317.

[28] a) L. D. Lavis, R. T. Raines, *ACS Chem. Biol.* **2008**, *3*, 142-155; b) L. D. Lavis, R. T. Raines, *ACS Chem. Biol.* **2014**, *9*, 855-866.

[29] a) R. Y. Tsien, *Annual Review of Biophysics and Bioengineering* **1983**, *12*, 91-116; b) A. Minta, J. P. Y. Kao, R. Y. Tsien, *J. Biol. Chem.* **1989**, *264*, 8171-8178; c) M. H. Lim, S. J. Lippard, *Acc. Chem. Res.* **2007**, *40*, 41-51; d) D. W. Domaille, E. L. Que, C. J. Chang, *Nature Chemical Biology* **2008**, *4*, 168; e) E. M. Nolan, S. J. Lippard, *Acc. Chem. Res.* **2009**, *42*, 193-203; f) T. Ueno, T. Nagano, *Nat. Methods* **2011**, *8*, 642-645; g) P. Rivera-Fuentes, S. J. Lippard, *Acc. Chem. Res.* **2015**, *48*, 2927-2934; h) T. Ikeno, T. Nagano, K. Hanaoka, *Chem. - Asian J.* **2017**, *12*, 1435-1446.

[30] S. Tyagi, F. R. Kramer, *Nature Biotechnology* **1996**, *14*, 303-308.

[31] D. Sahoo, V. Narayanaswami, C. M. Kay, R. O. Ryan, *Biochemistry* **2000**, *39*, 6594-6601.

[32] M. K. Smalley, S. K. Silverman, *Nucleic Acids Res.* **2006**, *34*, 152-166.

[33] D. Zink, N. Sadoni, E. Stelzer, *Methods* **2003**, *29*, 42-50.
[34] R. W. Sabnis, *Handbook of Biological Dyes and Stains: Synthesis and Industrial Application*, John Wiley & Sons, Inc., Hoboken, New Jersey, **2010**.
[35] P. A. Sontz, N. B. Muren, J. K. Barton, *Acc. Chem. Res.* **2012**, *45*, 1792-1800.
[36] a) A. Minta, J. P. Kao, R. Y. Tsien, *J. Biol. Chem.* **1989**, *264*; b) K. Kikuchi, K. Komatsu, T. Nagano, *Current Opinion in Chemical Biology* **2004**, *8*, 182-191; c) V. V. Martin, A. Rothe, K. R. Gee, *Bioorganic & Medicinal Chemistry Letters* **2005**, *15*, 1851-1855.
[37] J. Karolin, L. B. A. Johansson, L. Strandberg, T. Ny, *Journal of the American Chemical Society* **1994**, *116*, 7801-7806.
[38] A. Loudet, K. Burgess, *Chem. Rev. (Washington, DC, U. S.)* **2007**, *107*, 4891-4932.
[39] A. Waggoner, *Current Opinion in Chemical Biology* **2006**, *10*, 62-66.
[40] a) Y. Koide, Y. Urano, K. Hanaoka, T. Terai, T. Nagano, *ACS Chem. Biol.* **2011**, *6*, 600-608; b) E. D. Cosco, J. R. Caram, O. T. Bruns, D. Franke, R. A. Day, E. P. Farr, M. G. Bawendi, E. M. Sletten, *Angew. Chem., Int. Ed.* **2017**, *56*, 13126-13129.
[41] a) A. D'Aleo, A. Bourdolle, S. Brustlein, T. Fauquier, A. Grichine, A. Duperray, P. L. Baldeck, C. Andraud, S. Brasselet, O. Maury, *Angew. Chem., Int. Ed.* **2012**, *51*, 6622-6625; b) A. T. Bui, M. Beyler, Y.-Y. Liao, A. Grichine, A. Duperray, J.-C. Mulatier, B. L. Guennic, C. Andraud, O. Maury, R. Tripier, *Inorg. Chem.* **2016**, *55*, 7020-7025; c) A. T. Bui, M. Beyler, A. Grichine, A. Duperray, J.-C. Mulatier, Y. Guyot, C. Andraud, R. Tripier, S. Brasselet, O. Maury, *Chem. Commun. (Cambridge, U. K.)* **2017**, *53*, 6005-6008.
[42] M. Rajendran, E. Yapici, L. W. Miller, *Inorg. Chem.* **2014**, *53*, 1839-1853.
[43] A. Foucault-Collet, K. A. Gogick, K. A. White, S. Villette, A. Pallier, G. Collet, C. Kieda, T. Li, S. J. Geib, N. L. Rosi, S. Petoud, *Proc. Natl. Acad. Sci. USA* **2013**, *110*, 17199-17204.
[44] A. Foucault-Collet, C. M. Shade, I. Nazarenko, S. Petoud, S. V. Eliseeva, *Angew. Chem., Int. Ed.* **2014**, *53*, 2927-2930.
[45] a) Z. Liao, M. Tropiano, S. Faulkner, T. Vosch, T. J. Sørensen, *RSC Adv.* **2015**, *5*, 70282-70286; b) I. Martinić, S. V. Eliseeva, V. L. Pecoraro, S. Petoud, *Chem. Sci.* **2017**, *8*, 6042-6050.
[46] a) J. W. Walton, A. Bourdolle, S. J. Butler, M. Soulie, M. Delbianco, B. K. McMahon, R. Pal, H. Puschmann, J. M. Zwier, L. Lamarque, O. Maury, C. Andraud, D. Parker, *Chem. Commun.* **2013**, *49*, 1600-1602; b) B. K. McMahon, R. Pal, D. Parker, *Chem. Commun.* **2013**, *49*, 5363-5365; c) M. Starck, R. Pal, D. Parker, *Chem. - Eur. J.* **2016**, *22*, 570-580.
[47] B. Song, C. D. B. Vandevyver, A.-S. Chauvin, J.-C. G. Buenzli, *Org. Biomol. Chem.* **2008**, *6*, 4125-4133.
[48] A. T. Bui, A. Grichine, S. Brasselet, A. Duperray, C. Andraud, O. Maury, *Chemistry – A European Journal* **2015**, *21*, 17757-17761.
[49] a) P. R. Selvin, J. E. Hearst, *Proceedings of the National Academy of Sciences* **1994**, *91*, 10024-10028; b) J. M. Zwier, H. Bazin, L. Lamarque, G. Mathis, *Inorganic Chemistry* **2014**, *53*, 1854-1866.

[50] M. Delbianco, V. Sadovnikova, E. Bourrier, G. Mathis, L. Lamarque, J. M. Zwier, D. Parker, *Angewandte Chemie International Edition* **2014**, *53*, 10718-10722.
[51] L. Olofsson, S. Felekyan, E. Doumazane, P. Scholler, L. Fabre, J. M. Zwier, P. Rondard, C. A. M. Seidel, J.-P. Pin, E. Margeat, *Nature Communications* **2014**, *5*, 5206.
[52] A. Thibon, V. C. Pierre, *Anal. Bioanal. Chem.* **2009**, *394*, 107-120.
[53] a) E. Pershagen, J. Nordholm, K. E. Borbas, *J. Am. Chem. Soc.* **2012**, *134*, 9832-9835; b) H. Saneyoshi, Y. Ito, H. Abe, *J. Am. Chem. Soc.* **2013**, *135*, 13632-13635; c) E. Pershagen, K. E. Borbas, *Angew. Chem., Int. Ed.* **2015**, *54*, 1787-1790; d) Y. Yao, C. Kong, L. Yin, A. D. Jain, K. Ratia, G. R. J. Thatcher, T. W. Moore, T. G. Driver, L. W. Miller, *Chem. - Eur. J.* **2017**, *23*, 752-756.
[54] a) D. Parker, P. K. Senanayake, J. A. G. Williams, *Journal of the Chemical Society, Perkin Transactions 2* **1998**, *0*, 2129-2140; b) E. A. Weitz, J. Y. Chang, A. H. Rosenfield, V. C. Pierre, *J. Am. Chem. Soc.* **2012**, *134*, 16099-16102.
[55] a) R. Pal, D. Parker, *Organic & Biomolecular Chemistry* **2008**, *6*, 1020-1033; b) S.-Y. Huang, V. C. Pierre, *Chemical Communications* **2018**, *54*, 9210-9213.
[56] a) R. F. H. Viguier, A. N. Hulme, *J. Am. Chem. Soc.* **2006**, *128*, 11370-11371; b) A. Thibon, V. C. Pierre, *Journal of the American Chemical Society* **2009**, *131*, 434-435.
[57] M. S. Tremblay, M. Halim, D. Sames, *J. Am. Chem. Soc.* **2007**, *129*, 7570-7577.
[58] C. Szíjjártó, E. Pershagen, K. E. Borbas, *Dalton Transactions* **2012**, *41*, 7660-7669.
[59] a) H. Yamamoto, K. Mukoyoshi, K. Hattori, Fujisawa Pharmaceutical Co., Ltd., Japan . **2003**, p. 62 pp; b) P. Ge, P. R. Selvin, *Bioconjugate Chem.* **2004**, *15*, 1088-1094; c) H.-K. Lee, H. Cao, T. M. Rana, *Journal of Combinatorial Chemistry* **2005**, *7*, 279-284; d) K. E. Borbas, J. I. Bruce, *Org. Biomol. Chem.* **2007**, *5*, 2274-2282; e) A. Kathuria, N. Priya, K. Chand, P. Singh, A. Gupta, S. Jalal, S. Gupta, H. G. Raj, S. K. Sharma, *Bioorganic & Medicinal Chemistry* **2012**, *20*, 1624-1638.
[60] E. Pershagen, K. E. Borbas, *Coord. Chem. Rev.* **2014**, *273-274*, 30-46.
[61] W. J. Kruper, P. R. Rudolf, C. A. Langhoff, *The Journal of Organic Chemistry* **1993**, *58*, 3869-3876.
[62] A. Merbach, L. Helm, E. Toth, Editors, *The Chemistry of Contrast Agents in Medical Magnetic Resonance Imaging*, John Wiley & Sons Ltd., **2013**.
[63] J. Andres, A.-S. Chauvin, *Phys. Chem. Chem. Phys.* **2013**, *15*, 15981-15994.
[64] M. Y. Berezin, S. Achilefu, *Chem. Rev.* **2010**, *110*, 2641-2684.
[65] D. Parker, J. A. G. Williams, *J. Chem. Soc., Perkin Trans 2* **1995**, 1305-1314.
[66] T. Gunnlaugsson, D. Parker, *Chem. Commun.* **1998**, 511-512.
[67] A. K. R. Junker, L. R. Hill, A. L. Thompson, S. Faulkner, T. J. Soerensen, *Dalton Trans.* **2018**, *47*, 4794-4803.
[68] D. Parker, J. A. G. Williams, *J. Chem. Soc., Perkin Trans. 2* **1996**, 1581-1586.

[69] a) L. A. Ekanger, L. A. Basal, M. J. Allen, *Chem. Eur. J.* **2017**, *23*, 1145-1150; b) N.-D. H. Gamage, M. J. Allen, *Angew. Chem. Int. Ed.* **2010**, *49*, 8923-8925.
[70] a) M. Gál, V. Kolivoška, *Eur. J. Inorg. Chem.* **2013**, 3217-3223; b) L. A. Ekanger, M. J. Allen, *Inorg. Chem.* **2016**, *55*, 9981-9988.
[71] M. H. V. Werts, N. Nerambourg, M. Blanchard-Desce, *Photochem. Photobiol. Sci.* **2005**, *4*, 531-538.
[72] G. B. Barlin, W. Pfleiderer, *Journal of the Chemical Society B: Physical Organic* **1971**, 1425-1432.
[73] G. Saroja, N. B. Sankaran, A. Samanta, *Chem. Phys. Lett.* **1996**, *249*, 392-398.
[74] D. Kovacs, K. E. Borbas, *Coord. Chem. Rev.* **2018**, *364*, 1-9.
[75] D. R. Lide, *CRC Handbook of Chemistry and Physics, Internet Version 2005*, CRC Press, Boca Raton, FL, **2005**.
[76] G.-L. Law, D. Parker, S. L. Richardson, K.-L. Wong, *Dalton Transactions* **2009**, *0*, 8481-8484.
[77] T. Lazarides, M. A. H. Alamiry, H. Adams, S. J. A. Pope, S. Faulkner, J. A. Weinstein, M. D. Ward, *Dalton Trans.* **2007**, 1484-1491.
[78] D. Parker, P. K. Senanayake, J. A. G. Williams, *J. Chem. Soc., Perkin Trans. 2* **1998**, 2129-2139.
[79] M. Regueiro-Figueroa, J. L. Barriada, A. Pallier, D. Esteban-Gómez, A. d. Blas, T. Rodríguez-Blas, É. Tóth, C. Platas-Iglesias, *Inorganic Chemistry* **2015**, *54*, 4940-4952.
[80] M. Botta, M. Ravera, A. Barge, M. Bottaro, D. Osella, *Dalton Transactions* **2003**, 1628-1633.
[81] N. A. Piro, E. J. Schelter, *Coord. Chem. Rev.* **2014**, *260*, 21-36.
[82] G. J.-P. Deblonde, R. Abergel, *Nat. Chem.* **2017**, *9*, 843-849.
[83] M. Xiao, P. R. Selvin, *J. Am. Chem. Soc.* **2001**, *123*, 7067-7073.
[84] E. L. Yee, O. A. Gansow, M. J. Weaver, *Journal of the American Chemical Society* **1980**, *102*, 2278-2285.
[85] a) Z. Kovacs, A. D. Sherry, *J. Chem. Soc., Chem. Commun.* **1995**, 185-186; b) Z. Kovacs, A. D. Sherry, *Synthesis* **1997**, 759-763.
[86] L. E. Hopper, M. J. Allen, *Tetrahedron Lett.* **2014**, *55*, 5560-5561.
[87] a) L. M. D. León-Rodríguez, A. D. Miranda-Olvera, *Tetrahedron Lett.* **2006**, *47*, 6937-6940; b) I. Carreira-Barral, M. Mato-Iglesias, A. de Blas, C. Platas-Iglesias, P. A. Tasker, D. Esteban-Gómez, *Dalton Transactions* **2017**, *46*, 3192-3206.
[88] A. Beeby, D. Parker, M. Woods, *J. Chem. Soc., Perkin Trans. 2* **1999**, 493-503.
[89] M. P. Oude-Wolbers, D. N. Reinhoudt, *J. Chem. Soc. Perkin Trans. 2* **1998**, 2141-2150.
[90] J. Scholten, G. A. Rosser, J. Wahsner, N. Alzakhem, C. Bischof, F. Stog, A. Beeby, M. Seitz, *J. Am. Chem. Soc.* **2012**, *134*, 13915-13917.
[91] K. Binnemans, *Coordination Chemistry Reviews* **2015**, *295*, 1-45.
[92] a) T. P. Yoon, M. A. Ischay, J. Du, *Nat. Chem.* **2010**, *2*, 527-532; b) K. S. Joya, H. J. M. d. Groot, *Int. J. Hydrog. Energy* **2012**, 8787-8799.
[93] N. Hamon, O. Maury, R. Tripier, *Chem. Commun.* **2018**, *54*, 6173-6176.
[94] S. Shuvaev, D. Parker, *Chem. Sci.* **2018**, *9*, 2996-3003.
[95] J. Andres, A.-S. Chauvin, *Eur. J. Inorg. Chem.* **2010**, 2700-2713.

[96] C. R. Chang, E. S. Gould, *Inorg. Chem.* **1979**, *18*, 1294-1297.
[97] E. Vrachnou-Astra, D. Katakis, *J. Am. Chem. Soc.* **1975**, 5357-5363.
[98] a) A. Mohamadi, L. W. Miller, *Bioconjugate Chem.* **2016**, *27*, 2540-2548; b) S. Pillai, A. Mustaev, *JPPA: Chem.* **2013**, *255*, 16-23; c) D. R. Reddy, L. W. Miller, *Bioconjugate Chem.* **2011**, *22*, 1402-1409; d) L. N. Krasnoperov, A. Mustaev, *Bioconjugate Chem.* **2010**, *21*, 319-329; e) L. Wirpsza, A. Mustaev, *JPPA: Chem.* **2013**, *253*, 30-37.
[99] A. E. Martell, R. D. Hancock, *Metal Complexes in Aqueous Solutions*, 1 ed., Springer US, **1996**.
[100] J. Beld, H. Cang, M. D. Burkart, *Angew Chem Int Ed Engl* **2014**, *53*, 14456-14461.
[101] a) A. Ehrlich, M. Bienert, *J. Org. Chem.* **1996**, *61*, 8831-8838; b) K. J. Hale, L. Lazarides, *Org. Lett.* **2002**, *4*, 1903-1906; c) T. M. Kamenecka, S. J. Danishefsky, *Angew. Chem. Int. Ed.* **1998**, *37*, 2993-2995.
[102] a) L. A. Carpino, *Journal of the American Chemical Society* **1993**, *115*, 4397-4398; b) L. A. Carpino, H. Imazumi, B. M. Foxman, M. J. Vela, P. Henklein, A. El-Faham, J. Klose, M. Bienert, *Organic Letters* **2000**, *2*, 2253-2256.
[103] W. Watson, *Org. Process Res. Dev.* **2012**, *16*, 1877.
[104] W. I. O´Malley, K. L. Tuck, B. Graham, *Inorg. Chem.* **2016**, *55*, 1674-1682.
[105] a) E. W. Price, C. Orvig, *Dalton Trans.* **2014**, *43*, 7176-7190; b) P. Comba, H. Wadepohl, *Inorg. Chem.* **2016**, *55*, 12531-12543.
[106] J. Andres, K. E. Borbas, *Inorganic Chemistry* **2015**, *54*, 8174-8176.
[107] a) M. Polasek, P. Caravan, *Inorg. Chem.* **2013**, *52*, 4084-4096; b) S. Shuvaev, M. A. Fox, D. Parker, *Angew. Chem. Int. Ed.* **2018**, *57*, 7488-7492; c) M. Regueiro-Figueroa, C. Platas-Iglesias, *Inorg. Chem.* **2011**, *50*, 4125-4141.
[108] F. S. Richardson, *Chem. Rev.* **1982**, *82*, 541-552.
[109] A. K. R. Junker, T. J. Sørensen, *European Journal of Inorganic Chemistry* **2019**, *2019*, 1179-1179.
[110] A. S. Chauvin, F. Gumy, D. Imbert, J. C. G. Bünzli, *Spectroscopy Letters* **2004**, *37*, 517-532.
[111] K. Kumar, C. A. Chang, L. C. Francesconi, D. D. Dischino, M. F. Malley, J. Z. Gougoutas, M. F. Tweedle, *Inorganic Chemistry* **1994**, *33*, 3567-3575.
[112] M. Rajendran, Lawrence W. Miller, *Biophysical Journal* **2015**, *109*, 240-248.

Acta Universitatis Upsaliensis

Digital Comprehensive Summaries of Uppsala Dissertations from the Faculty of Science and Technology 1809

Editor: The Dean of the Faculty of Science and Technology

A doctoral dissertation from the Faculty of Science and Technology, Uppsala University, is usually a summary of a number of papers. A few copies of the complete dissertation are kept at major Swedish research libraries, while the summary alone is distributed internationally through the series Digital Comprehensive Summaries of Uppsala Dissertations from the Faculty of Science and Technology. (Prior to January, 2005, the series was published under the title "Comprehensive Summaries of Uppsala Dissertations from the Faculty of Science and Technology".)

Distribution: publications.uu.se
urn:nbn:se:uu:diva-381905

ACTA
UNIVERSITATIS
UPSALIENSIS
UPPSALA
2019